Physiological and molecular studies on the akinete differentiation of filamentous cyanobacteria

Dissertation

der Mathematisch-Naturwissenschaftlichen Fakultät

der Eberhard Karls Universität Tübingen

zur Erlangung des Grades

eines Doktors der Naturwissenschaften

(Dr. rer. nat.)

vorgelegt von

Zulema Rebeca Perez

Aus Mar del Plata, Argentinien

Tübingen

2016

Tag der mündlichen Prüfung:	4/11/2016
Dekan:	Prof. Dr. Wolfgang Rosenstiel
1. Berichterstatter:	PD Dr. Iris Maldener
2. Berichterstatter:	Prof. Dr. Karl Forchhammer

To my parents

Acknowledgements

I would like to thank all the people that supported me and helped me make this thesis possible.

First of all, I am especially grateful to my supervisor Dr. Iris Maldener for giving me the opportunity to work in this project, for all her support, her guidance and especially for her patience throughout my *Ph.D.* project. I deeply appreciate her advice and our fruitful discussions. Also, I would like to thank her for encouraging me to get involved in collaborations that broadened my horizons.

I would like to express my deepest gratitude to Prof. Karl Forchhammer for his continuous advice and inspiring discussions.

I am very thankful to the research training group GRK1708, SFB766 and University of Tübingen for the academic and personal enrichment in addition to their financial support. I am especially grateful to my colleagues and to the PICs of GRK. It was pleasant learning with you all.

I am thankful to all my colleagues of *Organismische Interaktionen* group for making the lab a pleasant place to work. In particular, Alexander Klotz, Waldemar Hauf, Björn Watzer, Jan Lüddecke and Jan Bornikoel for always be ready to help me with techniques, methods and some obstacles in the lab. Thank you for the laughs and the brewer's yeast!

I thank Claudia Menzel for teaching me how to prepare samples for transmission electron microscopy and using the TEM. I am thankful to Lenka Bucinska to teach me all the tips related to prepare samples for the TEM, and for her nice company. I appreciate the help of Martina with the TLC experiments; it was really nice to work with you. I am thankful to Nadine Silver and Ignacio Sanchez to teach me how to be a supervisor, I enjoyed working and learning with both of you.

I want to express my gratitude to Prof. Graciela Salerno to encourage me to follow my research interest and for her supervision during my research stay in Argentina. I thank to all people from FIBA lab, it was pleasant to work with you one more time. In special to Clara Fernandez and Dr. Macarena Perez Cenci for the technical support. I am especially grateful to Dr. Maria Kolman for her scientific and emotional support during this thesis, also for advise me when I needed.

I am thankful to Dr. Lars Wörmer for his wonderful cooperation in this thesis. I appreciate his patience to explain me the LC-MS methods and for his fruitful discussion.

I would like to express my gratitude to all the people that supported me emotionally during my long stay in Germany. To my dear Tübingen family: Edi, Amit and Katja. I have the best

memories of the times that we shared in Tübingen and I am glad to keep you as my friends. Thanks to Dr. Nishi "Caro" for the technical and emotional support in the initial and final stages of this project. I also want to thank to my lovely roommates: Inge, Agnes, Kerstin and my dear German *Schwester* Martina Goller. Thanks for your nice company, interesting talks and for feed me!. I am especially grateful to my dear friends in Tübingen: Martina, Pablo, Toni and the Torti Group (Lore, Clau, Julia). I really appreciate your friendship and spiritual support. Of course, I will not forget my precious Argentinian friends that supported me in spite of the distance: Maria, Alejandro, Luis, Naty, Vane, Noe, Martín, Ger, Romi and Lety.

Last but not least, I am deeply grateful to my sisters Melina and Julieta for their unconditional support in very difficult times from afar. All my gratitude to both of them for taking care of my dear parents. There are no words to explain my deepest gratitude to my beloved parents Zulema and Héctor! I am very grateful to you for supporting my dreams, especially in difficult times. This thesis is dedicated to you.

Table of Contents

List of tables

List of figures

Abbreviations

ATCC	American Type Culture Collection
ATP	adenosine triphosphate
Chl *a*	chlorophyll *a*
CM	cytoplasmic membrane
Cm	chloramphenicol
CP	cyanophycin
DAPI	4',6-diamidino-2-phenylindole
DCMU	photosynthesis inhibitor
DMSO	dimetyhl sulfoxide
E. coli	*Escherichia coli*
EDTA	ethylene-diamine-tetraacetic acid
Em	erythromycin
FRAP	fluorescent recovery after photobleaching
GFP	green fluorescent protein
HEP	heterocyst envelope polysaccharide layer
HGL	heterocyst-specific glycolipid layer
HGs	heterocyst glycolipids
Km	kanamycin
MOPS	3-N-morpholino propane sulfonic acid
Nm	neomycin
OD	optical density
OM	outer membrane
PBS	phosphate buffered saline
PCC	Pasteur Culture Collection
PCR	polymerase chain reaction
PSII	photosystem II
rpm	revolutions per minute
RT	room temperature
Sm	streptomycin
Sp	spectinomycin
TAE	Tris-acetate-EDTA
TEM	transmission electron microscopy
TLC	thin layer chromatography
TM	thylakoid membrane
TM (H)	transmembrane (helix)
WT	wild-type

Abstract

Akinetes are spore-like cells of filamentous cyanobacteria that allow these organisms to survive long periods of unfavourable conditions. The akinete differentiation and germination processes were studied in detail in two model species of cyanobacterial cell differentiation, the planktonic freshwater *Anabaena variabilis* ATCC 29413 and the terrestrial or symbiotic *Nostoc punctiforme* ATCC 29133. The best trigger of akinete differentiation of *A. variabilis* was low light, while of *N. punctiforme* was phosphate starvation. Akinetes differed from vegetative cells by their larger size, different cell morphology, and the presence of a large number of intracellular granules. The akinete envelopes of both strains were composed by the same glycolipids as heterocysts and by an exopolysaccharide layer. Also, an unknown and new lipid was detected in lipid extracts of *A. variabilis* akinetes. During akinete development the storage compounds cyanophycin, glycogen and lipid droplets transiently increased, and the photosynthesis and respiration activities decreased.

In both strains, germination was an asynchronous process triggered by light. Fast cell divisions occurred inside of the akinetes envelope and did not need endogenous carbon or nitrogen resources but a functional photosystem to complete the process. Unusual fast heterocyst differentiation was observed during akinete germination in *A. variabilis*. Fast cell divisions and heterocysts differentiation during germination could have been supported by the high DNA content in akinetes. In the end of the germination process, the akinete envelope was opened (*A. variabilis*) or partially degraded (*N. punctiforme*) allowing the emergence of the short filament formed. At this point, the photosynthesis and respiration rates were similar to a vegetative cells culture.

Focusing on the specific modulation of the cell wall and cell envelope, proteins were identified that are differentially expressed in akinetes or where shown to be involved in cell differentiation in *N. punctiforme*. One mutant was created in the *ΔAva_2312* gene of *A. variabilis* encoding a protein with putative function associated to cell wall proteins and characterized. This mutant showed a severe filament dystrophy and it was not able to differentiate heterocysts and to grow without a combined nitrogen source. In addition, a thicker peptidoglycan with more non-crosslinked peptides residues was observed in the septum. Finally, this mutant differentiated akinete-like cells lacking a lipid envelope.

Mutants in genes encoding the cell wall lytic enzymes *ΔamiC1* and *ΔamiC2* of *A. variabilis* were also created and characterized in this study. Both mutant strains showed filaments of longer vegetative cells, which differentiated non-functional heterocysts and akinete like-cells. The heterocysts with aberrant morphology showed an abnormal or no deposition of glycolipids, absence of cyanophycin polar bodies and accumulation of glycogen characteristic for a phenotype with hampered N_2 fixation. Accumulation of a thicker peptidoglycan in the septum between the heterocyst and the vegetative cells was observed in both mutant strains. Moreover, *ΔamiC1* and *ΔamiC2* mutants formed akinete like-cells with rounded-shape, irregular or missing lipid envelope than in wild type.

In this study, clear differences in the metabolic and morphological adaptation mechanisms of akinetes from two important cyanobacterial species were found. For the first time a detailed characterization of the germination process of these species was presented. The results paved the way for further genetic and functional studies of akinete differentiation and germination in these species. In fact, three new mutants in cell wall genes involved in akinete development were characterized showing the relevance of the cell wall proteins in cell differentiation.

Zusammenfassung

Akineten sind sporenartige Zellen von filamentösen Cyanobakterien, die es diesen Organismen erlauben lange Zeiträume in ungünstigen Bedingungen zu überleben. Die Akinetendifferenzierung und Keimungsprozesse in den zwei Modellorganismen der cyanobakteriellen Zelldifferenzierung, das planktonische Süßwasserbakterium *Anabaena variabilis* ATCC 29413 und das terrestrische oder symbiontische *Nostoc punctiforme* ATCC 29133, wurden ausführlich studiert. Der beste Trigger der Akinetendifferenzierung für *A. variabilis* war Lichtmangel, und für *N. punctiforme* war es Phosphatmangel. Akineten unterscheiden sich von vegetativen Zellen durch ihre Größe, unterschiedliche Zellmorphologie und die Anwesenheit einer großen Anzahl von intrazellulären Körnchen. Die Zellhüllen von Akineten beider Stämme wurden durch die gleichen Glycolipide wie die von Heterozysten und durch einen Exopolysaccharidschicht zusammengesetzt ist. Auch ein unbekanntes und neues Lipid wurde in der Hülle von *A. variabilis* Akineten identifiziert. Während der Entwicklung der Akineten stiegen die Speicherstoffe Cyanophycin, Glykogen und Lipidtröpfchen vorübergehend an und die Photosynthese und Atmungaktivität verringerten sich.

In beiden Stämmen war die Akinetenkeimung ein durch Licht ausgelöster asynchroner Prozess. Schnelle Zellteilungen traten innerhalb der Akineten Zellhülle auf und benötigten keine endogenen Kohlenstoff- oder Stickstoff-Ressourcen, aber brauchten ein funktionelles Photosystem um den Vorgang abzuschließen. Ungewöhnlich schnelle Heterozystendifferenzierung wurde während der Akinetenkeimung in *A. variabilis* beobachtet. Schnelle Zellteilungen und Heterocystendifferenzierung während der Keimung könnten durch den hohen DNA-Gehalt in Akineten unterstützt werden. Am Ende des Keimungsprozesses wurde die Akinetenzellhülle durchbrochen (*A.variabilis*) oder teilweise abgebaut (*N. punctiforme*), was die Entstehung des kurzen Filaments ermöglicht. Zu diesem Zeitpunkt waren die Photosynthese und Atmungsraten ähnlich einer vegetativen Zellkultur.

Bezüglich der spezifischen Modulationen der Zellwand und Zellhülle wurden Proteine, die differentiell in Akineten exprimiert werden, bzw. in *N. punctiforme* an der Zelldifferenzierung beteiligt sind, im Genom von *A. variabilis* identifiziert. So wurde eine Mutante im *ΔAva_2312* Gen von *A. variabilis* erstellt und charakterisiert. Das Gen kodiert ein Zellwandprotein mit einer sogenannten GerM-Domäne, die in zahlreichen bakteriellen Proteinen mit Zellwandfunktion vorkommt., Die Mutante zeigte eine starke Filamentdystrophie, konnte keine Heterozysten differenzieren und ohne ein Stickstoffquelle nicht wachsen. Mikroskopisch konnte eine stark

verdickte Peptidoglycanschicht mit mehreren nicht vernetzten Peptidresten in den Septen zwischen den Zellen beobachtet werden. Diese Mutante differenzierte akinetenähnliche Zellen mit einer fehlenden Lipidhülle. Folgich scheint das Ava_2312-Protein eine wichitge Rolle bei der Zellwandsynthese und –modulation zu spielen.

Mutanten in Genen, die die zellwandlytischen Enzyme AmiC1 und AmiC2 von *A. variabilis* kodieren, wurden ebenfalls in dieser Studie erstellt und charakterisiert. Die vegetativen Zellen in beiden Mutanten waren deultich länger als im Wildtyp und die gebildeten Heterozysten waren nicht funktional, so dass diese Stämme nicht auf N_2 als einziger Stickstoffquelle wachsen konnten. Die Heterozysten wiesen eine veränderte Morphologie auf und waren defekt in der Bildung der Glycolipidschicht., Das Fehlen von polaren Cyanophycinkörperchen und die Akkumulation von Glykogen ist charakteristisch für einen Phänotyp, der eine Unfähigkeit zur N_2-Fixierung aufweist. Die Akkumulation einer dickeren Peptidoglykanschicht im Septum zwischen der Heterozyste und den vegetativen Zellen wurde in beiden Mutantenstämmen beobachtet. Nach Induktion konnten beide Mutanten nur akinetenähnliche Zellen ausbilden. Die Zellwandamidasen AmiC1 und AmiC2 haben somit eine wichtige Funktion in der Differenzierung von Heterozysten und Akineten in *Anabaena variabilis*.

In dieser Studie wurden deutliche Unterschiede in den metabolischen und morphologischen Anpassungsmechanismen von Akineten aus zwei wichtigen Cyanobakterienarten gefunden. Zum ersten Mal wurde eine detaillierte Charakterisierung der Sporenkeimung dieser Arten vorgestellt. Die Ergebnisse ebneten den Weg für genetische und funktionelle Studien dieses ökologisch wichtigen Zelldifferenzierungsvorgangs und es wurden drei neue Mutanten in Zellwandgenen, die an der Akinetenentwicklung beteiligt sind, charakterisiert, was die Bedeutung der Zellwand bei der Zelldifferenzierung dieser Bakterien zeigt.

Introduction

1 THE CYANOBACTERIA

The cyanobacteria are photosynthetic prokaryotes found in almost all illuminated habitats of our planet, including extreme environments as hot springs and polar regions (Castenholz, 1969; Vincent, 2007). They are in quantity the most important organisms on the Earth with a global biomass estimated in 3×10^{14} g C or a thousand million tonnes (10^{15}g) wet biomass (Garcia-Pichel *et al*., 2003). Cyanobacteria were the first organisms to employ oxygenic photosynthesis, and their burgeoning growth during the Precambrian began to change the Earth's atmosphere from anoxic to oxic (Adams & Duggan, 1999). All cyanobacteria synthesize chlorophyll *a* (Chl*a*) and water is the typical electron donor during photosynthesis. In addition, cyanobacteria contribute greatly to global primary production fixing a substantial amount of carbon, and they are key contributors to global nitrogen fixation (Whitton & Potts, 2012; Garcia-Pichel *et al*., 2003).

1.1 Classification and phylogeny of cyanobacteria

Cyanobacteria include a wide range of morphologies reflected by traditional taxonomic studies, which organized them into five subsections based on morphology and development. Subsection I (Chroococcales) comprise solitary and colonial unicellular forms. Subsection II (Pleurocapsales) unicellular forms that reproduce through multiple fissions in three planes creating smaller daughter cells, baeocytes. Strains in subsection III (Oscillatoriales) comprise filamentous cyanobacteria without cell differentiation, while organisms in subsections IV (Nostocales) and V (Stigonematales) are able to differentiate specific cells (heterocysts, akinetes and hormogonia). Subsection V is further distinguished by the ability to form branching filaments (Rippka *et al*., 1979). Figure 1 illustrates the phylogenetic relationship among cyanobacteria, based on molecular sequence comparison that cover a broad range of morphologies, lifestyles, and metabolisms (Shih *et al*., 2013).

Fig. 1. Maximum-likelihood phylogeny of cyanobacteria with bootstrap support. Branches are color coded according to morphological subsection. Phylogenetic subclades are grouped into seven major subclades (A–G), some of which are made up of smaller subgroups (taken from Shih *et al*., 2013).

1.1.2 The life cycle of filamentous cyanobacteria

Filamentous cyanobacteria of the order *Nostocales* are primordial multicellular organisms, whose filaments are composed of hundreds of mutually dependent vegetative cells, which under certain conditions can differentiate to carry out specialized functions. These differentiated cells include nitrogen fixing heterocysts, motile hormogonia and resistant spore-like cells called akinetes (Fig. 2). The hormogonia and akinetes are transient growth stage in the life cycle of cyanobacteria, which means that they can de-differentiate back to vegetative cells, while heterocysts represent a terminal differentiated cell (Flores & Herrero, 2010; Maldener *et al*., 2014; Adams & Duggan, 1999).

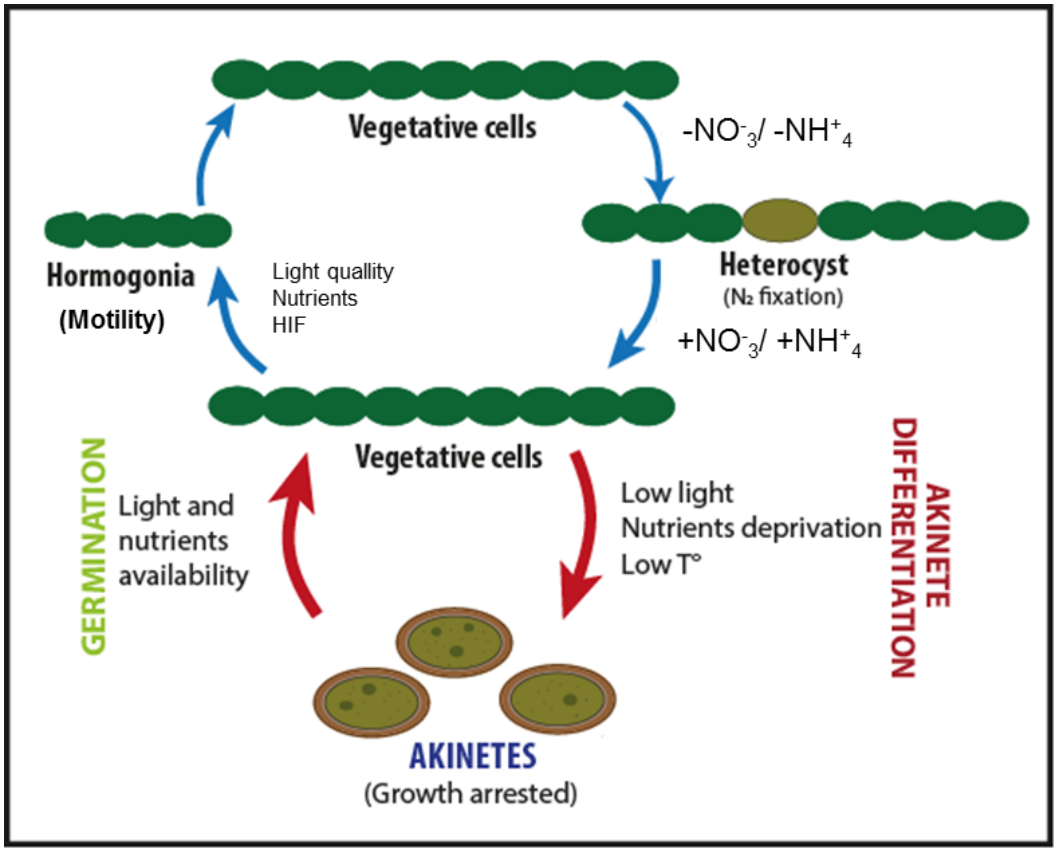

Fig. 2. Scheme of life cycle in *Nostocales*. Vegetative cells can successively grow and divide forming long filaments, when nutrients are available. In absence of combined nitrogen sources (NO_3/NH_4^+), about 5-10% of the vegetative cells differentiate into heterocysts, which can performe N_2 fixation and supply the vegetative cells with nitrogen compounds. Akinetes are formed under unfavorable conditions, as nutrient deprivation, low light and low temperatures. They are arrested in growth, but when the light and nutrients are available they can germinate forming a new filament. The third developmental alternative is the transient symbiotic filament called hormogonia.

1.2 Multicellularity and cell-cell communication

The multicellularity and cell differentiation in *Nostocales* species requires intercellular metabolite exchange between the cells in the filament (Fig.3). Signal and regulatory molecules responsible for the development of specialized cells from vegetative cells must be recruited to the destination (Flores & Herrero, 2010). When the nitrogen sources are scarce, heterocysts appear at semiregular intervals forming a developmental pattern of a single heterocyst every 10 - 20 vegetative cells along filaments (Kumar *et al*., 2010). Heterocyst and vegetative cells are mutually dependent: while the vegetative cells supply carbon compounds, the heterocysts supply combined nitrogen compounds (Golden & Yoon, 2003). Hormogonium differentiation involves synchronous and fast cell division that is controlled by the rapid exchange of information in the filament. In addition, hormogonia requires a sophisticated intercellular signaling system to move coordinated in one direction (Maldener *et al.,* 2014; Meeks & Elhai, 2002).

The exact mechanisms for cell-cell communication in filamentous cyanobacteria remained unclear, however two routes have been proposed: the exchange of information via a continuous periplasm (Fig. 3, blue arrows), or by direct diffusion from cytoplasm to cytoplasm via cell-cell junctions involving the septal proteins SepJ (also known as FraG), FraC and FraD (Fig. 3 purple arrows). These proteins have been localized to the septum or cell junction, between the cells, and could form or be part of the septal junctions, in the literature also described as microplasmodesmata, channels or septosomes (Flores *et al*., 2007; Merino-Puerto *et al*., 2010; Giddings & Staehelin, 1978 & 1981; Wilk *et al*., 2011; Omairi-Nasser *et al*., 2014).

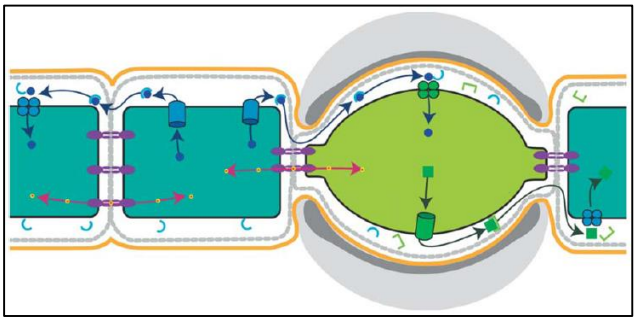

Fig. 3. Schematic representation of intercellular material exchange in filamentous cyanobacteria. Barrels represent exporter, as putative sugar transporters. Protein complexes are localized in the septum, putatively composed of SepJ and Fra proteins. Small yellow dots represent small solutes. Half circles and half squares represent binding proteins and dots represent solutes that diffuse through the periplasmic space (taken from Maldener & Muro-Pastor, 2010).

Recently, the cell wall amidases AmiC2 (NpF1846) and AmiC1 (Alr0092) of *N. punctiforme* and *Anabaena* sp. PCC 7120 respectively, were shown blocked in cell differentiation and cell-cell metabolite exchange (Lehner *et al*., 2011; Berendt *et al*., 2012). The *amiC1* mutant of *Anabaena* sp. PCC 7120 was not able to differentiate heterocysts and therefore to grow without a combined nitrogen source (Berendt *et al*., 2012). Also, a mutant in the *amiC2* gene of *Anabaena* sp. PCC 7120, named *hcwA,* was required for heterocyst formation (Zhu *et al*., 2001). However, a mutant of that gene in another study did not show such phenotype (Berendt *et al*., 2012). In *N. punctiforme*, the *amiC2* mutant showed a severe filament dystrophy with aberrant position of the septa resulting in cell clumps. This mutant was unable to differentiate heterocysts, hormogonia and akinetes; a phenotype that coincides with the complete loss of cell-cell communication demonstrated by calcein fluorescent recovery after photobleaching (FRAP) experiments (Lehner *et al*., 2011). In addition, it was shown that AmiC2 is abundant in the septa of the hormogonia but disappears in maturing akinetes, which do not need communication any more. This enzyme drills holes into the septum forming a nanopore array that may serve as frame work for cell-joining proteins allowing the cell-cell communication and cell differentiation (Lehner *et al.,* 2013; Büttner *et al*., 2016).

1.3 Cell differentiation

1.3.1 Hormogonia

Hormogonia are relatively short gliding filaments composed of cells with smaller and different shape than vegetative cells (Meeks & Elhai, 2002). The smaller cell size results from cell divisions that are not accompanied by an increase in cell biomass (Herdman & Rippka, 1998). Hormogonia serve as spread agent at short distance and are the infective units of cyanobacterial symbiotic associations (Meeks, 1998). Hormogonia move by a gliding mechanism that can involve pili structures (Duggan *et al*., 2007; Khayatan *et al*., 2015) or directional secretion of polysaccharide (Hoiczyk & Baumeister, 1998). They are able to positively move at short distance in response to photo- and chemotaxis stimulus (Meeks & Elhai, 2002). Sudden changes in the habitat, such as the concentration of nutrients or the spectral composition of light lead to hormogonia differentiation (Tandeau De Marsac, 1994). Furthermore, hormogonia are induced and attached to symbiotic plants, which emit a chemical signal called hormogonia inducing factor (HIF) (Meeks & Elhai, 2002).

1.3.2 Heterocysts

Heterocysts are specialized N_2-fixing cells, which do not fix CO_2 by photosynthesis. They develop from the vegetative cells at semiregular intervals along the filament under nitrogen deprived conditions (Wolk *et al*., 1994; Maldener et al., 2014). Heterocysts are easily distinguished from vegetative cells by their larger and rounder shape, loss of pigmentation, thicker cell envelopes, and usually prominent cyanophycin (CP) granules at poles adjacent to vegetative cells (Kumar *et al*., 2010). The differences in ultrastructure of vegetative cells and heterocysts are shown in the figure 4.

The heterocyst differentiation involves complex metabolic and morphological changes to protect nitrogenase from the atmospheric O_2 as well from O_2 produced by the adjacent vegetative cells (Wolk, 1996; Maldener *et al*., 2014). The microoxic cytoplasm in the heterocysts is generated by increasing the rate of respiration, dismantling the O_2 producing photosystem PSII, and the deposition of a multilayered envelope (Wolk *et al*., 1994). This envelope consists of an inner "laminated" layer composed of two heterocyst-specific glycolipids (HGL) and an outer polysaccharide layer (HEP) (Cardemil & Wolk, 1979 & 1981; Nicolaisen *et al*., 2009). Mutants defective in genes involved in the synthesis and deposition of HGL and HEP are not able to grow under diazotrophic conditions (Ernst *et al*., 1992; Maldener *et al*., 2014).

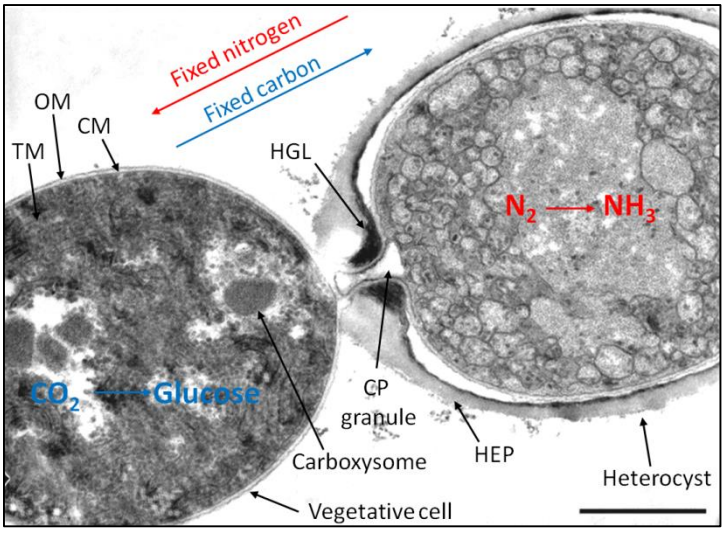

Fig. 4. Ultrastructure of *Anabaena variabilis* ATCC 29413. The structures of a terminal heterocyst and a vegetative cell visualised by transmission electron microscopy. CM, cytoplasmic membrane; OM, outer membrane; TM, thylakoid membrane; CP, cyanophycin; HGL, heterocyst-specific glycolipid layer; HEP, polysaccharide layer.

1.3.3 Akinetes

Akinetes are spore-like, thicker walled, nonmotile cells that differentiate from vegetative cells in response to diverse unfavourable environmental conditions (like temperature, light and nutrients limitation) depending on the cyanobacterial species. They are dormant cells that do not resemble endospores in structure and differentiation mechanism and are not heat resistant. However, since akinetes are resistant to cold and desiccation they are called spore like cells. Akinetes are larger and have a thicker wall than vegetative cells and contain large amount of reserve materials (Kaplan-Levy *et al*., 2010). The shape and position in the filament differs among species, in some cases the heterocyst influence their location (Wolk, 1965). They can germinate to produce new filaments under suitable conditions. Therefore, akinetes provide cyanobacteria with a means of overwintering or surviving dry periods and play a superior role in survival of filamentous cyanobacteria living in habitats with fluctuating conditions as planktonic species (Adams & Carr, 1981b; Kaplan-Levy *et al*., 2010; Maldener *et al*., 2014) (Fig. 5).

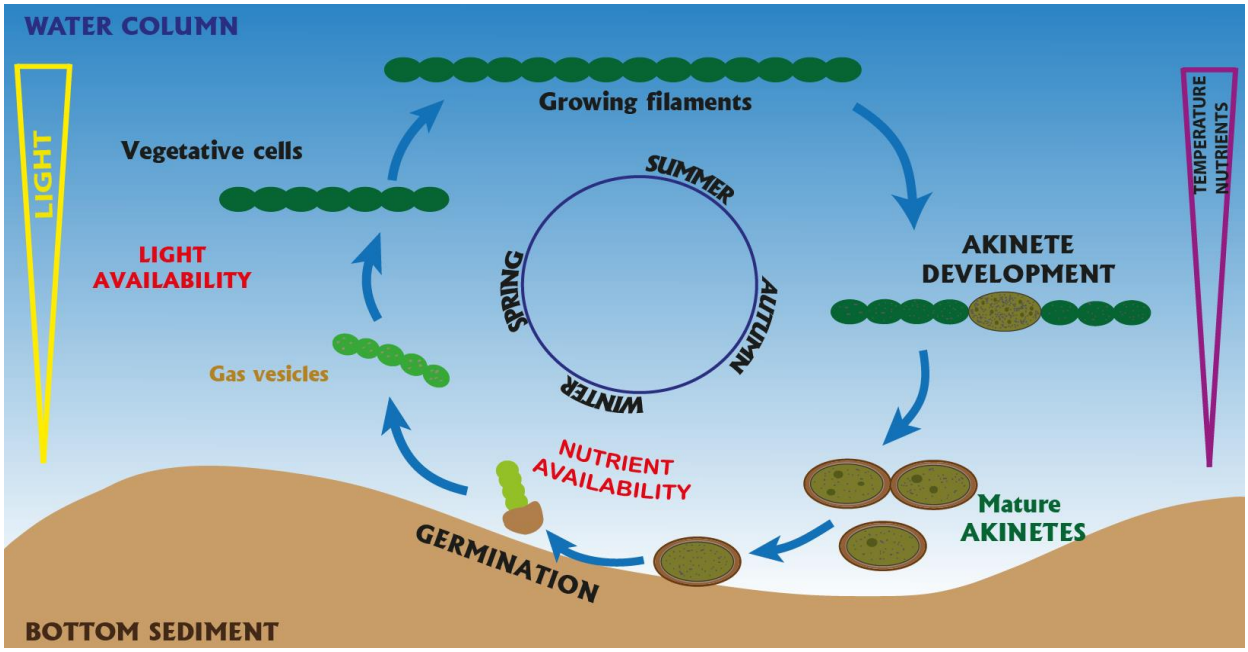

Fig. 5. Annual life cycle of planktonic Nostocales (ie. *A. variabilis* ATCC 29413). In autumn, the vegetative cells start to differentiate in akinetes, which are able to survive under harsh environmental conditions in the bottom sediments. When the environmental conditions improve, a short filament of vegetative cells with gas vesicles emerge from the akinete and float through the water column. Finally, when the light is available the filament formed grow in long filaments. Adopted from Kaplan-Levy *et al*., 2010.

Structure and composition

The development from vegetative cell to a mature akinete involves many structural changes as an increase of cell size, rearrangement of thylakoid membranes, accumulation of intracellular granules like cyanophycin and glycogen (Simon, 1986), and formation of a multi-layered extracellular envelope present in many strains as *A. variabilis* Kützing (Braune, 1980; Nichols & Adams, 1982). The composition of an external akinete polysaccharide layer varies between strains, but structurally is similar to those found in the heterocyst as was reported in *A. variabilis* and *A. cylindrica* (Cardemil & Wolk, 1981). In addition, the akinete envelope of *Cyanospira rippkae* contains the same glycolipids as the heterocyst envelope (Soriente *et al*., 1993).

A conspicuous feature of akinete differentiation is the accumulation of reserve materials as glycogen and cyanophycin (CP), a non-ribosomal produced polymer composed of an aspartate backbone with arginine groups that serves as nitrogen storage (Shi & Carmichael, 1997; Simon, 1987; Sutherland *et al*., 1979). In *Anabaena torulosa* and *Nostoc* PCC 7524 was reported glycogen accumulation during akinete formation (Sarma & Khattar, 1986; Sutherland *et al*., 1979). In addition, in akinetes of *A. torulosa* and *Aphanizomenon ovalisporum* a large amount of CP was detected (Sarma & Khattar, 1986; Sukenik, 2015). However, the accumulation of reserve material is not specific for akinete formation, hence vegetative cells also accumulate glycogen and cyanophycin in stationary growth phase and under stress conditions (Herdman, 1987; Lawry & Simon, 1982). Furthermore, mutation of the arginine biosynthesis gene (*argL*) in *Nostoc ellipsosporum* resulted in the production of akinetes lacking cyanophycin, suggesting that its accumulation is not essential for the formation of akinetes (Leganés *et al.*, 1998). On the other hand, it was reported a massive accumulation of nucleic acids in akinetes of *A. ovalisporum,* which may be supported by polyphosphate bodies that were abundantly present in vegetative cells, but absent in mature akinetes (Sukenik *et al.*, 2007 & 2012).

Metabolic activities

All metabolic activities during the akinete formation and maturation process are strongly affected in several strains. For example, the CO_2 fixation rate was reduced in *A. cylindrica* and *Nostoc* PCC 7524, whereas the respiration rate was often elevated but lost in older akinetes (Fay, 1969; Sutherland *et al*., 1985). Isolated mature akinetes of *N. spongiaeforme* show reduced respiration in the dark. The mature akinetes rather than being completely dormant, maintain a low level of metabolic activity (Thiel & Wolk, 1983). *In vivo* fluorescence measurements of

akinetes from *A. variabilis* Kützing showed the presence of the reaction centre chlorophyll, but also suggested that akinetes lack a functional photosystem II (PSII) (Bjorn *et al*., 1983). Photosynthetic activity was strongly reduced in mature isolated akinetes of *Aphanizomenon ovalisporum* and *A. cylindrica* (Fay, 1969; Sukenik *et al*., 2007 & 2015).

Germination

Germination of akinetes is a metabolic complex process induced by various environmental conditions such as temperature, light and nutrient availability. Also, the sediment mixing and resuspension is a significant factor, triggering germination of akinetes previously localized in the bottom of the sediments (Kaplan-Levy *et al*., 2010). In addition, germination was reported to be dependent on light intensities and did not occur in the dark or in the presence of the photosynthesis inhibitor DCMU (Yamamoto, 1976; Braune, 1979). The ambient conditions that trigger akinete germination in different species, generally correspond to the conditions that support growth of vegetative cultures (Kaplan-Levy *et al*., 2010).

The germination of akinetes was reported as an asynchronous process in some cyanobacterial species (Miller & Lang, 1968; Wildman *et al*., 195; Braun, 1980), while in *Nostoc* PCC 7524 synchronous germination of akinets was observed (Sutherland *et al*., 1985). Akinete germination begins with reorganization of the cellular material followed by elongation and cell division, which take place inside the akinete envelope. The successive cell divisions result in an increase in turgor pressure, which consequently leads to a rupture of the envelope and emergence of the germling from the akinete envelope. The rupture or degradation of the akinete envelope was observed in the polar regions and sometimes the envelope remains associated with the developing filament for some time. By contrast, in some strains such as *N. punctiforme* the entire akinete wall may dissolve during germination, hence, it was not microscopically visible (Adams & Duggan 1999; Skill & Smith, 1987; Sili *et al*., 1994; Moore *et al*., 2004; Meeks *et al*., 2002). Germination of *Cyanospira* akinetes was accompanied by *de novo* synthesis of proteins which took place prior to the first cell division (Sili *et al*., 1994). In *A. circinalis*, photosynthetic activity provided the energy for akinete germination (Kezhi *et al*., 1985), but the rate of germination was determined by the respiratory oxygen uptake of the akinetes, in a temperature-dependent manner (Fay, 1988).

Genes Involved in Akinete Differentiation

In contrast to our profound knowledge on the differentiation of ecological important heterocysts, which was gained in the last decades due to molecular genetics, little is known about the adaptation strategy by akinete differentiation (Kumar *et al*., 2010). Few genes were found to be involved in akinete formation, one of those genes is *hepA* encoding an ABC transporter required for the deposition of polysaccharides in the envelope of akinetes and heterocysts in *A. variabilis* (Leganés *et al*., 1994). In *N. punctiforme* the overexpression of *devR*, a gene implicated in polysaccharide synthesis, resulted in an increase in akinete differentiation (Campbell *et al*., 1996). Furthermore, *hetR* which is a regulator of heterocyst genes, is expressed in akinetes and its deletion led to a failure to differentiate heterocysts or akinetes in *N. ellipsosporum (*Leganés *et al*., 1994), but was not required for akinete formation in *N. punctiforme* (Wong & Meeks, 2001). An akinete marker gene, *avaK,* was identified in *A. variabilis* (Zhou & Wolk, 2002). This gene was differentially expressed in akinetes of *A. variabilis* and *N. punctiforme* but its function is still unknown (Argueta *et al*., 2005). Finally, a mutation in the gene *amiC2* of *N. punctiforme* abolished differentiation of hormogonia, heterocysts and akinetes (Lehner *et al*., 2011). A global expression analysis carried out in the *N. punctiforme zwf* mutant strain that is able to differentiate akinetes in few days, revealed the up-regulation of 255 genes, 41% of which encoded known proteins (Campbell *et al*., 2007).

Aim of the thesis

Over the past decades, our understanding of the heterocyst as a nitrogen-fixing cell has improved considerably, and the ultrastructure, physiology, biochemistry, and molecular biology of this differentiated cell type has been extensively studied in *Nostoc* PCC 7120, but also in *N. punctiforme* (Elhai & Wolk, 1988; Flores & Herrero, 2010). In addition, the differentiation process and N_2 fixation were studied in the genetically accessible strain *A. variabilis* ATCC 29413 (Fiedler *et al*., 1998; Thiel & Pratte, 2014). Several complete genome sequences are available and the method of plasmid transfer by conjugation has successfully been used for formerly inaccessible strains (Nürnberg *et al*., 2014; Stucken *et al*., 2012). These achievements make the study of akinete differentiation on a molecular level feasible in the model organisms for complex multicellular lifestyle as the planktonic freshwater strain *A. variabilis* ATCC 29413 and the terrestrial or symbiotic *N. punctiforme* ATCC 29133, both facultative heterotroph that form akinetes as resting cells (Argueta & Summers, 2005; Argueta *et al.*, 2006; Argueta *et al.*, 2004; Meeks *et al.*, 2001).

This work aims to deepen our knowledge on the akinete differentiation and germination processes in these two model strains. The metabolic and morphologic changes that take place during both processes will be analysed in detail by measurement of O_2 photosynthesis and respiration rates, by chemical determination of reserve materials, and various microscopic techniques such as light, fluorescence and electron microscopy.

Furthermore, mutants in cell-wall proteins (AmiC1, AmiC2 and Ava_2312) of *A. variabilis,* putatively involved in akinete differentiation will be generated by site-directed mutagenesis. Their morphology and ability to differentiate functional heterocyst and akinetes, will be analysed by various microscopic techniques such as light, fluorescence and electron microscopy.

Materials and Methods

2 MATERIALS

2.1 Bacterial strains, plasmids and oligonucleotides

Table 1: Cyanobacterial strains

Strain	Genotype or relevant properties	Source or reference
Anabaena variabilis ATCC 29413 FD	Wild-type	ATCC (obtained from Peter Wolk)
A. variabilis ATCC 29413 *ΔamiC1*	*Ava_1465*::pIM503; Nm^r	This study
A. variabilis ATCC 29413 *ΔamiC2*	*Ava_1466*:: pIM507; Nm^r	This study
A. variabilis ATCC 29413 *ΔAva_2312*	*Ava_2312*::pIM620; Sm^r, Sp^r	This study
Nostoc punctiforme ATCC 29133	Wild-type	ATCC (obtained from Jack Meeks)

Sm, streptomycin; Sp, spectinomycin; Nm, neomycin

Table 2: *E. coli* strains

Strain	Genotype or relevant properties	Source or reference
HB101	F-, *thi*-1, *hsd*S20 (rB–, mB–), *sup*E44, *rec*A13, *ara*-14, *leu*B6, *pro*A2, *lac*Y1, *gal*K2, *rps*L20 (strr), *xyl*-5, *mtl*-1	Sambrook *et al*., 1989
J53 (RP-4)	R+, *met, pro* (RP-4:*Ap,Tc, Km, Tra+, IncP)*	Wolk *et al*., 1984
TOP10	F- *mcr* Δ*(mrr-hsd*RMS-*mcr*BC) φ80lacZ ΔM15 l Δ*lac*X74 *rec*A1 *ara*Δ139 Δ(*ara-leu*)7697 *gal*U *gal*K *rps*L (Str^R) *end*A1 *nup*G	Thermofisher

Table 3: Plasmids

Plasmid	Genotype or relevant properties	Source or reference
pIM503	2.14 kbp *amiC1* in pRL271; Cm^r, Km^r, Em^r	Amorelli, 2012 Diploma thesis, University of Tübingen

pIM507	2.48 kbp *amiC2* in pRL271; Cm^r, Km^r, Em^r	Amorelli, 2012 Diploma thesis, University of Tübingen
pIM620	340 bp from *Ava_2312* in pRL277 Sp^r ,Sm^r	This study
pRL277	integrative vector containing *sacB* gene and Sp^r ,Sm^r	Black *et al.,* 1993
pRL528	Helper plasmid for conjugation Cm^r	Elhai & Wolk, 1988

Sm, streptomycin; Sp, spectinomycin; Cm, chloramphenicol; Km, Kanamycin

Table 4: Oligonucleotides

Oligonucleotide	Sequences (5´➔3´)
Oligo859	CTCGAGATCTTCCCGTTTCCGTCCTGAG
Oligo860	CTCGAGCTGCGGAGTTGGCGTGAATAC
Oligo861	CTCGAGGAGATGATGCTGCTAAACTACG
Oligo862	CTCGAGCTGAGAAACCGTAAAGATTACC
Oligo1297	ATAATAAGCGGATGAATGGCAGAAATTCGATATCTAGATC **ATGAATAACCAACAAGGATCTAAC**
Oligo1298	CCGGCATGTCCCCCTGGCGGACGGGAAGTATCCAGCTCGA **TGGAGTCTGTTCCTTCTGTC**
Oligo1350	GTGATAATAAGCGGATGAATGGCAGAAATTCGATATCTA **CAGCTAATTCTAGACAATAAATATATAA**
Oligo1351	CCCTGGCGGACGGGAAGTATCCAGCTCGAGAT **CTTATTTATATAATTCATCCATACCATG**

Bold letters, sequences binding to the gene; no bold letters, sequences overlapping to the vector.

2.2 Databases and software used

Table 5: List of databases and internet pages used

Description	Internet address
Cyanobase	http://bacteria.kazusa.or.jp/cyanobase/
NCBI (CDART/BLSAT)	http://www.ncbi.nlm.nih.gov/
Meeks Lab Home Page	http://microbiology.ucdavis.edu/meeks/

Table 6: List of software used

Description	Source
Clonemanager 9 (Cloning simulation)	purchased
TMHMM server 2.0 (transmembrane helices prediction)	(http://www.cbs.dtu.dk/services/TMHMM/)

WinASPECT	purchased
Leica LAS AF Deconvolution (3D-Reconstruction)	purchased
Adobe-Photoshop CS6	purchased
Adobe-Illustrator CS6	purchased
GraphPad Prism 6	purchased

2.3 Buffers and reagents

MOPS-Buffer

500 mM MOPS
6.0 M NH_4Cl
7.4 pH NaOH

PBS-Buffer (pH 7,4)

140 mM NaCl

2.5 mM KCl
10 mM Na_2HPO_4
2.0 mM KH_2HPO_4
7.4 pH HCl

TAE-Buffer 10 x, pH 7,9

48.4 g Tris
11.4 ml Acetic acid
20.0 ml EDTA [0.5 M], pH 8.0

ISO-Buffer 5X

500 mM Tris-HCl pH 7.5
50 mM MgCl2
1.0 mM dGTP
1.0 mM dATP
1.0 mM dTTP
1.0 mM dCTP
50 mM DTT
1.5 g PEG-8000
5.0 mM NAD
Add water to 6 ml

Gibson reagents

5X isothermal (ISO) reaction buffer
T5 exonuclease (Epiecntre)
Phusion DNA polymerase (New England Biolabs)
Taq DNA ligase (New England Biolabs)

Gibson Master Mix

320 µl 5X ISO buffer
0.64 µl 10 U/µl T5 exonuclease
20 µl 2 U/µl Phusion DNA polymerase
160 µl 40 U/µl Taq DNA ligase
Add water to 1.2 ml
Aliquot 15 µl

2.5 MICROBIAL METHODS

2.5.1 Growth of cyanobacteria

Cyanobacteria were grown in liquid BG11-medium according to Rippka *et al*., (1979) or in Allen and Arnon (A+A)-medium (Allen & Arnon, 1955) diluted fourfold with water (A+A/4) and supplemented with 5 mM MOPS (pH 7.5), 2.5 mM NH_4Cl, 2.5 mM $NaNO_3$ and 2.5 mM KNO_3. Cultures were incubated under continuous illumination (17–22 µmol photons m^{-2} s^{-1}) at 28 °C with shaking at 120 rpm. For A+A or BG11 solidified media, 1% (w/v) of Bacto agar (Difco, Laurence, USA) was added. Nitrogen source was added in the form of 17.2 mM $NaNO_3$ (BG11) or 5 mM KNO_3 (A+A). Mutants of *A. variabilis* were treated under the same conditions with the addition of the corresponding antibiotics (Table 10).

Table 7: Composition of BG11 medium

Medium	Chemicals	Concentration [mM]
$BG11_o$	$CaCl_2$ x $2H_2O$	0.25
	Citric acid	0.03
	Ammonium citrate	0.023
	K_2HPO_4	0.2
	$MgSO_4$ x $7H_2O$	0.3
	Na_2CO_3	0.18
	Na_2EDTA x $2H_2O$	2.5
Trace element solution	$CoCl_2$ x $6H_2O$	0.2
	$CuSO_4$ x $5H_2O$	0.32
	H_3BO_3	46
	$MnCl_2$ x $4H_2O$	9.2
	Na_2MoO_4 x $2H_2O$	1.6
	$ZnSO_4$ x $7H_2O$	0.77

Table 8: Composition of A+A-Medium

Medium	Chemicals	Concentration [mM]
A+A	$MgSO_4 x 7H_2O$	1,0
	$CaCl_2 x 2H_2O$	0.5
	NaCl	4,0
	K_2HPO_4	2,0
Trace element solution	$MnCl_2 x 4H_2O$	9,24
	MoO_3	1.25
	$ZnSO_4 x 7H_2O$	0.77
	$CuSO_4 x 5H_2O$	0.32
	H_3BO_3	46,0
	KOH	39,0
	$Na_2EDTA x 2H_2O$	23,0
	$FeSO_4 x 7H_2O$	21,0
	NH_4VO_3	0.20
	$CoCl_2 x 6H_2O$	0.17

2.5.2 Growth of *E. coli*

The *E. coli* cells were grown in LB medium, and when was necessary supplemented with the appropriate antibiotics (Table 10). The cells were grown at 37 °C in the dark until the desired cell density. Flasks were shaken at 140 rpm and test tubes in the carousel moved shaker for ventilation.

Table 9: Composition of LB medium (Miller, 1972)

Medium	Chemicals	Concentration [mM]
LB -Liquid medium	Yeast extract	0.5%
	Pepton	1,0%
	NaCl	0.5%
LB- Solid medium	LB liquid medium	
	Agar (Roth, Karlsruhe)	1.5%

2.5.3 Antibiotics

Table 10: Antibiotic concentrations

Antibiotics	Concentration for *E. coli*	Concentration for *A. variabilis*
Kanamycin/Neomycin	100 µg/ml	50 µg/ml
Spectinomycin	100 µg/ml	2.5 µg/ml
Streptomycin	25 µg/ml	2.5 µg/ml
Chloramphenicol	20 µg/ml	

2.5.4 Cryopreservation

For long-term storage bacterial cells were harvested from late log or early stationary growth phases by centrifugation (4,000 rpm; RT, 7 min) and resuspended carefully with 1 ml of the corresponding growth medium supplemented with either 20% (w/v) glycerol (*E. coli*) or 8% (v/v) dimethyl sulfoxide (DMSO) (cyanobacteria). Cells were immediately frozen in liquid nitrogen and stored at -80 °C.

2.5.5 Cell density determination

The growth of bacteria was measured from 1 ml of culture by determining the optical density (OD) and using the medium as reference. The measurement was performed in a spectrophotometer (Specord 205, Analytik Jena) at a wavelength of 600 nm for *E. coli* and of 750 nm for cyanobacteria.

2.5.6 Determination of Chlorophyll *a* concentration

(Mackinney, 1941)

Chl *a* was extracted from 1 ml of cyanobacterial cells in triplicate by adding methanol to a final concentration of 90% (v/v) and vortexing the suspension for 1 min at RT. After removing cell by centrifugation (12,000 rpm; RT, 2 min) the absorption of the supernatant was measured at 665 nm in a spectrophotometer (Specord 205, Analytik Jena). The final concentration of Chl *a* was calculated in terms of the formula Chl *a* [µg ml^{-1}] = 13.43 * A_{665} nm (Mackinney, 1941).

2.5.7 Cultivation methods for cell differentiation

Akinete induction

Akinete differentiation was induced in stationary phase cultures by either low light or phosphate starvation in *A. variabilis* and in *N. punctiforme*. Low light conditions (2 µmol x photons m^{-2} s^{-1}) were maintained by covering flasks with paper towels. Phosphate starvation was brought about by washing filaments three times with A+A/4 media without inorganic phosphate and transferring to A+A/4 media supplemented with 5 mM MOPS buffer (pH 7.5), 2.5 mM NH_4Cl, 2.5 mM $NaNO_3$ and 2.5 mM KNO_3 but lacking inorganic phosphate. Phosphate starvation was also performed with nutrient enrichment by adding 5 mM fructose or 10 mM KNO_3. All induced cultures were maintained at 28 °C with shaking at 50 rpm. Low temperature induction was achieved by transferring the cultures to 15 °C with shaking (Perez *et al*., 2015).

Akinete germination

Cultures containing akinetes were induced to germinate by transfer to normal light conditions or by washing and transferring the akinetes to a fresh medium containing all nutrients (as phosphate).

Heterocyst induction (N step-down)

In liquid medium

Heterocyst differentiation was induced by growth in $BG11_0$ medium under the conditions described above. Previously, the cells were grown in BG11 medium, then harvested by centrifugation (4,000 rpm; RT, 7 min) and washed three times and incubated in $BG11_0$ medium.

In solidified medium

Filaments of wild-type and mutant strains from a liquid culture were washed three times, resuspended with $BG11_0$ medium to obtain different chlorophyll concentrations, spotted in 10 µl aliquots on agar plates and incubated on agar plate medium without combined nitrogen (A+A) for one week.

2.6 GENETIC METHODS

2.6.1 Plasmid isolation

Plasmid isolation was performed with the commercial kit from peqlab (peqGOLD Plasmid Miniprep Kit I) according to the manufacturer´s protocol. For this, 3 ml of an *E. coli* overnight culture were used.

2.6.2 DNA quantification

DNA was quantitated by measuring the absorbance at 260 nm and 280 nm. At 260 nm the optical density of a 50 µg ml^{-1} solution of double strand DNA equals 1.0. Using a TayCell cuvette (Hellma), 3 µl of DNA solution were measured (DNA concentration = Absorbance 260nm × 50 × dilution factor × 10). To get an indication of the purity of the DNA solution the OD_{260}:OD_{280} ratio was calculated with WinASPECT software; solutions with a ratio above 1.8 were considered as pure.

2.6.3 Polymerase chain reaction (PCR)

The "Q5 High-fidelity" DNA polymerase (BioLabs) was used for the amplification of PCR products, that later were used for cloning (section 2.6.7). The "RedTaq DNA" polymerase (Genaxxon bioscience) was used to check the presence of a plasmid or insertion fragment in single colonies of *E. coli* and *A. variabilis* after transformation. The PCR reactions were performed in 0.2 ml PCR reaction tubes in Labcycler (SensoQuest, Goettingen). For the PCR reaction the following components were used:

Table 11: Composition for 25 µl of PCR reaction with "Q5 High-fidelity" polymerase

Component	Volume (µl)	Concentration [mM]
5X Q5 Reaction Buffer	5.0	1X
10X mM dNTPs	0.5	200 µM
10 µM Oligo A	1.25	0.5 µM
10 µM Oligo B	1.25	0.5 µM
Template DNA	2.0	5-100 ng
Q5 High-fidelity polymerase	0.25	0.02 U/µl
ddH_2O	to 25	

Table 12: Composition for 20 µl of PCR reaction with "RedTaq DNA" polymerase

Component	Volume (µl)	Concentration [mM]
2x RedMaster mix	10	1X
10 µM Oligo A	1	0.5 µM
10 µM Oligo B	1	0.5 µM
Template DNA/colony	1	5-100 ng
ddH_2O	to 20	

Table 13: PCR cycling procedure

Step	Temperature (°C)	Time	N° Cycle
Initial denaturation	94	8 min	1
Denaturation	94	45 s	30
Annealing*	49-60	30 s	30
Elongation	72	1 min/1 Kb	30
Final elongation	72	5 min	1
Stop	4	∞	

***** Annealing temperatures were generally 5-10 °C below the lowest melting temperature of the pair of primers used.

2.6.4 Agarose gel electrophoresis

PCR products and digested plasmids were separated according to their size by agarose gel electrophoresis. The agarose (Genaxxon bioscience) was dissolved in TAE buffer (see page 14) to a final concentration of 0.8 to 1.0% (w/v). The samples were mixed with 6x DNA loading buffer (Fermentas), loaded into the pockets of the gel and separated in TAE buffer at 100-130 V. The gel was stained by "Midori Green Advance" (Nippon Genetics EUROPE GmbH) and analyzed using the "Professional Visualization System" (phase HL GmbH).

2.6.5 DNA extraction from agarose gels

DNA fragments were extracted from agarose gels by using the purification kit QIAquick® Gel Extraction Kit" (Qiagen), according to the manufacturer's specifications.

2.6.6 Restriction digestion

The DNA was digested with specific restriction enzymes following the information provided by the manufacturer (Fermentas, Inc. New England BioLabs): 2 µg plasmid (pRL277) together with 1U/µl restriction enzyme (*Xho*I) and 0.5 µl of buffer R were mixed and incubated for 2 h at 37 °C. After that, *Xho*I was inactivated by incubation at 80 °C for 20 min and the restriction mixture was separated on agarose gel.

2.6.7 Creation of the plasmid pIM620

The pIM620 plasmid (see Table 3) was generated by cloning according to Gibson *et al*., (2009). The *Ava_2312* overlapping fragment (340 bp) was obtained by amplification from *A. variabilis* genome with overhanging primers (see Table 4). This fragment has 40 bp at the 5´and 3´ ends, which overlap with the pRL277 vector. The PCR products were purified from the agarose gel and the DNA concentration was determined. A total of 5 µl DNA (4 µl of pRL277 digested and 1 µl of *Ava_2312* fragment in equimolar amounts) and 15 µl of Gibson Master Mix (see section 2.3 Buffers and reagents) were incubated for 1 h at 50 °C.

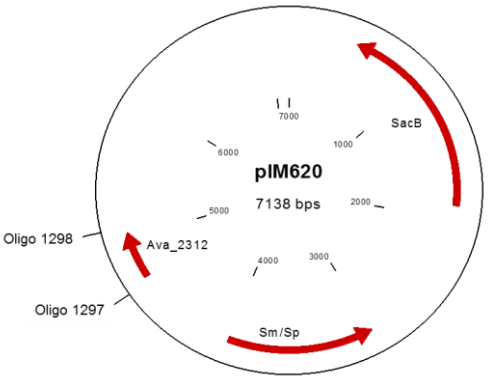

Fig. 6. Schematic representation of the pIM620 plasmid. The pIM620 carrying a fragment of *Ava_2312* gene will be used for conjugation of *A. variabilis*. Oligo 1297 and Oligo 1298 are the primers used to obtain the *Ava_2312* overlapping fragment (see Table 4).

2.6.8 Preparation of electro-competent *E. coli* cells

Initially, 5 ml of LB medium were inoculated with a single colony of *E. coli* (from agar plate) and incubated overnight at 37 °C. This culture was used to inoculate 1 L of fresh medium and grown at 37 °C until an OD_{600} of 0.5-0.7 was reached. To stop cell division, the cells were incubated on ice for 10 min and harvested by centrifugation (4,000 rpm, 4 °C, 10 min.), the supernatant was

carefully discarded and the pellet resuspended in 40 ml cold ddH_2O. In order to remove salts and other components of the medium that could interfere later in the electroporation, the cells were washed twice (4,000 rpm, 4 °C, 20 min) and dissolved in 10% cold glycerol. After re-centrifugation, the cells were dissolved up in 15% glycerol and stored in aliquots of 50 µl into pre-cooled (-80 °C) eppendorf tubes at -80 °C.

2.6.9 Electroporation of *E. coli* cells

The electro-competent cells (50 µl) were thawed on ice and mixed with 1 µl of the pIM620 plasmid resulted from Gibson cloning (see section 2.6.7). The mixture was incubated on ice about 1 min and then transferred to a cold electroporation cuvette (25 x 2 mm, Peqlab), The mixture was electroporated at 2.5 kV, 25µF and 200 Ω in a "Bio Rad Gene Pulser®". Then 1 ml LB of warm medium was quickly added to the mixture and incubated for 1 h at 37 °C on a rotary shaker. A portion of this suspension was plated on an LB plate with the required final concentration of antibiotics and grown at 37 °C overnight.

2.6.10 Triparental conjugation

For the triparental conjugation, late exponential growth cultures of *A. variabilis* were sonicated with Branson SONIFIER 250 (output 3; 50% duty), washed with medium and incubated overnight for recovering. The cells were concentrated at 75 - 100 µg Chl *a*/ml by centrifugation. Both *E. coli* strains HB101 [pRL528 + cargo plasmid (pIM: see Table 3)] and J53 (RP4) were grown in 2 ml of LB medium supplemented with the appropriate antibiotics overnight at 37 °C. 300 µl of each *E. coli* overnight cultures were used to inoculate 30 ml of fresh LB medium without antibiotics that were incubated for 3.5 h at 37 °C. Both cultures were concentrated at OD_{600} of 9 and 1 ml of each were combined with 0.5 ml of LB medium and incubated for 1.5 h at 30 °C in the dark. Half ml of the *E. coli* suspension and 0.5 ml of *A. variabilis* cells were carefully mixed in an eppendorf tube, centrifuged (6,000 rpm, RT, 30 s) and 800 µl of the supernatant discarded. The resuspended pellets were spread out with glass beads on millipore filters (Immobilon-NC, Merck REF08250) on agar BG11 plates without antibiotics and incubated at low light at 28 °C for 24 h. The filters were then transferred to selection plates (50 µg/ml of Nm or 2.5 µg/ml of Sp and Sm) and incubated at 28 °C with normal light for approximately 10 days. Colonies were picked and restreaked on 1% (w/v) agar BG11 plates supplemented with antibiotics until strains were fully segregated.

2.7 BIOCHEMICAL METHODS

2.7.1 Cyanophycin extraction and quantification

(Perez *et al*., 2015)

Cyanophycin was extracted from cells in triplicate according to Watzer *et al*. (Watzer *et al*., 2015) with the following modifications: aliquots (25 ml) of liquid cultures were taken at 1, 18, 30 and 60 days after akinete differentiation was induced by low light or phosphate starvation. The cells were harvested by centrifugation, resuspended in 100% acetone and incubated for 90 min at room temperature with constant shaking (1,400 rpm). Cells were collected by centrifugation at 25,000 × *g* for 15 min. The pellet was resuspended in 1 ml 0.1 M HCl and incubated for 2 h with constant shaking (1,400 rpm) at 60 °C; the suspension was centrifuged at 25,000 × *g* for 20 min. To precipitate cyanophycin, 1 ml of 1 M Tris/HCl pH 9.0 was added to the clear supernatant. The mixture was incubated for 90 min at 4 °C and centrifuged at 25,000 × g for 30 min at 4 °C. The supernatant was discarded, and the cyanophycin pellet was dissolved in 1 ml 0.1 M HCl. Cyanophycin was quantitated in the samples and in a standard curve generated with isolated cyanophycin (Watzer *et al*., 2015) by determining the arginine concentration using the Sakaguchi reaction according to Messineo (1966). For that, following solutions were added in the following order to 1 ml of sample: 500 µl of 1 M KOH, 100 µl of 2,4-Dichloro-1-naphthol solved in absolute ethanol (w/v) and 100 µl of NaClO (sodium hypochlorite). The reaction was mixed by inversion of the tube 2-4 times and arginine was estimated by absorbance at 510nm.

2.7.2 Glycogen determination

(Perez *et al*., 2015)

Glycogen was extracted from triplicate aliquots (50 ml) of cultures of both species taken after 0, 18 and 30 days after akinete formation was induced by phosphate starvation. The samples were centrifuged, lyophilized and the pellets boiled in water brought to pH 9 with ammonium. After centrifugation the cell pellet was washed with 80% ethanol (v/v), resuspended in 400 µl H_2O and autoclaved at 120 °C for 1 h (Curatti *et al*., 2008). The remaining pellets were solubilized by heating to 100 °C during 20 min in 500 µl of 50mM HCl/sodium-acetate mixture (pH 4.8). Glycogen was quantitated in the samples and in a standard curve generated with commercial glycogen by determining the reducing sugars concentration using the Somogyi and Nelson reagents (Porchia *et al*.,1999). After acidification to pH 4.9, part of the suspension was digested at 60 °C during 1 h with α-Amyloglucosidase. This reaction was stopped by boiling for 20 min in 500 µl of Somogyi

reagent, and after addition of 800 µl of Nelson reagent, the reducing sugar concentration was estimated by absorbance at 520nm.

Somogyi (25A + B + 26 H_2O)

Solution A:	Na_2CO_3 (anhydrous)	25 g
	$KNaC_4H_4O_6$ x $4H_2O$	25 g
	$NaHCO_3$	20 g
	Add water to	1000 ml
Solution B:	$CuSO_4$ x $5H_2O$	15 g
	H_2SO_4	2 drops
	Add water to	100 ml

Nelson (1Nelson + 1 H_2O)

$(NH_4)6Mo_7O_{24}$ x $4H_2O$	25 g
H_2SO_4	21 ml
Na_2HAsO_4 x 7 H_2O	3 g
Add water to	500 ml

2.7.3 Lipid composition of the heterocysts and akinetes envelopes

Thin layer chromatography

For thin layer chromatography, lipids were extracted by the method of Winkenbach *et al*. (Winkenbach *et al*., 1972). 50 ml of cultures grown with and without nitrogen source, and from cultures induced to form akinetes by low light (*A. variabilis*) and phosphate starvation (*N. punctiforme*) for 2 months were used to determine the lipid composition of heterocysts and akinetes. Also, 50 ml of *A. variabilis* and its mutants (*ΔamiC1* and *ΔamiC2*) were grown in media with and without nitrogen source to analyse the presence of glycolipids in the mutant strains. The cultures were centrifuged (4,000 rpm; RT; 10 min) and the pellets dissolved in methanol-chloroform mixture (1:1). The lipids were concentrated by evaporation and dissolved in 200 µl of chloroform. The solution was spotted on a thin-layer silica plate (Merk, Germany). Separation occurred in a mobile phase of chloroform-methanol-acetic acid-water mixture (85:15:10:3.7). The lipids were visible by spraying the plates with 25% H_2SO_4 and subsequent heating at 220 °C for 1 to 2 minutes.

UHPLC-MS analysis

The following steps were performed by Lars Wörmer (University of Bremen, Germany)

Lipid content from the TLC bands were extracted according to Sturt e*t al*. (2004). Reversed phase chromatographic separation was achieved on a Waters Acquity $BEHC_{18}$ column with a Dionex Ultimate 3000RS UHPLC (Wörmer *et al*., 2013) coupled by an electrospray ionization source to a maXis quadrupole time-of-flight mass spectrometer (Q ToF-MS, Bruker Daltonics, Bremen, Germany). The chromatographic gradient was slightly modified to improve detection of cyanobacterial heterocyst glycolipids (HGs). Detection of lipids was performed in positive ionization mode while scanning a mass-to-charge (m/z) range from 150 to 2,000. MS^2 scans were obtained in data-dependent mode, for each MS full scan up to three MS^2 experiments, targeting the most abundant ions, were performed. Active exclusion limits the times a given ion is selected for fragmentation (3 times every 0.5 min) and thus allowed to also obtain MS^2 data of less abundant ions (Fig. 7) (Yoshinaga *et al*., 2015).

Lipid identification was achieved by monitoring exact masses of possible parent ions (present as either H^+, NH_4^+ or Na^+ adducts) in combination with characteristic fragmentation patterns as outlined by Sturt *et al*. (2004), Bauersachs *et al*. (2009) and Wörmer *et al*. (2012).

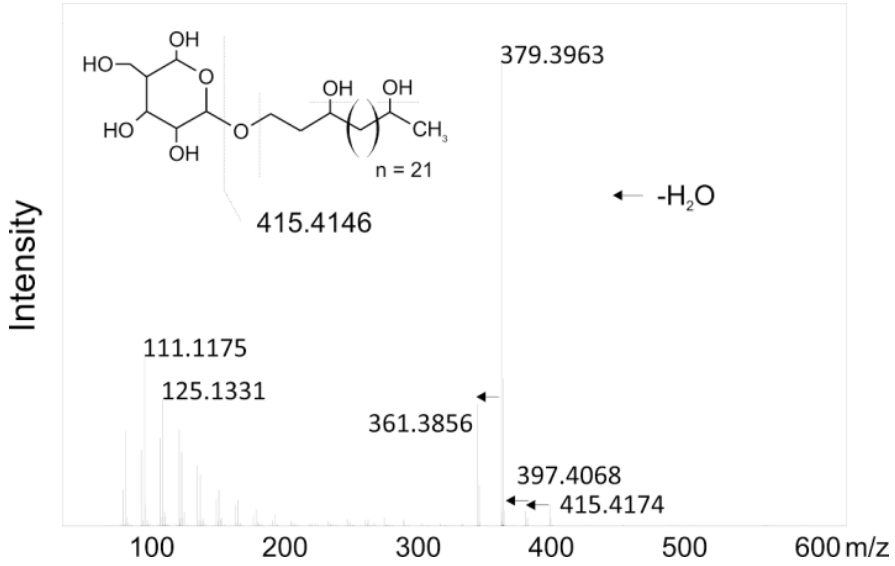

Fig. 7. MS^2 spectrum showing the characteristic fragmentation pattern of HGs. The glycosyl moiety is initially cleaved off, followed by sequential losses of the OH groups.

2.7.4 Photosynthetic oxygen evolution measurement

(Perez *et al*., 2015)

Photosynthetic oxygen evolution was measured *in vivo* using a Clark-type oxygen electrode (Hansatech DW1, King's Lynn, Norfolk, UK). Light (55 µmol photons m^{-2} s^{-1}) was provided from a high-intensity white light source (Hansatech L2). Oxygen evolution was measured at room temperature from 2 ml aliquots of both strains, after induction of akinete differentiation by phosphate starvation for 0, 18, 30 and 60 days or after akinete germination for 0, 12, 24, 30, 48 and 72 hours. The activity of photosystem II (PS II) was measured using the Hill reaction according to Dai *et al.* (2014) with a light intensity of 1,500–2,000 µmol photons $m^{-2}s^{-1}$. As artificial electron acceptors, 2.5-dimethyl-*p*-benzoquinone and potassium ferricyanide were used. Respiratory activity was determined by measuring O_2 consumption in the dark.

2.8 MICROSCOPY METHODS

2.8.1 Electron microscopy

(Fiedler *et al*., 1998)

Contrasting and sample embedding for ultrathin sections

For electron microscopy studies, cultures were harvested by centrifugation (4,000 rpm; RT; 10 min) and fixed with glutaraldehyde (2.5% final concentration) for 5 min at RT. After washing three times with 5 mM HEPES (pH 8.0), the samples were post-fixed with 2% potassium permanganate solution at 4 °C overnight. This step served to better contrasting of the glycolipid layers. Then, the cells were washed 8 to 10 times with ddH_2O and immersed in 2% Sea Kem agarose (FMC Bioproducts, Rockland, USA). After solidification the agar blocks were cut into small cubes with an edge length of ~2 mm and dehydrated by incubation on increasing alcohol concentrations (v/v) (70%, 80%, 90% and 95%) 2 times each for 10 minutes and then 20 min with three times changing in 100 % ethanol. For successful infiltration of Epon in the samples they were first pretreated by incubation with propylene oxide for 15 minutes. The first infiltration of the samples with resin was carried out in a 1:2 mixture of propylene oxide and Epon for 30 min, followed by a 1:3 mixture for 90 min at RT. Finally, the agarose cubes were embedded in Epon pure, polymerized for 24 hours at 40 °C and for 48 h at 60 °C.

Production of ultra-thin sections for TEM analysis

Ultrathin sections (60-90 nm) were made with the Leica EM UC6 and transferred to copper grids pioloform covered. The samples were contrasted by incubation of the grids for 17 min in uranyl acetate 2% in ethanol (w/v), followed by 5 minutes in lead citrate 1% (according to Reynolds).

Transmission Electron Microscopy

The analysis of ultrathin sections was made in a Transmission Electron Microscope (TEM) Philips Tecnai 10 at 80 kV and micrographs recorded with an exposure time of 2 sec on a medium format film and then digitized using a transmitted light scanner. Images were post edited using Adobe Photoshop CS6.

2.8.2 Light and fluorescence microscopy

Light and fluorescence microscopy images were obtained with a Leica DM 2500 light microscope connected to a Leica DFC420C camera and with a Leica DM 5500B microscope connected to a Leica DFC420C monochrome camera, respectively. The wavelength of excitatoion of fluorescent stains was 470/440 nm. Autofluorescence was monitored after excitation with 535/50 nm. For three-dimensional imaging, a series of images derived from different focal planes (Z-stack) was recorded, and the scatter was re-calculated by deconvolution using the built-in function of the Leica ASF software. Images were recolored by the Leica ASF software based on the filter used, and intensity levels were adjusted using Adobe Photoshop CS6.

2.8.3 Staining of bacteria

Alcian Blue

Alcian Blue stained the polysaccharide containing envelope layers of heterocysts and akinetes. For that, 2 to 10 µl of Alcian blue solution 1.5% in H_2O (w/v) was added to 1 ml of culture and incubated for 10 to 15 min. Cells were placed on a slide covered with 1% agarose and observed by light microscopy.

BODIPY

Neutral lipoid structures and lipid envelopes were visualized by stained with BODIPY 493/503 (Molecular Probes). One ml of culture was resuspended in 1 ml PBS buffer (pH 7.5), centrifuged and resuspended in 1 ml 4% (w/v) paraformaldehyde. The mixture was incubated for 1 h at room

temperature, the cells were centrifuged and resuspended in 0.5 ml PBS buffer (pH 7.5) and 1 µl of 50 ng/ml BODIPY in DMSO was added. The cell suspension was incubated in the dark for 15 min at room temperature, centrifuged and resuspended in 100 µl PBS buffer (pH 7.5). Cells were placed on a slide covered with 1% agarose and observed by fluorescent microscopy.

DAPI

The nucleic acid of vegetative cells and akinetes was visualized by stained with DAPI, a blue fluorescent nucleic acid stain (Sigma-Aldrich). For that, 0.5 ml of culture was resuspended in 1 ml PBS buffer (pH 7.5), centrifuged and resuspended in 1 ml 4% (w/v) paraformaldehyde. The cells were incubated for 1 h at room temperature and washed with PBS buffer (pH 7.5). Finally, the cell pellet was resuspended in 100 µl PBS buffer (pH 7.5) and 1 µl of 1 mg/ml DAPI solution was added. The cell suspension was incubated in the dark for 30 min at room temperature, washed twice and resuspended in 100 µl PBS buffer (pH 7.5). Cells were placed on a slide covered with 1% agarose and observed by fluorescent microscopy.

Neisser

In order to observe the presence of polyphosphate bodies in the cells, 0.5 ml of culture was centrifuged and washed with 1 ml PBS buffer (pH 7.5). The pellet was resuspended and stained with 200 µl of (2A + B) Neisser solution for 1 min. Cells were washed with ddH_2O and stained with 500 µl of 0.3% chrysoidin solution in water for 15 min. finally, the cells were washed and placed on a slide covered with 1% agarose and observed by light microscopy. Polyphosphate bodies stained dark purple-black (Pelczar, 1957).

Solution A:	Methylene blue	0.1 g
	Glacial acetic acid	5 ml
	Ethanol 96%	5 ml
	Distilled water	100 ml
Solution B:	Crystal violet, 10% in 96% ethanol	3.3 ml
	Ethanol 96%	6.7 ml
	Distilled water	100 ml
Chrysoidin solution:	Chrysoidin Y, 1% aqueous solution	33.3 ml
	Destilled water	100 ml

Sakaguchi

(Watzer *et al*., 2015)

To visualize cyanophycin granules by light microscopy, cells and differentiated cells were collected by centrifugation from 1 ml of culture and pellets resuspended in 1 ml PBS buffer (pH 7.5). For fixation, the cells were centrifuged and resuspended in 1 ml 4% (w/v) paraformaldehyde for 1 h at 4 °C. Fixed cells were centrifuged and washed once with PBS buffer (pH 7.5). The pellet was resuspended very gently in 80 µl KOH and 10 µl 1% (w/v) 2,4-Dichloro-1-napthol (solved in absolute ethanol) and 10 µl 5% (w/v) sodium hypochlorite were added and mixed very gently. After centrifugation, the cells were resuspended in 100 µl PBS buffer (pH 7.5), placed on a slide covered with 1% agarose and observed by light microscopy.

Van-FL

(Lehner *et al*., 2013)

For the *in vivo* staining of peptidoglycan, 100 µl of culture was stained with Van-FL (BODIPY® FL Conjugate) (1 µg/ml) and incubated for 1 h at RT in the dark. The excess of unlinked dye was removed by washing two times with PBS buffer (pH 7.5). Cells were placed on a slide covered with 1% agarose and observed by fluorescent microscopy. For the detection of the fluorescence signal of the GFP filter was used.

Results

3. 1 AKINETE DIFFERENTIATION

3.1.1 Triggers of akinete differentiation

When the nutrients become limited in stationary phase cultures, akinetes were commonly observed in *A. variabilis* (Fig. 8c) and *N. punctiforme* (Fig. 8d). In general, they can be identified in the light microscope by their larger size and intracellular granules (Fig. 8a-d). To study the physiological and morphological changes that take place during akinete formation, it was necessary to determine the best conditions for synchronized differentiation and to obtain cultures with as close to 100% akinetes as possible. For this purpose, various conditions were tested to induce akinete formation in stationary phase cultures: low temperature, low light and phosphate starvation without and with nutrient enrichment. Akinete differentiation was efficiently induced by low light in stationary phase cultures of *A. variabilis* that reached up to 95% akinetes after 10 days of induction. By contrast, after 30 days of phosphate starvation, cultures contained only about 70% of mature akinetes (Fig. 9). In stationary phase cultures of *N. punctiforme,* phosphate starvation was the most efficient trigger and led to 70% of akinetes after 18 days (Fig. 10). All other conditions tested (see Methods), as low temperature, were less effective. After two months, cultures of *A. variabilis* and *N. punctiforme* induced by phosphate starvation consisted of 90 to 100% fully matured akinetes (Fig. 8e, f).

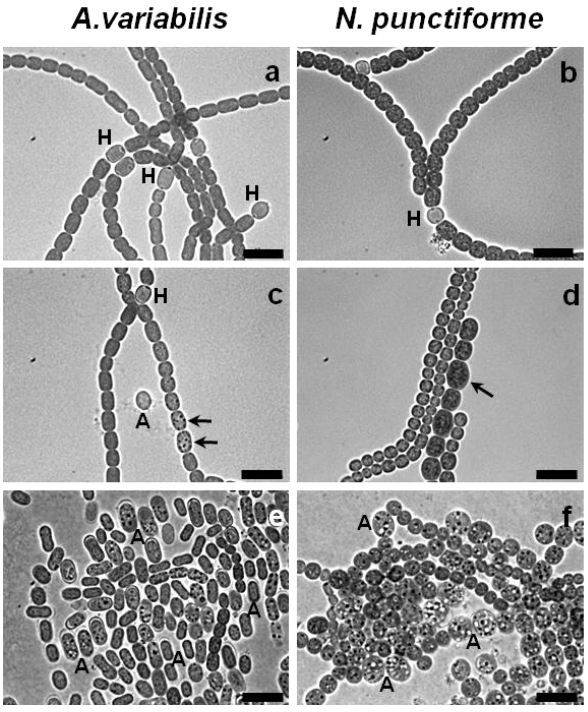

Fig. 8. Different cell types found in cultures of *A. variabilis* ATCC 29413 (a, c, e) and *N. punctiforme* ATCC 29133 (b, d, f). (a, b) Bright-field images of filaments composed of vegetative cells and heterocysts. (c, d) Immature akinetes (arrows) in filaments of stationary-phase cultures. (e, f) Mature akinetes after 60 days of phosphate starvation. H, Heterocyst; A, mature akinete. Bars, 10 µm.

3.1.2 Morphological changes during akinete formation

Akinetes developed within groups of adjacent vegetative cells in the filaments of both *A. variabilis* and *N. punctiforme* (Fig. 8c–f). These spore-like cells were distinguished from vegetative cells by their larger size (*A. variabilis*: 7.45 µm × 4.24 µm; *N. punctiforme*: 8.12 µm × 5.7 µm), large number of intracellular granules and different cell shape (Figs. 9, 10). The large, oval-shaped mature akinetes of *A. variabilis* were mostly detached from the filaments and were surrounded by an envelope (Figs. 8e, 9a-c, e-g). Even though, some mature akinetes were still connected (Fig 9 d, e).

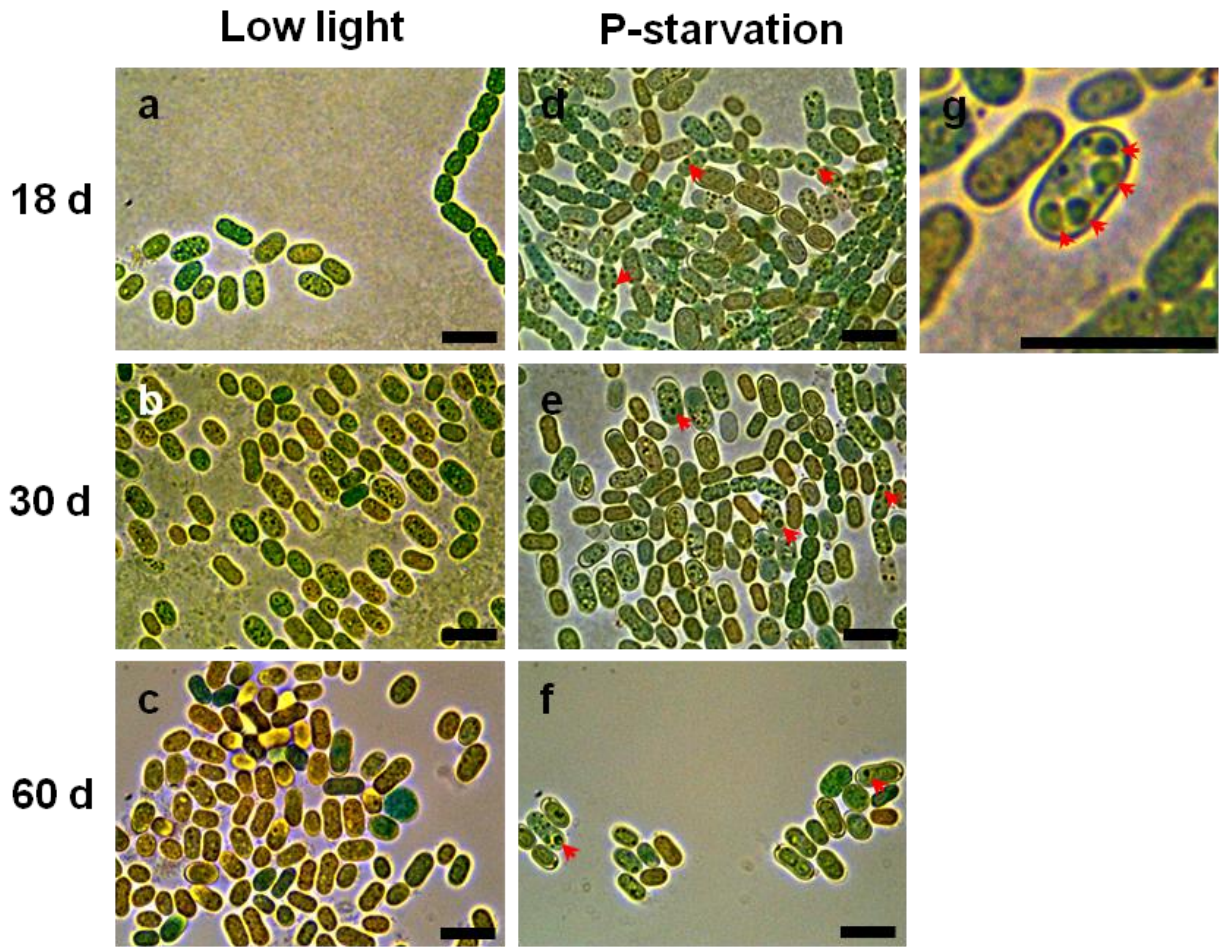

Fig. 9. Induction of akinetes in *A. variabilis* by various conditions. Bright-field micrographs of cultures after (a, d, g) 18, (b, e) 30 and (c, f) 60 days of incubation under (a, b, c, g) low light or (d, e, f) phosphate starvation. High magnification of akinetes (g). Red arrows, granules in akinetes. Bars, 10 µm.

Most of *N. punctiforme* akinetes remained attached to each other, but the septum between the enlarged spherical cells was constricted. In addition, a thicker envelope was not visible in the light microscope (Figs. 8d, f, 10). Frequently, a brownish sheath can be seen surrounding a group of akinetes (Fig. 10f, S1).

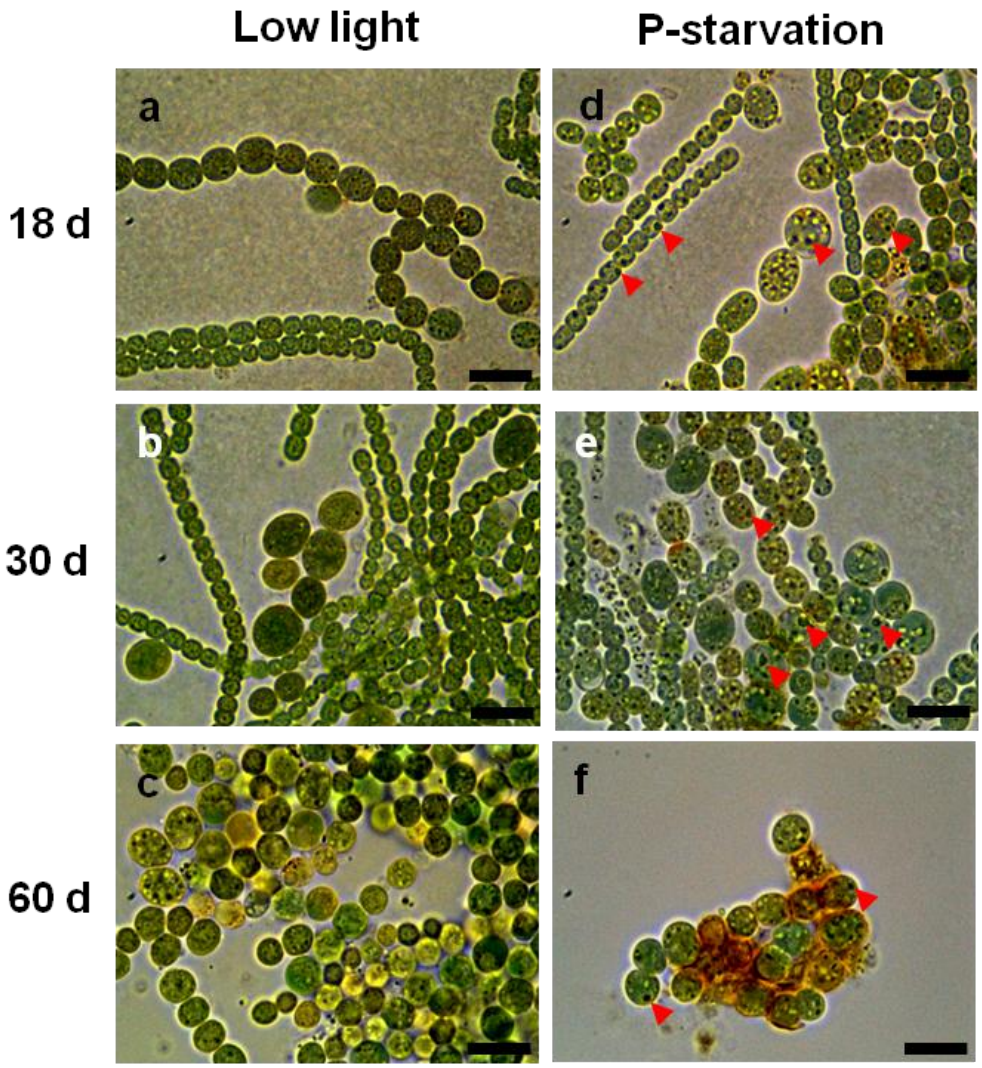

Fig. 10. Induction of akinetes in *N. punctiforme* by various conditions. Bright-field micrographs of cultures after (a, d) 18, (b, e) 30 and (c, f) 60 days of incubation under (a, b, c) low light or (d, e, f) phosphate starvation. Red arrow heads, granules in akinetes. Bars, 10 µm.

The akinete ultrastructure was analysed by preparing samples at different stages after akinete differentiation was induced by low light (*A. variabilis*) or phosphate starvation (*N. punctiforme*). The ultrastructure of *A. variabilis* akinetes 20 days after induction (Fig. 11b) clearly differed from

that of vegetative cells, in which polyhedral carboxysomes and the typical arrangement of thylakoid membranes were observed (Fig. 11a). The large granules consisting of cyanophycin (nitrogen storage) and a large number of smaller glycogen granules (carbon storage) were observed in akinetes. The thylakoid organization was already disordered, carboxysomes were lacking and an extra envelope surrounding the Gram-negative cell wall started to develop. By contrast, large cyanophycin granules were not present in mature akinetes (Fig. 11c, d), and their envelope was thicker and composed of five distinct layers as described by Braune (1980) for the strain *A. variabilis* Kützing.

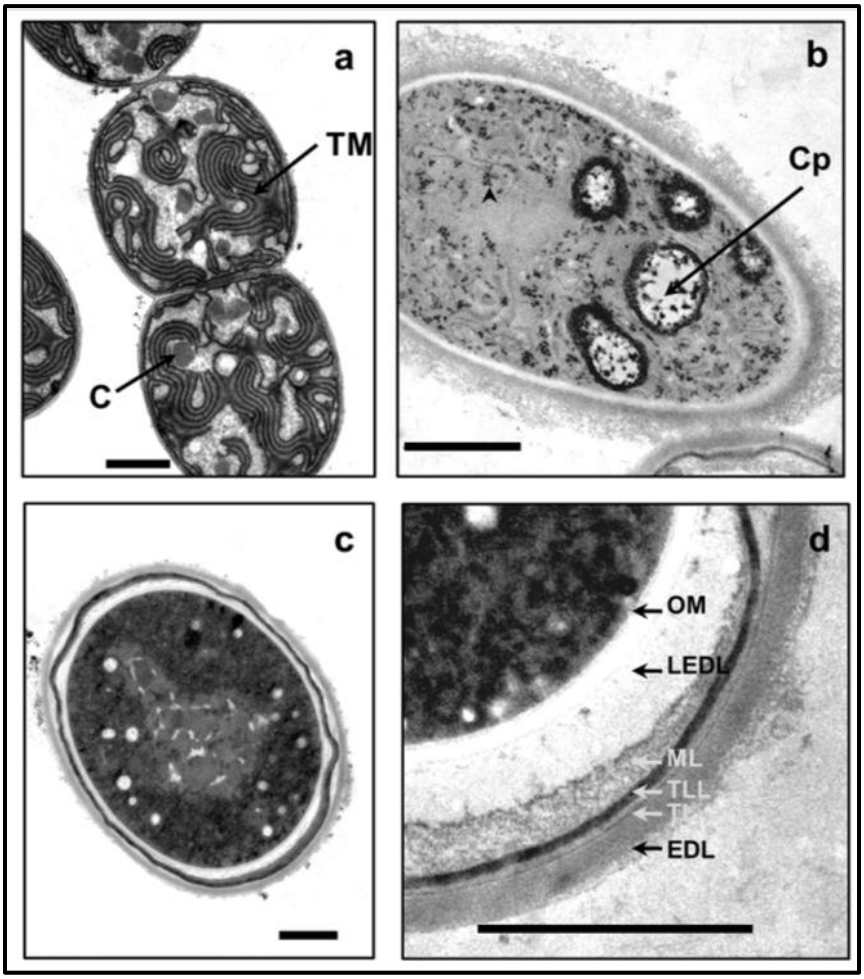

Fig. 11. Ultrastructure of *A. variabilis* akinetes. Transmission electron micrographs of vegetative cells (a) and akinetes (b–d) in cultures exposed to low light for 20 (b) or 60 days (c, d). (d) High magnification of the akinete envelope. C, Carboxysome; Cp, cyanophycin; EDL, electron-dense layer; LEDL, less electron-dense layer; ML, mucilaginous layer; OM, outer membrane; TL, thin laminated layer; TLL, thick laminated layer; TM, thylakoid membrane; arrowhead, glycogen granules. Bars, 1 µm.

The ultrastructure of akinetes of *N. punctiforme* was also analysed in cultures starved of phosphate for 32 (Fig. 12b, c) and 60 days (Fig. 12d). Vegetative cells of *N. punctiforme* were similar to those of *A. variabilis*, contained polyhedral carboxysomes and had the typical arrangement of the thylakoid membranes (Fig. 12a). Different morphologies of akinetes representing different maturation stages, were observed at both time points after induction, which indicated that they developed asynchronously in the culture. The immature akinete showed glycogen granules, cyanophycin granules, carboxysomes, lipid droplets and rearrangement of thylakoid membranes (Fig. 12c). In mature akinetes, carboxysomes, cyanophycin granules and lipid droplets were lacking, thylakoid membranes were pronouncedly rearranged and two visible layers of the envelope were present (Fig. 5d).

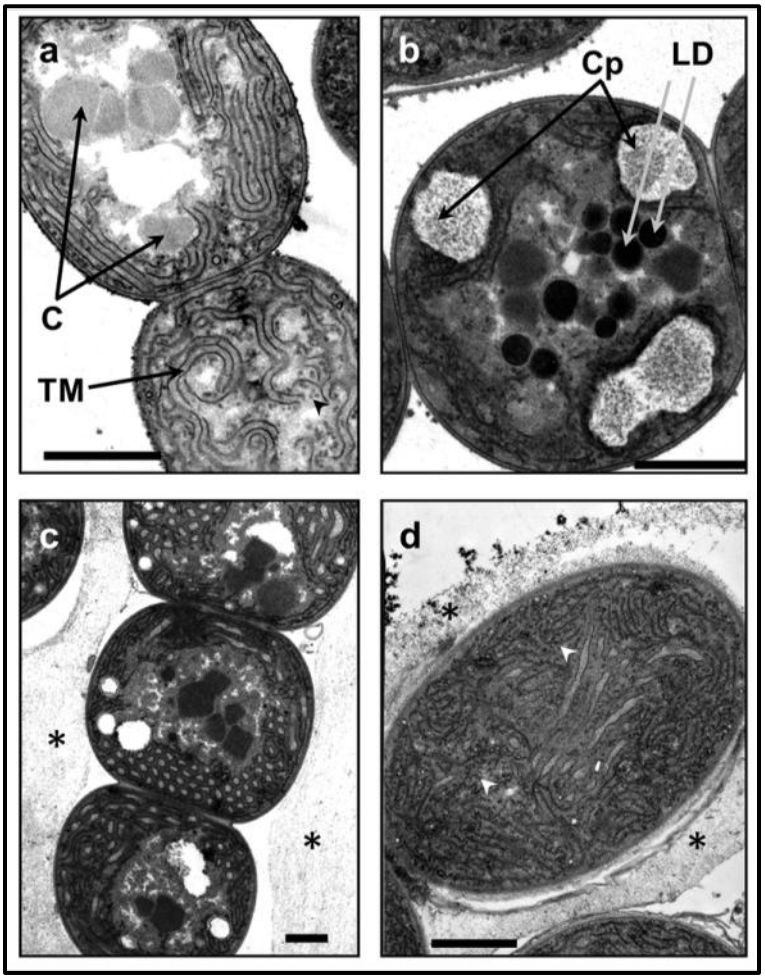

Fig. 12. Ultrastructure of *N. punctiforme* akinetes. Transmission electron micrographs of vegetative cells (a) and akinetes (b–d) in cultures starved of phosphate for 32 (b, c) or 60 days (d). C, Carboxysome; Cp, cyanophycin; LD, lipid droplets; star, exopolysaccharide layer; TM, thylakoid membrane; arrowheads, glycogen granules. Bars, 1 µm

3.1.3 Ultrastructure of the akinete envelope

In order to thoroughly investigate the akinete envelope in both strains, cultures were induced to form akinetes by low light (*A. variabilis*) or phosphate starvation (*N. punctiforme*) during 60 days and their ultrastructure was analyzed. Clearly, most of the mature akinetes in *A. variabilis* were detached from the filaments; but in some cases two or more mature akinetes with their envelope totally developed were still connected (Figs. 9d, 13a, b). The ultrastructure of this connection shows that both akinetes were surrounded by the same merged exopolysaccharide layer and connected by a thick laminated layer (TLL) probably composed of glycolipids (Fig. 13b). In the case of *N. punctiforme*, the mature akinetes were either separated or still connected by a narrow septum. They were embedded in high amounts of extra cellular material, probably exopolysaccharides (Figs. 13d-f). Also, a laminated layer similar to the TLL in *A. variabilis* akinetes (Fig. 11d) was observed in several mature akinetes of *N. punctiforme* (Figs. 13e, f).

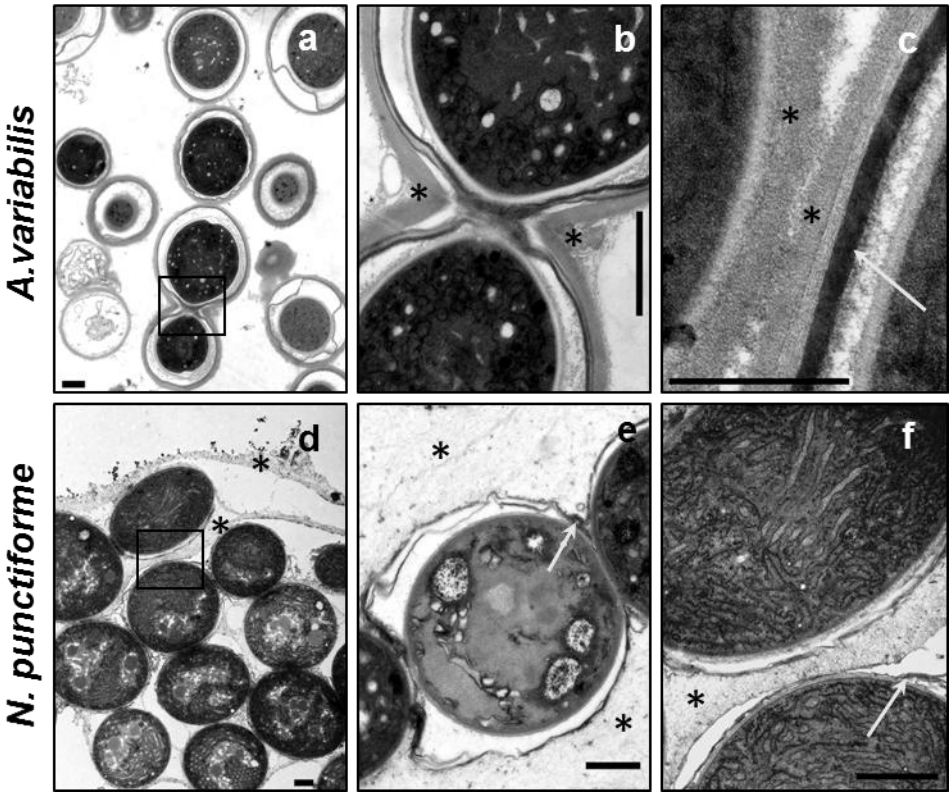

Fig. 13. Ultrastructure of *A. variabilis* (a-c) and *N. punctiforme* akinetes (a–f). akinetes in cultures exposed to (a-c) low light or (d-f) phosphate starvation by 60 days. (a, d) Transmission electron micrographs of group of akinetes, (b, e) akinetes connection and (c–f) high magnification of the akinete envelope. Star, exopolysaccharide layer and arrow, glycolipid layer. (a, b, d, e, f) Bars, 1 µm; (c) bar, 500 nm. Squares show area of magnification in b, f respectively in a, d.

3.1.4 Composition of the akinete envelope

The presence of lipids in the akinete envelope was investigated by BODIPY staining. This dye stains specifically neutral lipids that afterwards can be visualized by fluorescence microscopy (Peramuna & Summers, 2014). Cultures induced to form akinetes by phosphate starvation for two months were stained with BODIPY and observed by fluorescence microscopy. In *A. variabilis*, a defined thicker envelope around the akinetes was stronger stained with BODIPY. In addition, this stain was more intense at the poles of the akinetes (Fig. 14a). By contrast, in *N. punctiforme* the envelope of some akinetes was less stained than the envelope of *A. variabilis* akinetes (Fig. 14b).

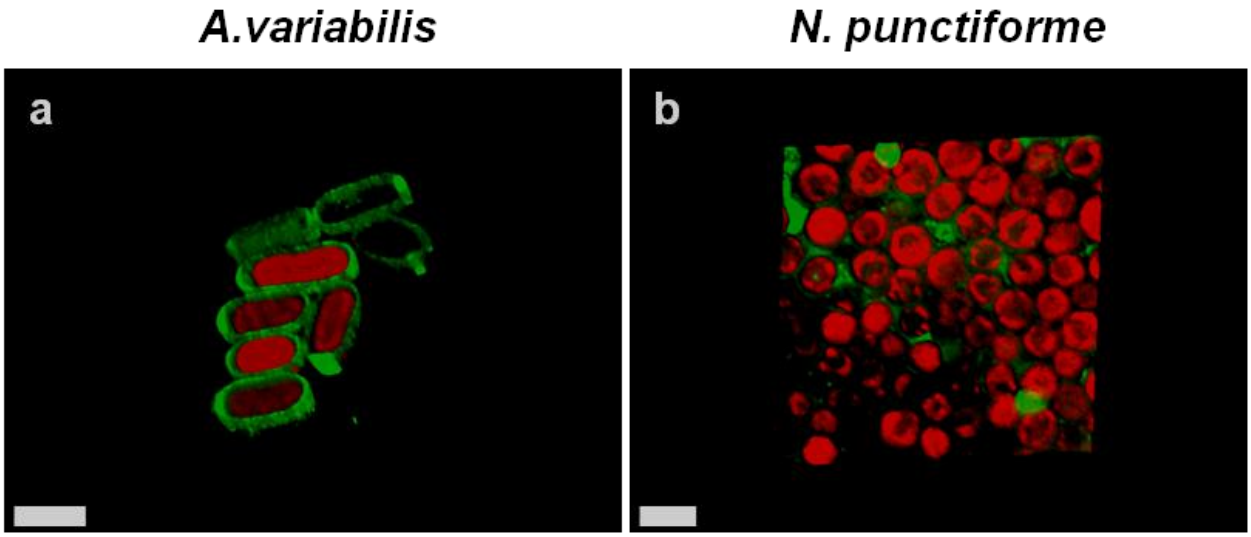

Fig. 14. Staining and visualization of the lipid layer in akinetes of *A. variabilis* (a) or *N. punctiforme* (b). Cultures exposed for two months to phosphate starvation were stained *in vivo* with green fluorescent BODIPY. (a, b) Shown are overlaid BODIPY fluorescence and autofluorescence images. Bars, 5 µm.

In order to investigate the glycolipid composition of the akinetes in both strains, a thin layer chromatography (TLC) was performed with lipid extracts from cultures grown with NO_3^- (only vegetative cells), starved from nitrate by 48 hours (with heterocysts) and exposed to low light (*A. variabilis*) or phosphate starvation (*N. punctiforme*) by two months (with akinetes). In the extracts corresponding to akinetes induced cultures of both strains, a spot was detected in the same region as does a heterocyst-specific glycolipid (Fig.15a). Furthermore, an additional spot was observed in the akinete extract of *A. variabilis* (Fig. 15a).

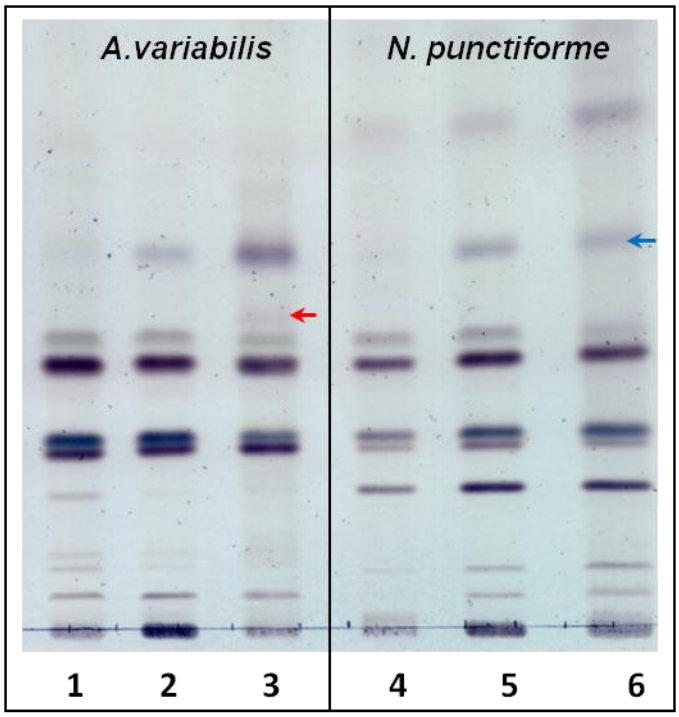

Fig. 15. Thin-layer chromatogram of lipids from different cell types of *A. variabilis* (1-3) and *N. punctiforme* (4-6). (1, 4) Vegetative filaments grown with NO_3^-. (2, 5) Filaments containing heterocysts grown without NO_3^-. (3) Akinetes induced by low light or (6) phosphate starvation for 2 months. Blue arrow, heterocyst-specific glycolipid. Red arrow indicates an unknown lipid.

The TLC bands from akinete extracts of *A. variabilis* corresponding to heterocyst-specific glycolipid (blue arrow) and the unknown band (red arrow) were scratched and analyzed by LC-MS. The presence of three characteristic heterocyst glycolipids HG_{26}-diol, HG_{28}-diol and HG_{26}-keto-ol (Wörmer *et al.*, 2012) were confirmed in the TLC bands of *A. variabilis* akinetes (Fig. 16a, b). Also five prominent di-glycosyl diacylglycerols (2G-DAG), which are compounds found in photosynthetic organisms (Wörmer, *et al.*, 2013), were detected (Fig. 16a). Finally, four compounds tentatively identified as $C_nH_{n-2}N_2O_8$ were detected in akinetes of *A. variabilis* (Fig. 16b).

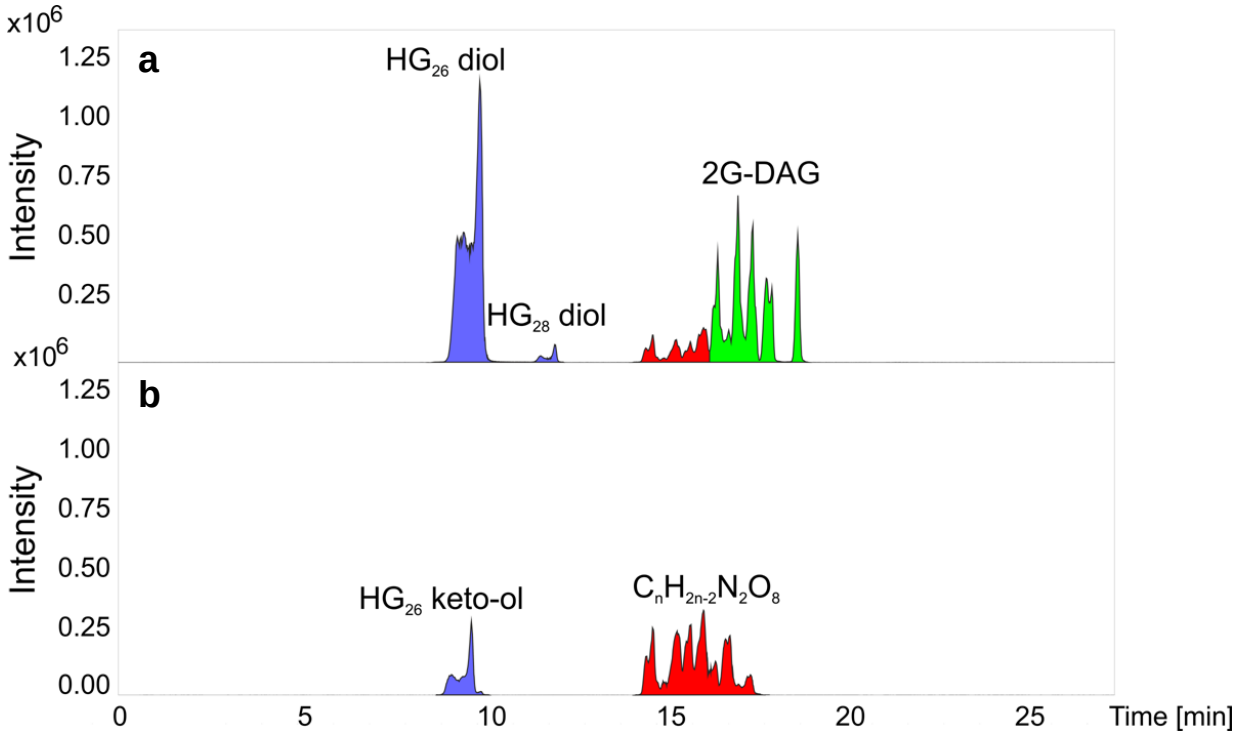

Fig. 16. Chromatogram of putative glycolipids extracted from *A. variabilis*. (a) Sum of the extracted ion chromatograms of two heterocyst glycolipids (HG) and five prominent diglygosyl diacylglycerols (2G-DAG) from heterocyst glycolipid band (indicated by a blue arrow in TLC). (b) Sum of the extracted ion chromatograms of one heterocyst glycolipid (HG) and four of the compounds tentatively identified as $C_nH_{n-2}N_2O_8$ (indicated by a red arrow in TLC).

Furthermore, to verify that the exopolysaccharide layer observed in the electron micrograph from akinetes is similar in composition to the heterocyst envelope (Fig. 14), an Alcian Blue staining was performed in cultures containing mature akinetes or heterocysts. The Alcian blue staining is specific for carbohydrates with acid groups and is frequently used to detect the polysaccharide layer of the heterocysts (Humason 1967; Argueta & Summers 2005). As was expected, a blue staining around the heterocysts and mature akinetes was observed in *A. variabilis* (Fig. 17a, b) and *N. punctiforme* (Fig. 17c, d).

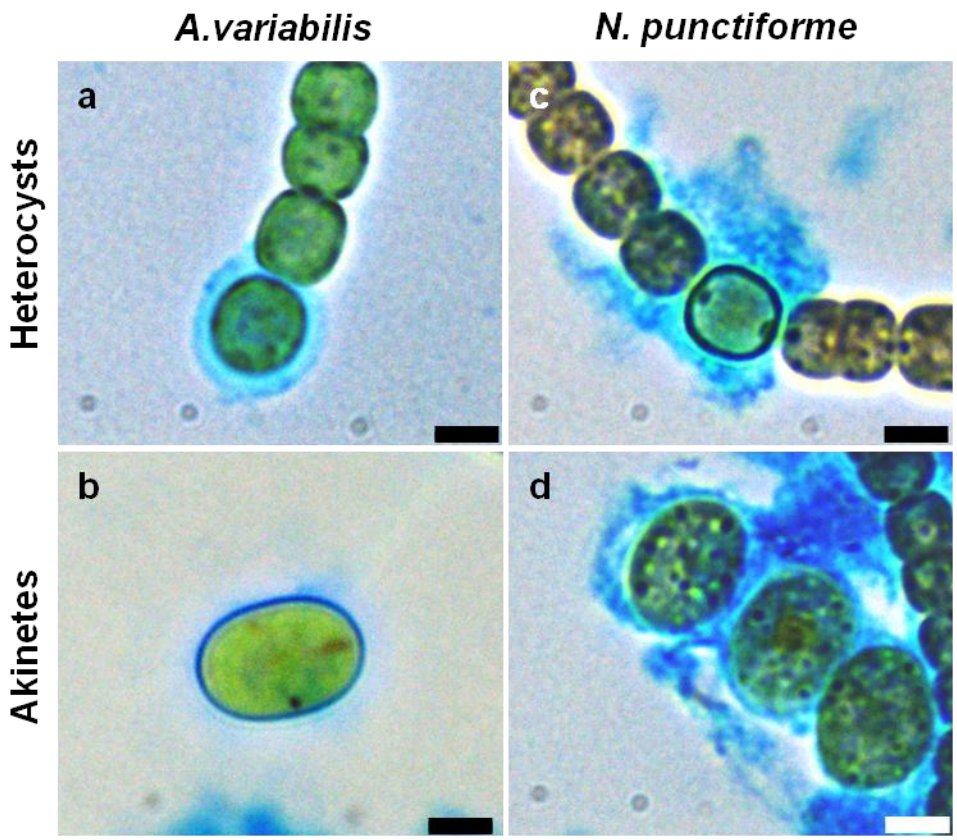

Fig. 17. Staining and visualization of the exopolysaccharide layer from heterocysts and akinetes. Bright-field images of (a, c) heterocysts or (b, d) akinetes stained with Alcian blue. (a, b) *A. variabilis* and (c, d) *N. punctiforme*. Bars, 3 µm.

3.1.5 Intracellular storage compounds of akinetes

To confirm that the large granules observed in immature akinetes of *A. variabilis* and *N. punctiforme* are composed of cyanophycin, two approaches were used: *in vitro* measurement of extracts and *in situ* staining of the granules. Cyanophycin was extracted from cultures exposed to low light or starved of phosphate for 1, 18, 30 and 60 days, and its concentration was determined by Sakaguchi reaction. Cyanophycin was not detectable in *A. variabilis* cultures starved of phosphate for one day, but the content was much higher after 18 and 30 days of phosphate starvation and was much lower after 60 days. Cyanophycin also appeared in cultures exposed to low light but in lower amounts (Fig. 18a). Cyanophycin in *N. punctiforme* cultures starved of phosphate for one day was also not detectable. The content was much higher after 18 days of phosphate starvation and decreased after 30 and 60 days of starvation. As in *A. variabilis,* lower amounts of cyanophycin was detectable in cultures exposed to low light (Fig. 18d). The granules in akinetes induced by phosphate starvation were much larger than those

induced by low light in both cyanobacterial species (Figs. 9, 10). To correlate the cyanophycin determined chemically with the large granules observed in micrographs, cyanophycin was stained *in situ* using the Sakaguchi reaction (Watzer *et al.,* 2015). The results of the staining were in accordance with the measurements in cell extracts (Fig. 18a, d). The numerous large granules were stained dark red in akinetes induced by phosphate limitation (*A. variabilis*: 6.0 ± 1.5 cyanophycin granules/akinete, n = 10; *N. punctiforme*: 6.0 ± 3.0 cyanophycin granules/akinete, n = 10) (Fig. 18c, f). As expected, fewer granules were observed in cultures exposed to low light in both species and were weaker stained (*A. variabilis*: 3.0 ± 2.1 cyanophycin granules/akinete, n = 10; *N. punctiforme*: 2.0 ± 1.6 cyanophycin granules/akinete, n = 0) (Fig.18, e).

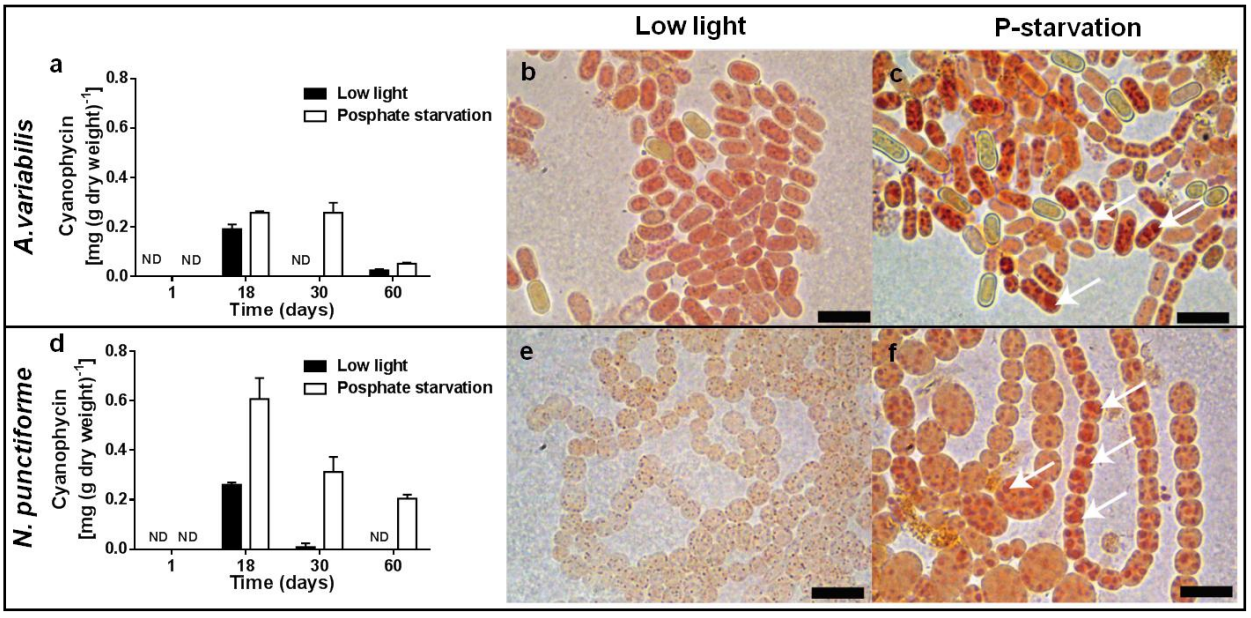

Fig. 18. Cyanophycin accumulation during akinete development. Cellular cyanophycin concentration of cultures of (a) *A. variabilis* and (d) *N. punctiforme* exposed to low light or starved of phosphate at 1, 18, 30 or 60 days. The data are the means of at least three independent samples ± SD. Bright-field images of Sakaguchi-stained akinetes of (b, c) *A. variabilis* and (e, f) *N. punctiforme*. Akinete formation was induced by (b, e) low light or (c, f) phosphate starvation for 18 days. Arrows, examples of individual stained granules. ND, not detectable Scale bars, 10 µm.

Many smaller granules were observed in akinetes at different stages of differentiation in transmission electron micrographs. To correlate these granules with the carbon storage polymer glycogen, whole cellular glycogen was extracted from the cultures after 0, 18 and 30 days of phosphate starvation and enzymatically determined using α-amyloglucosidase (Curatti *et al*.,

2008). In *A. variabilis* cultures starved of phosphate for 18 days, the amount of glycogen per cell dry weight increased by 150% compared to unstarved cultures and the level after 30 days of phosphate starvation was almost as low as in unstarved cultures (Fig. 19). By contrast, in akinetes of *N. punctiforme* cultures, the amount of glycogen per cell dry weight was nearly the same than in unstarved cultures and those starved of phosphate for 18 or 30 days (Fig. 19). This result fits to the appearance of small granules detected in electron micrographs.

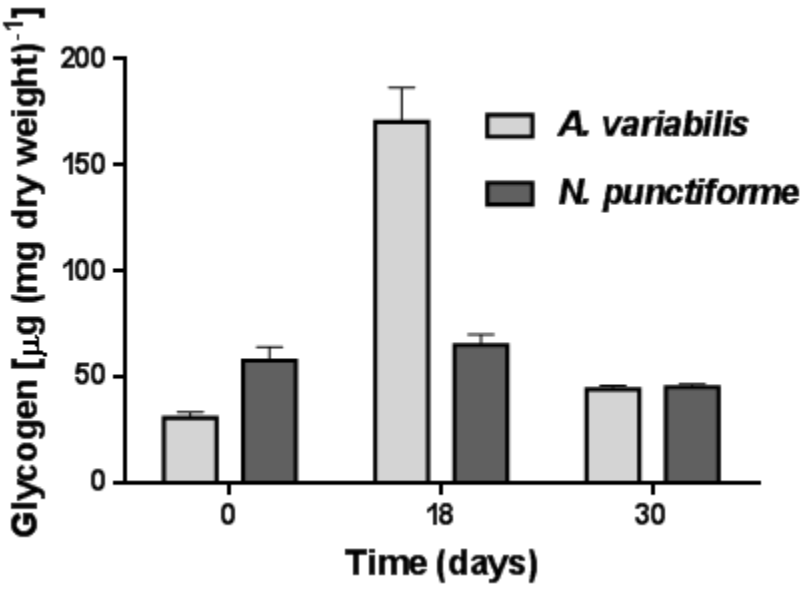

Fig. 19. Glycogen storage during akinete development. The glycogen concentration in culture extracts of *A. variabilis* and *N. punctiforme* starved of phosphate to induce akinete formation was measured using α-amyloglucosidase at the times indicated. The data are the means of at least three independent samples ± SD.

The presence of lipoid structures in akinetes of *N. punctiforme* was investigated by fluorescent BODIPY staining of vegetative cells and akinetes in cultures starved of phosphate for 30 days. Green fluorescent spots (1.0 ± 1.2 lipid droplets/cell; n = 10) corresponding to lipid droplets were identified in vegetative cells of *N. punctiforme* (Fig. 20a). Such spherical droplets accumulated in immature akinetes (8.0 ± 5.0 lipid droplets/cell; n = 10) and were rarely present in mature akinetes (0.0 ± 1.0; n = 10; Fig. 20b). BODIPY staining did not reveal any lipid droplets in *A. variabilis* vegetative cells or akinetes (Figs. 14a, 28a).

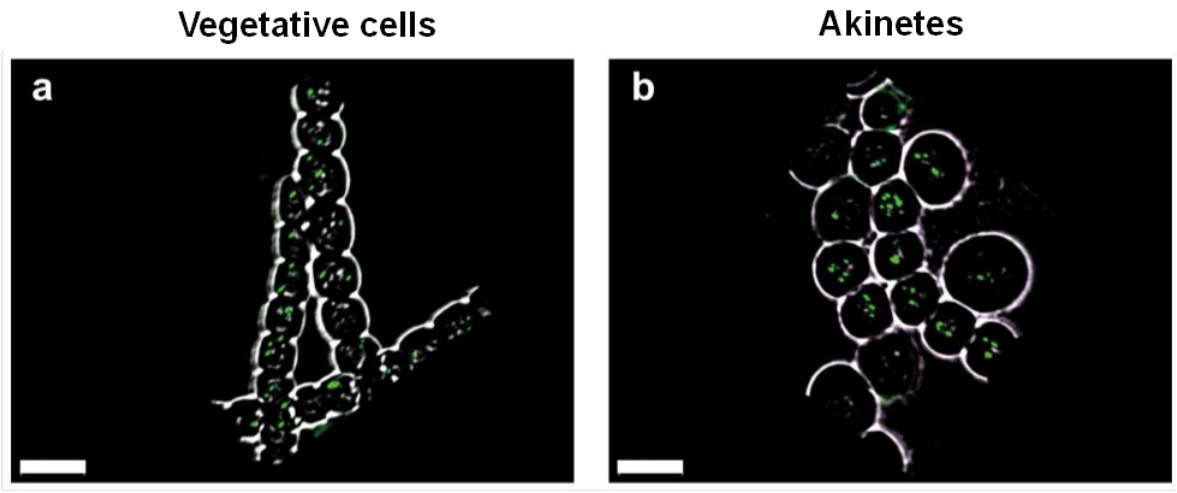

Fig. 20. Imaging of lipid droplets in *N. punctiforme*. Intracellular lipoid structures were stained *in situ* with green fluorescent BODIPY. (a) Vegetative cells and (b) immature and mature akinetes in cultures starved of phosphate for 30 days. Shown are overlaid BODIPY fluorescence and bright-field images. Bars, 5 µm.

To investigate the presence of polyphosphate bodies during akinete differentiation, cultures of *A. variabilis* and *N. punctiforme* were exposed to low light for 0, 18 and 60 days and then cells were stained with Neisser stain and observed by bright-field microscopy (Pelczar, 1957). Dark purple spots corresponding to polyphosphate bodies were detected in vegetative cells of both species (Fig. 21a, d). By contrast, polyphosphate bodies were rarely observed in immature akinetes (Fig. 21b, e) and were absent in mature akinetes (Fig. 21c, f).

In order to analyse the organization of nucleic acids in *A. variabilis* and *N. punctiforme* akinetes, vegetative cells and akinetes in cultures starved of phosphate for 60 days were stained with the fluorescent DAPI stain, which is specific for nucleic acids. In vegetative cells of *A. variabilis* one or two blue spots corresponding to nucleic acids were detected, but only one blue spot that became larger in the case of dividing cells was observed in *N. punctiforme* (Fig. 22a, c). In contrast, many or larger blue spots were observed in akinetes of *A. variabilis* and several blue spots in akinetes of *N. punctiforme* (Fig, 22b, d). Eventually, a blue stain around some *A. variabilis* akinetes was observed because the thicker envelope prevented the entrance of the DAPI stain.

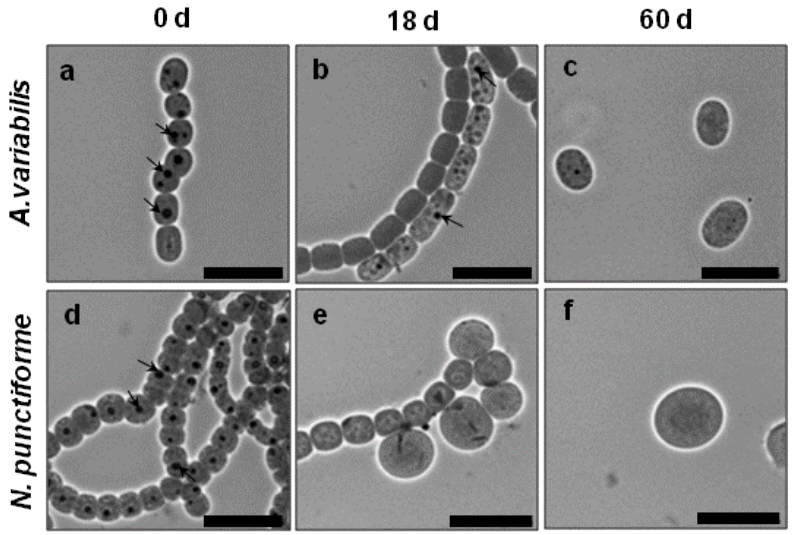

Fig. 21. Occurrence of polyphosphate bodies in vegetative cells and akinetes of *A. variabilis* (a–c) and *N. punctiforme* (d–f). (a, d) Vegetative cells in cultures before induction, (b, e) vegetative cells and akinetes in cultures exposed to low light for 18 days, and (c, f) akinetes in cultures exposed to low light for 60 days. Polyphosphate bodies (arrows) were stained with Neisser stain. Bars, 10 µm.

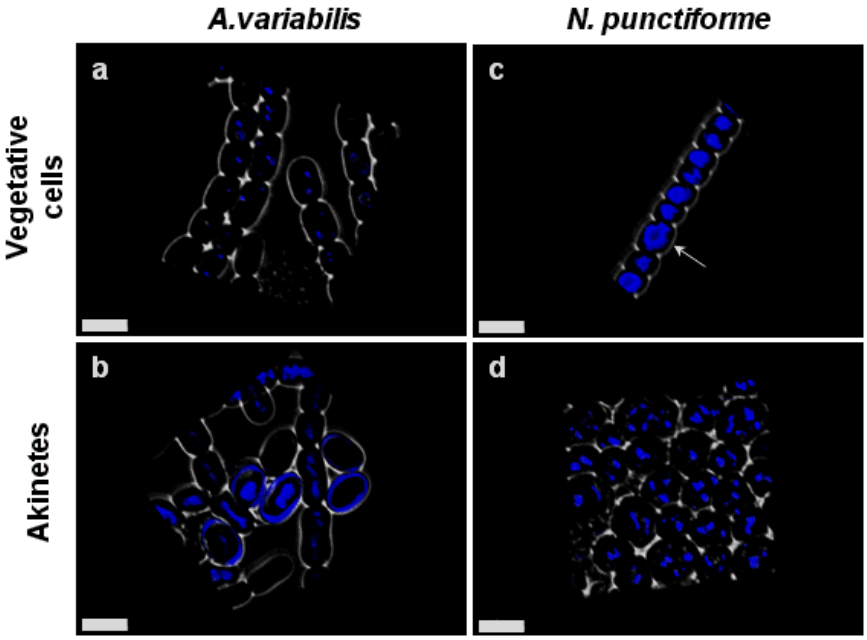

Fig. 22. Staining and visualization of DNA in different cell types of *A. variabilis* (a, b) and *N. punctiforme* (c, d). DNA was stained *in vivo* with the fluorescent DAPI stain. (a, c) vegetative cells and (b, d) mature akinetes in cultures starved of phosphate for 60 days. Shown are overlaid bright field and DAPI 3D images. Arrow, dividing cell. Bars, 5 µm.

3.1.6 Changes in photosynthetic and respiratory activities during akinete development

Metabolic activities in cultures of both species induced to differentiate akinetes by phosphate starvation for 18, 30 or 60 days and in unstarved stationary phase cultures (day 0) were measured. The photosynthetic oxygen evolution of cultures was estimated *in vivo* using a Clark-type oxygen electrode. In cultures of both *A. variabilis* (Fig. 23a) and *N. punctiforme* (Fig. 23d), after 18 days of phosphate starvation the rate of O_2 evolution was lower than that of stationary phase cultures. After 30 days it decreased to approximately 30% of that of unstarved cultures (Fig. 23a, d).

To investigate solely photosystem II (PSII) activity and not the entire electron transport chain, oxygen evolution was measured at high light intensity in the presence of an artificial electron acceptor system (Hill reaction). PSII-dependent O_2 evolution was approximately 50% of that of vegetative cells in cultures of *A. variabilis* starved of phosphate for 18, 30 or 60 days, (Fig. 23b). The *N. punctiforme* cultures starved of phosphate maintained almost the same level of PSII activity as vegetative cells in the stationary phase (Fig. 23e).

The respiratory activity was determined by measuring O_2 consumption in the dark. The respiration rate was lower after 18 days of phosphate starvation than in unstarved cultures of *A. variabilis* and was even lower after 30 and 60 days of starvation (Fig. 23c). By contrast, in cultures of *N. punctiforme* respiration after 18, 30, and 60 days of phosphate starvation, was much lower than in unstarved cultures (Fig. 23f).

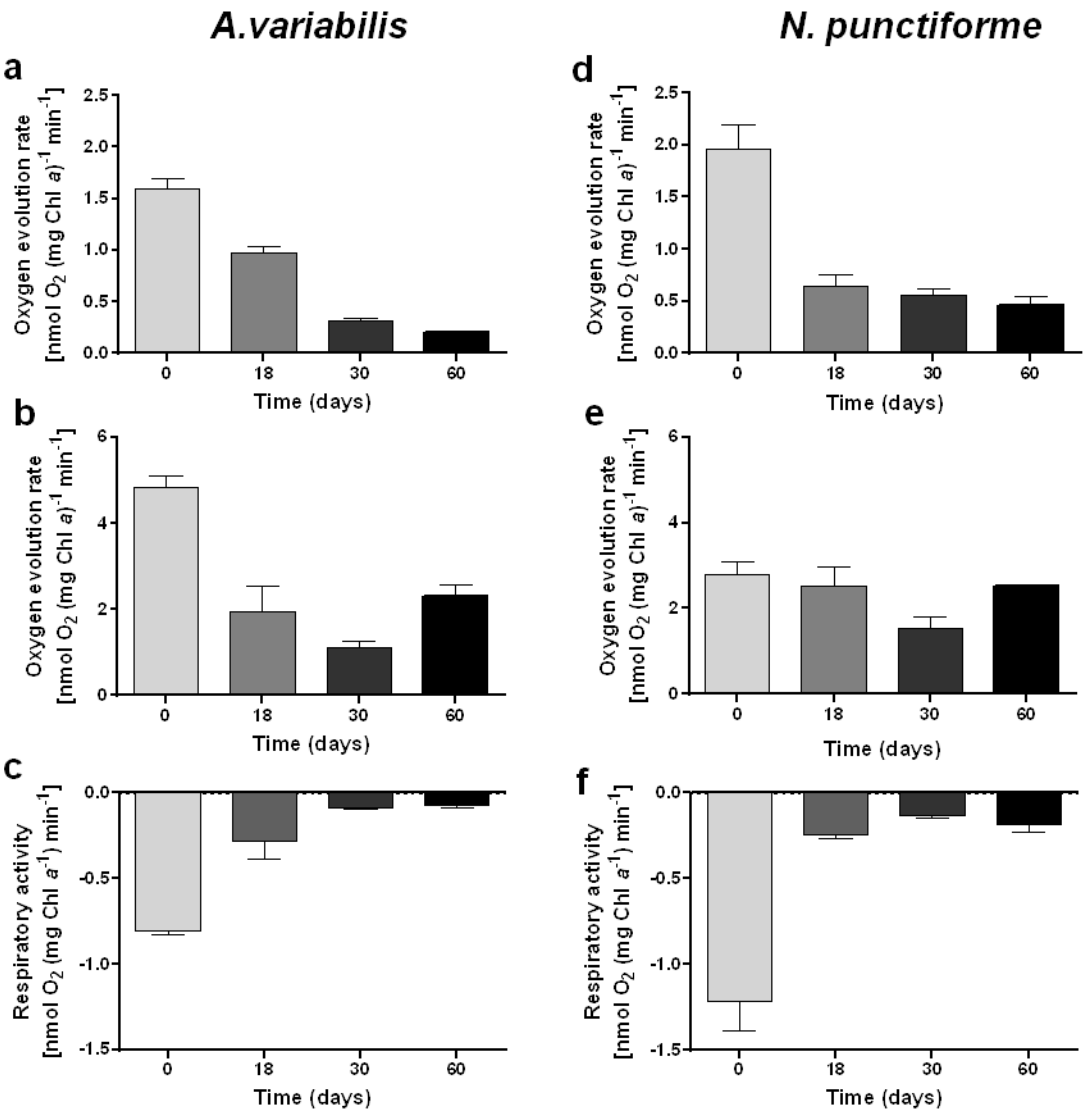

Fig. 23. Metabolic activities in *A. variabilis* (a–c) and *N. punctiforme* (d–f) during akinete differentiation. (a, d) Photosynthetic oxygen evolution, (b, e) Hill reaction, and (c, f) respiration of vegetative cells in stationary-phase cultures (0 days) and akinetes in stationary-phase cultures starved of phosphate for 18, 30 and 60 days measured in vivo using a Clark-type oxygen electrode. In the Hill reaction, oxygen evolution was measured at high light intensity (1,500-2,000 µmol photons m^{-2} s^{-1}) as described in Methods. Respiratory activity was measured as oxygen consumption in the dark. Chl *a*, Chlorophyll *a*. The data are the means of at least three independent samples ± SD.

3. 2 GERMINATION

3.2.1 Morphological changes during akinete germination

The germination process in *A. variabilis* and *N. punctiforme* akinetes was followed by light and electron microscopy. Germination was induced in cultures containing akinetes (26 days in low light or 33 days without phosphate) by exposure to normal light (*A. variabilis*) or by transferring the akinetes to fresh media supplemented with phosphate (*N. punctiforme*).

In the beginning of germination in *A. variabilis* (3-6 h) the cells started to divide inside the akinete envelope. Successive cell divisions resulted in a release from the surrounding envelope and the emergence of a short filament from a pore at one end (Fig. 24). In some cases, filaments still attached to the envelope were observed (6 h). Frequently an irregular plane of cell division was detected. Also, short filaments with a terminal heterocyst were observed between 9 and 48 h. Long filaments were detected after 48 h. The process of akinete germination was quite asynchronous, since after 9 h of induction, akinetes were still present and cell division inside the akinete envelope was observed up to 48 h (Fig. 24).

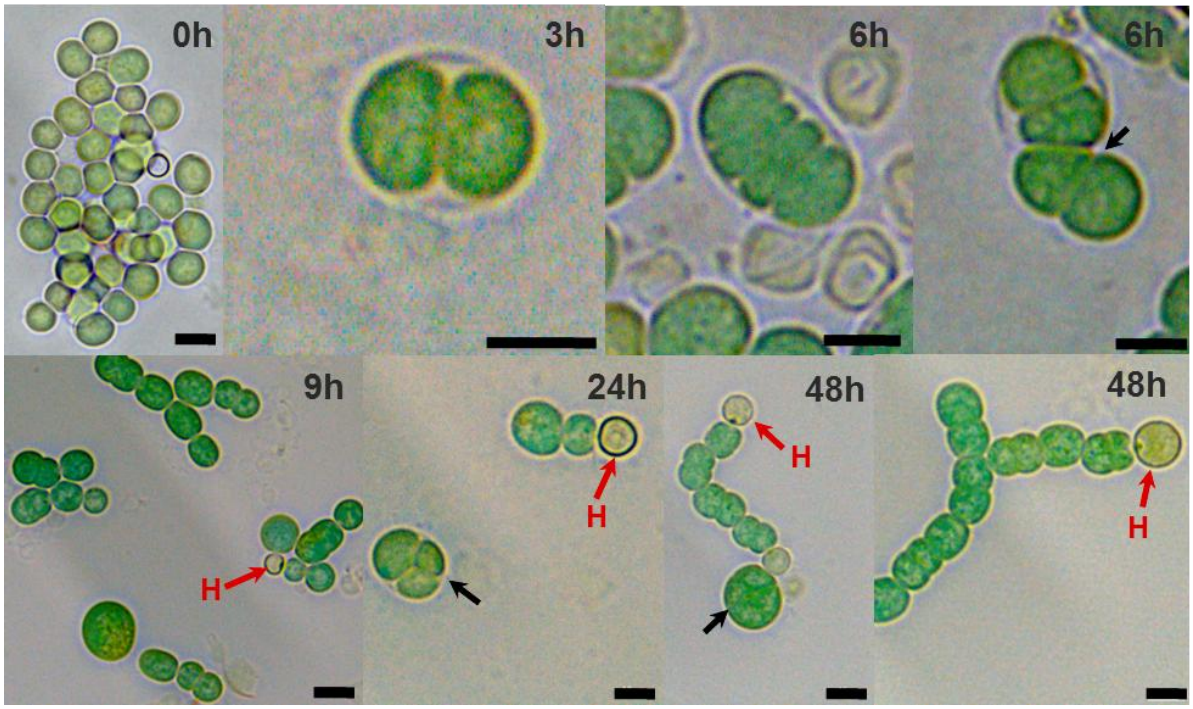

Fig. 24. Progress of akinete germination in *A. variabilis*. Germination of mature akinetes was induced by returning cultures to normal light conditions. Mature akinetes (0 h); cell division inside the akinete envelope (3-24 h), small filament emerging (6 h), small filament with terminal heterocyst (9-48 h). H, heterocyst. Black arrow, irregular plane of division. Bars, 10 µm.

The ultrastructure of germinating filaments of *A. variabilis* in different stages was also investigated by TEM. Cells characterized by undeveloped thylakoid membranes, initial carboxysomes, presence of glycogen and cyanophycin granules were observed in the beginning of the process (Figs. 25b-d). In figure 17c a fully developed heterocyst attached to a vegetative cell were still surrounded by the residual exopolysaccharide layer from the akinete envelope. After 48 h, many cells showed the typical vegetative cell ultrastructure with fully developed thylakoid membranes, carboxysomes and absence of reserve granules (Fig. 25e, f). The original multilayered akinete envelope kept intact and covered the growing filament until rupture and emergence of the short filament (Fig. 25f; and see also Fig. 24).

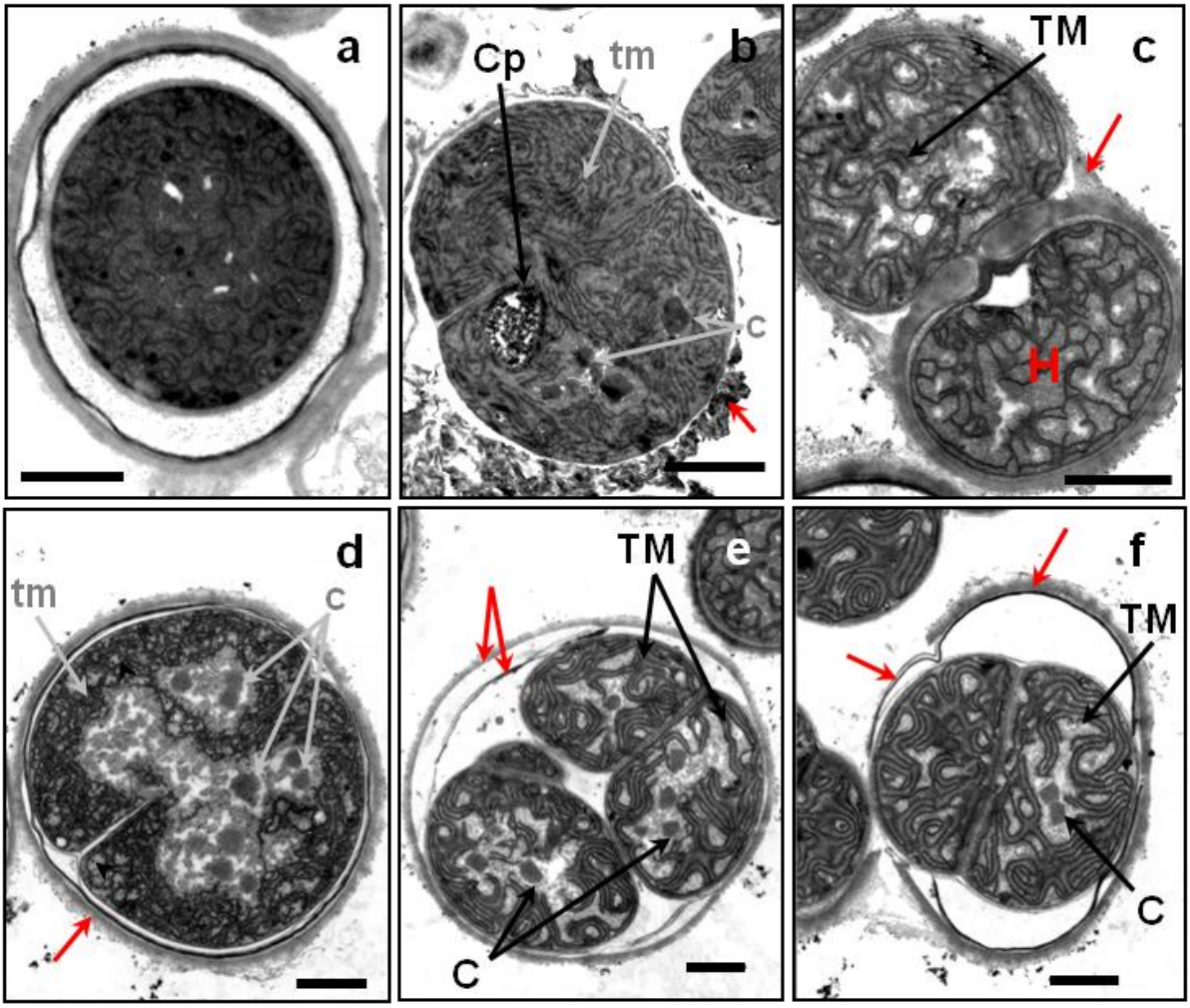

Fig. 25. Morphological phases of akinete germination in *A. variabilis*. (a) Transmission electron micrographs of akinetes at 3 (b, c) 6 and (d-f) 48 hours after akinete germination induced by light. Cp, cyanophycin; C, carboxysome; c, initial carboxysomes; TM, thylakoid membranes; tm, undeveloped thylakoid membranes; arrow head, glycogen; H, heterocyst; red arrow, akinete envelope. Bars, 1 µm.

Germination in *N. punctiforme* was induced by transferring akinetes to fresh medium and samples at 0, 3, 6, 9, 24 and 48 h were analyzed by light and electron microscopy. The first cell division was observed after 3h of germination. Short filaments were observed between 3-48 h and finally, long filaments were detected at 48 h. However, after 24 h still mature akinetes were observed showing that germination in *N. punctiforme* is also a highly asynchronous process (Fig. 26).

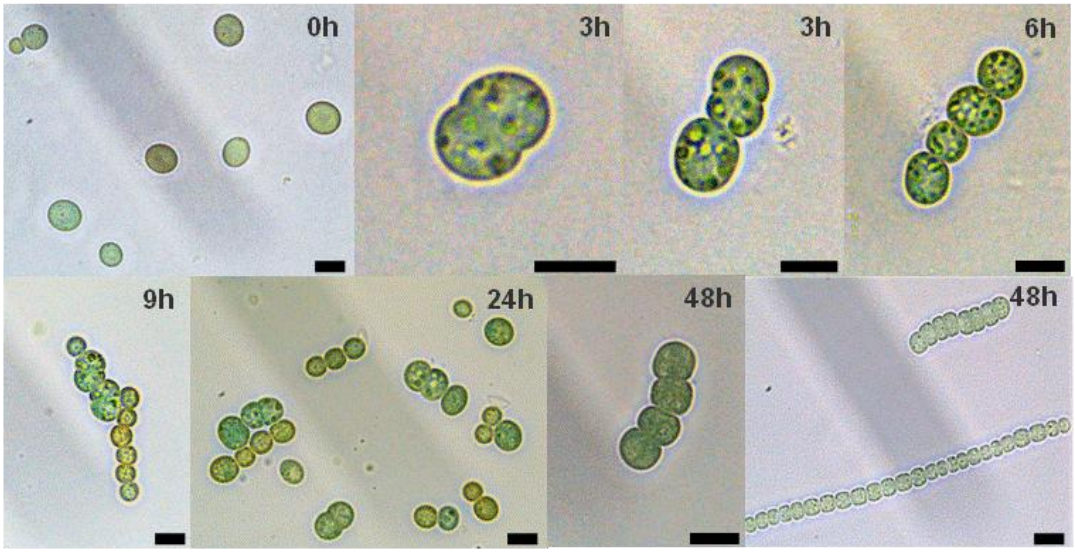

Fig. 26. Progress of akinete germination in *N. punctiforme*. Germination of akinetes was induced by transferring the akinetes to fresh media with phosphate. Free akinetes (0 h), cell division of akinetes (3-24 h), long filaments (48 h). Bars, 10 µm.

Furthermore, the germination process in *N. punctiforme* was analysed by TEM (Fig. 27). Cell division occurred inside the akinete envelope (Fig. 27c-e). Several germinating akinetes were embedded in an extra cellular matrix (Fig. 27c). Some intracellular glycogen granules were observed next to the underdeveloped thylakoid membranes (Fig. 27b). In addition, several cyanophycin granules were detected in the beginning of the germination process, which later disappeared in the small filament formed (compare Figs. 27c-e with Fig. 27f). The regeneration of the thylakoid membranes and carboxysomes with typical shape were observed during cell division and in the end of the process (Fig. 27d-f). Instead of envelope rupture, as observed for *A. variabilis*, the extra cellular matrix seems to be dissolved during the germination process in *Nostoc*. Occasionally, empty envelopes were also seen and not completely dissolved during

germination (Fig. 27c). In the end of the germination process short filaments made of vegetative cells with the typical structures were formed (Fig. 27f).

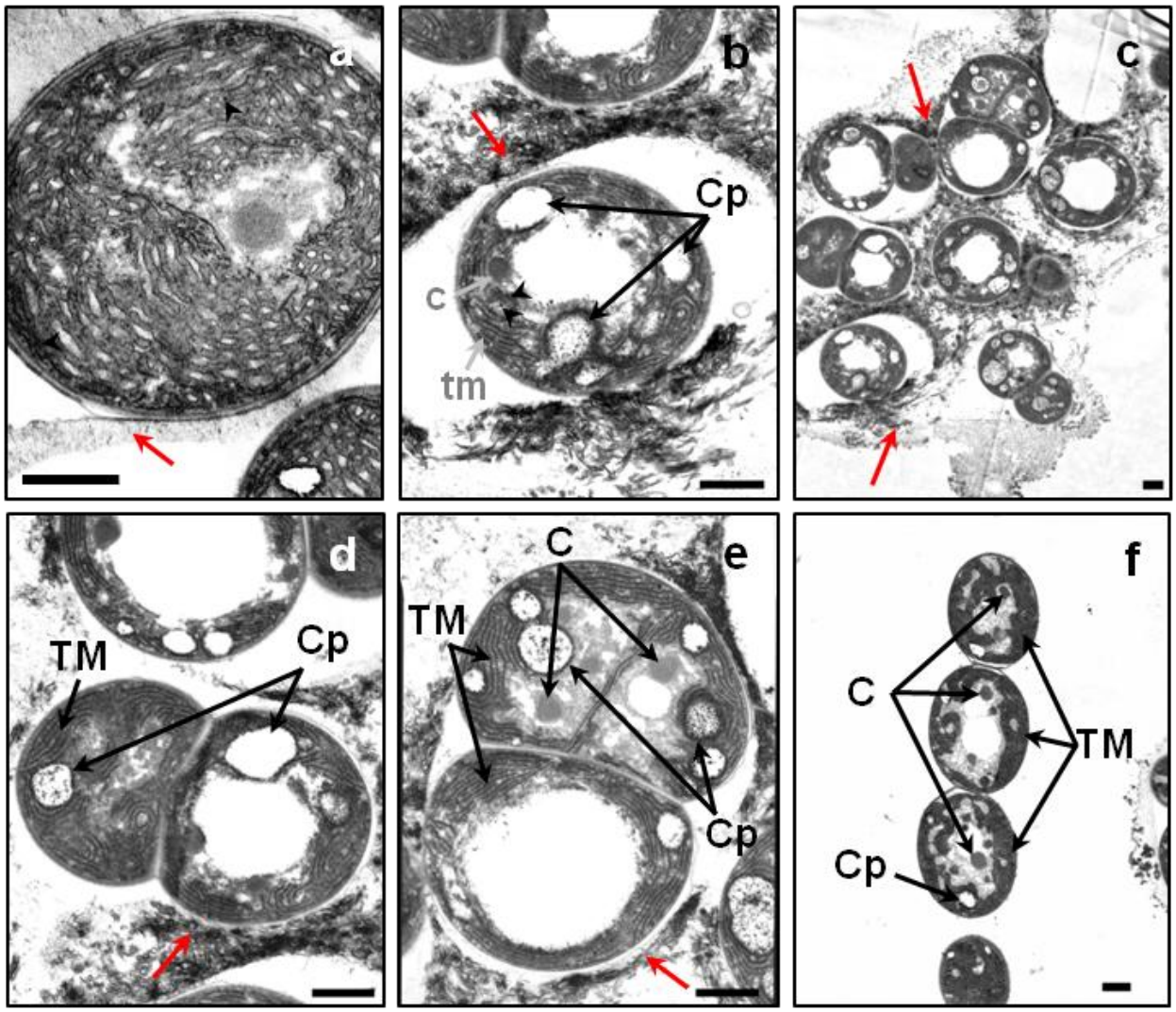

Fig. 27. Morphological phases of akinete germination in *N. punctiforme*. (a) Transmission electron micrographs of akinetes at 0 and (b-f) 48 hours of akinete germination induced by transferring the akinetes to fresh media with phosphate. Cp, cyanophycin; C, carboxysome; c, initial carboxysomes; TM, thylakoid membranes; tm, undeveloped thylakoid membranes; arrow head, glycogen; red arrow, akinete envelope. Bars, 1 µm.

3.2.2 The fate of the akinete envelope during germination

The fate of the akinete envelope during germination was investigated by BODIPY staining of cultures induced to form akinetes for 16 months by low light (*A. variabilis*) or phosphate starvation (*N. punctiforme*) followed by germination induction by washing and transferring to

fresh medium. As shown above in *A. variabilis,* a defined thicker envelope around the akinetes was stronger stained with BODIPY (Fig. 28a, also Fig. 21a). During germination, the cell division took place inside the lipid envelope, which stayed attached to the newly formed short filament (Fig. 28b-d). By contrast in *N. punctiforme* akinetes, a week stain of the envelope was detected (Fig. 28e, g). Occasionally, a weekly stained envelope around the germinating akinetes was observed (Fig. 28g).

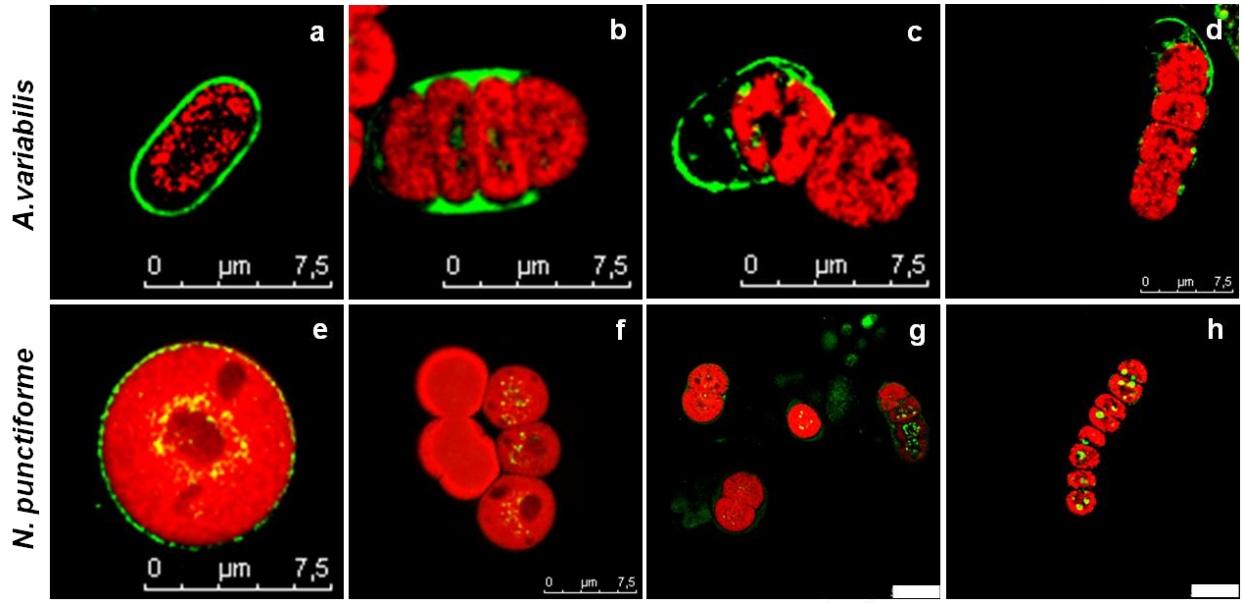

Fig. 28. Staining and visualization of akinete envelope during germination in *A. variabilis* (a-d) and *N. punctiforme* (e-h). Glycolipid layer of akinete envelope was stained *in vivo* with green fluorescent BODIPY. (a, e) akinetes at 0 h of germination and (b-d, f-h) cell division during asynchronous germination. Shown are overlaid BODIPY fluorescence and autofluorescence images.

3.2.3 The fate of the intracellular storage compounds during germination

The intracellular storage compounds, as glycogen and cyanophycin, were analysed during akinete germination in both strains by TEM. As described before, glycogen and cyanophycin granules were consumed during germination process (Figs. 25, 27).

In addition, smaller lipid droplets were detected by BODIPY staining in some germinating akinetes. Finally, bigger lipid droplets were detected in each vegetative cell of the short filament formed in *N. punctiforme* in the end of the germination (Figs. 28f-h).

In order to investigate the occurrence of polyphosphate bodies during germination, cultures of *A. variabilis* and *N. punctiforme* induced to form akinetes by phosphate starvation during 16 months were washed and transferred to the fresh media with phosphate and samples at

different time points of germination were stained with Neisser stain (Fig. 29). Polyphosphate bodies were not detected in mature akinetes of both cultures as shown above (Figs. 29a, e; see also Fig. 21c, f). Occasionally, dark spots corresponding to polyphosphate bodies were detected at 6 and 30 h of germination (Figs. 29b, c, f, g). At the end of the germination process, black spots were observed in all vegetative cells of the newly formed short filaments (Figs. 29d, h).

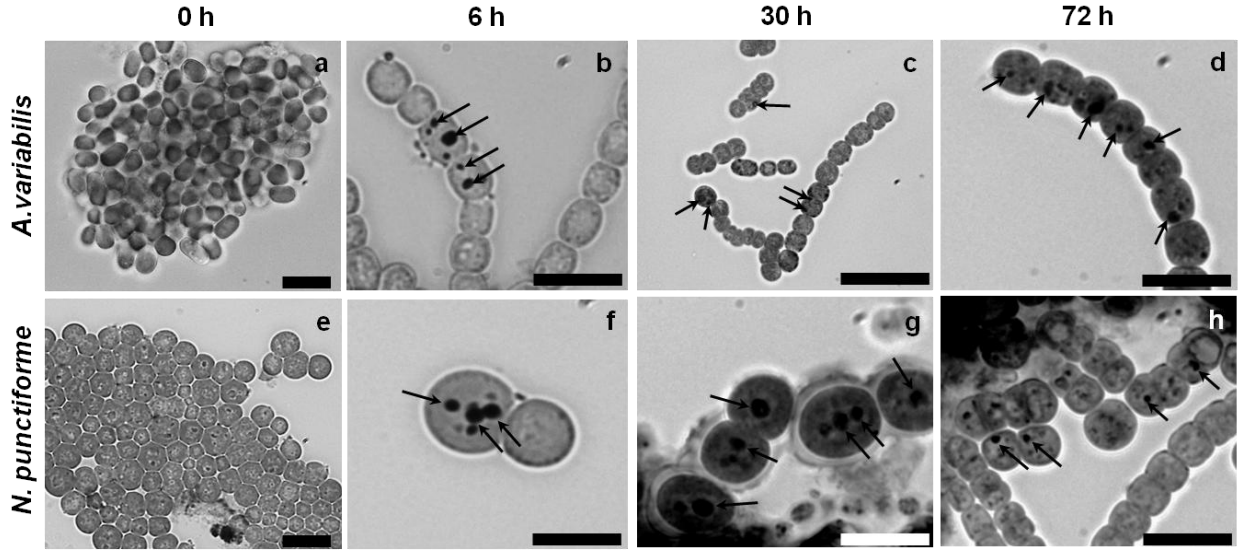

Fig. 29. Occurrence of polyphosphate bodies during germination in *A. variabilis* (a–d) and *N. punctiforme* (e–h). Cultures induced to form akinetes by phosphate starvation during 16 months were washed and transferred to fresh media with phosphate. (a, e) Samples were taken and stained with Neisser stain at 0, (b, f) 6, (c, g) 30 and (d, h) 72 hours of germination. Polyphosphate bodies (arrows) were dark stained. Bars, 10 µm.

3.2.4 Changes in photosynthetic and respiratory activity during germination

Metabolic activities were measured in cultures of both strains exposed to phosphate starvation by 3 months (0 hours) and induced to germinate by washing and transferring the akinetes to fresh media and normal growth conditions. Samples were taken and measured at 0, 6, 12, 30, 24, 48 and 72 h of germination. The photosynthetic oxygen evolution and respiration of germinating cultures was measured *in vivo* using a Clark-type oxygen electrode.

Before the induction in akinete cultures of both *A. variabilis* (Fig. 30a) and *N. punctiforme* (Fig. 30c), O_2 evolution was very low and similar to the results described above for cultures induced to form akinete by 60 days (compare with Fig. 23a, d). The O_2 evolution rate remained the same value until 24 h of germination in both strains (Fig. 30a, c) and after that increased three times more in *A. variabilis* cultures (Fig. 30a) and approximately five times in *N. punctiforme* cultures

(Fig. 30c). In both strains at 72 h of germination, the O_2 evolution rates were similar to the vegetative cells cultures as shown above (Fig. 23a, d).

The respiratory activity was determined by measuring O_2 consumption in the darkness. In cultures of both strains, respiration was very low in akinete cultures before of induction and similar to the respiration at 60 days of akinete induction cultures described above (compare Fig. 30b, c with Fig. 23c, f). Respiration rate increased about the double during the first 12 h, remained a bit lower between 12 and 48 h, and finally increased three times at 72 h of germination in *A. variabilis* culture (Fig. 30b). By contrast, a slight increase in respiration was observed between 0 to 48 h of germination in *N. punctiforme* cultures. Finally, respiration rate reached to the double at 72 h of germination (Fig. 30d).

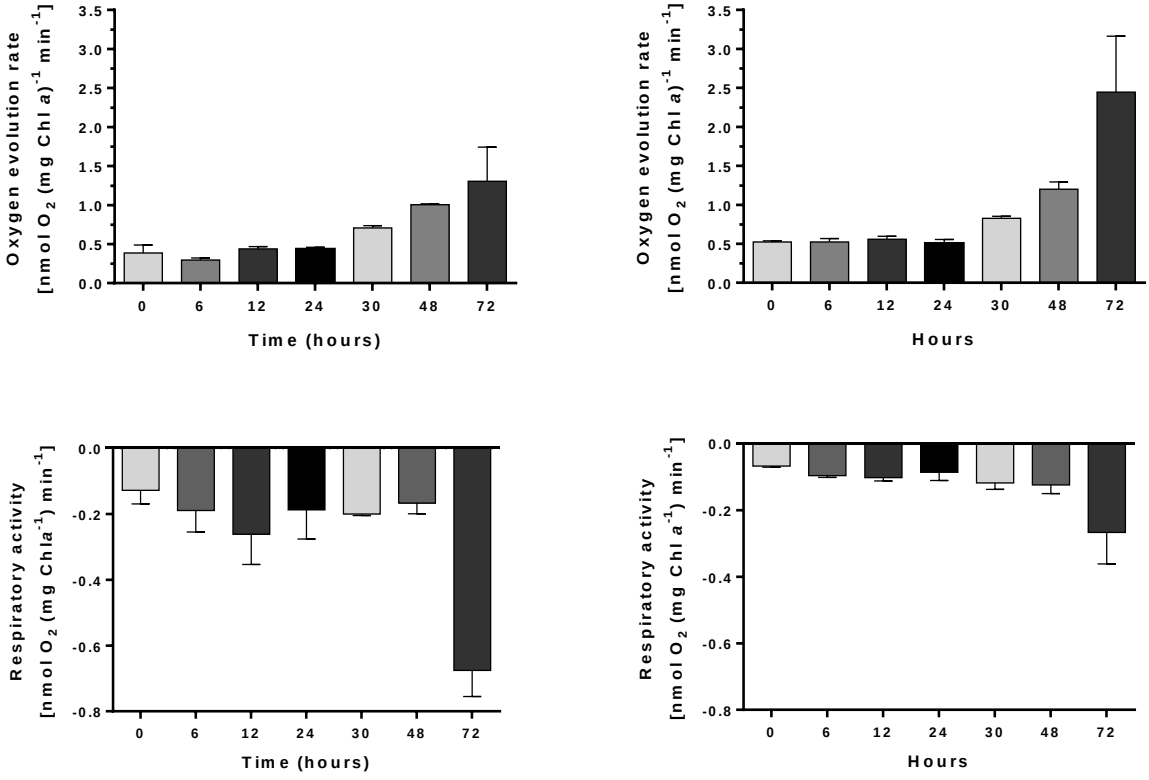

Fig. 30. Metabolic activities in *A. variabilis* (a–b) and *N. punctiforme* (c–d) during germination. (a, c) Photosynthetic oxygen evolution and (b, c) respiration of cultures with akinetes (0 hours) induced to germinate by washing and transfer cells to fresh medium with phosphate were measured *in vivo* using a Clark-type oxygen electrode during 72 hours. Respiratory activity was measured as oxygen consumption in the dark. Chl *a*, Chlorophyll *a*. The data are the means of at least three independent samples ± SD.

3.3 CHARACTERIZATION OF CELL WALL MUTANTS IN *A. variabilis*

3.3.1 Functional characterization of the putative germination protein Ava_2312

3.3.1.1 *In silico* analysis of the Ava_2312 protein

A global gene expression analysis in cultures of a *N. punctiforme zwf*⁻ mutant strain, which is able to differentiate akinetes in a few days, revealed the up-regulation of 255 genes after akinete induction, 41 % of which encoded known proteins (Campbell *et al*., 2007). In order to investigate possible candidates involved in akinete differentiation or germination, the microarray data were analyzed in detail. The gene *Npun_F0437* that encodes a putative spore germination protein was found up-regulated only during akinete differentiation. The homologue gene in *A. variabilis* is annotated as *Ava_2312*.

In silico analysis of the *Ava_2312* gene, predicted a product of 204 amino acids with a putative conserved germane domain (Fig. 31a). A transmembrane helix (TM) analysis revealed a possible N-terminal signal sequence (1-11 aa) and a TM helix (12-34 aa) from the Ava_2312 amino acid sequence. Besides, the bigger part of this protein is localized outside of the cell, in the periplasm (34-204 aa) (Fig. 31b). Using the CDART database from NCBI, conserved domain analysis and functional site prediction of the Ava_2312 protein were identified. It confirmed the presence of one conserved domain (germane domain) that is found in a number of different bacterial species both alone and in association with other domains involved in peptidoglycan processing such as Amidase_3 pfam01520, NTF2-like and Gmad2. Also, gerM domain was founded associated to Sigma 70 domain of *E. coli* related to sigma-factors, and to SH2 domain that is involved in signal transduction (Fig. 32).

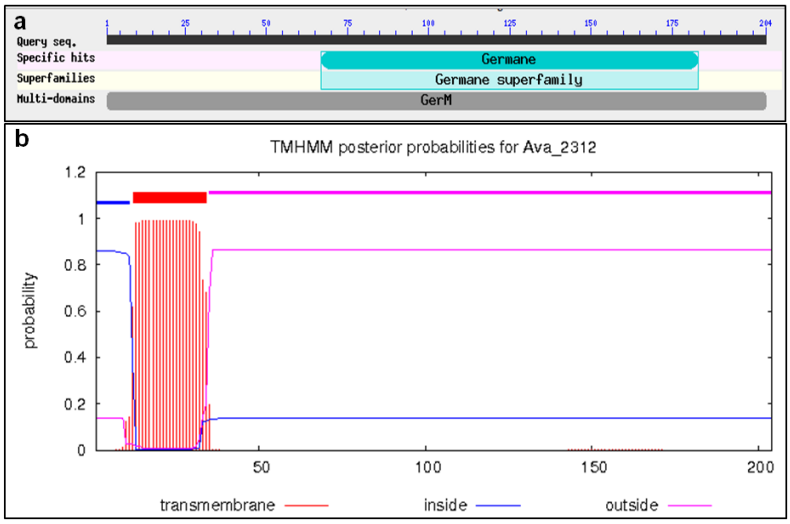

Fig. 31. Conserved domains and transmembrane prediction of the Ava_2312 protein. (a) The putative conserved domains were detected by BLAST analysis. (b) The transmembrane helix prediction was analyzed using TMHMM 2.0 program.

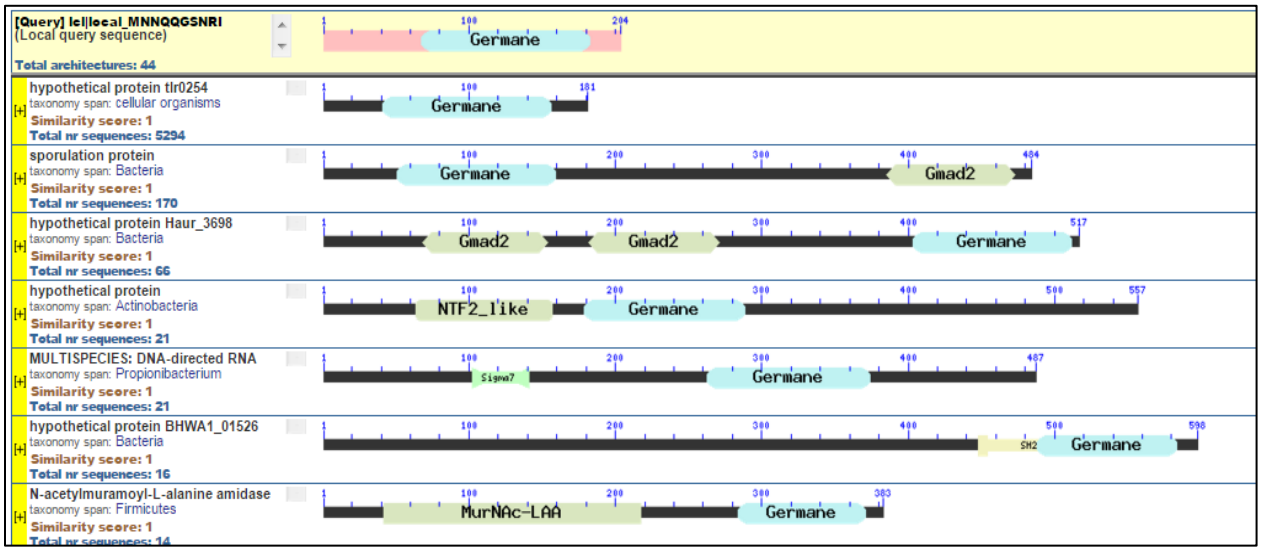

Fig. 32. Domain analysis of the Ava_2312 sequence from *A. variabilis*. Domains similar to the Ava_2312 sequence are grouped and scored by architecture using CDART.

The 24 hits from BLAST search showed sequences corresponding to filamentous cyanobacteria, most of them from Nostocales order that can differentiate akinetes, as *Nostoc sp*. PCC 7425, *N. punctiforme*, *A. cylindrica* and *Aphanizomenon flos-aquae* (Table 14).

	E value	Ident
conserved hypothetical protein [Anabaena variabilis ATCC 29413]	6e-144	100%
hypothetical protein [Nostoc sp. PCC 7120]	1e-139	97%
germination protein [Nostoc sp. PCC 7524]	5e-108	80%
transmembrane protein [Nostoc sp. PCC 7120]	3e-103	93%
hypothetical protein NOS3756_28630 [Nostoc sp. NIES-3756]	4e-99	81%
hypothetical protein [Nostoc punctiforme]	2e-93	75%
spore germination protein [Anabaena sp. wa102]	3e-92	72%
hypothetical protein [Anabaena cylindrica]	1e-91	76%
hypothetical protein [Dolichospermum circinale]	2e-89	70%
hypothetical protein [Anabaena sp. 90]	3e-89	70%
hypothetical protein [Microchaete sp. PCC 7126]	8e-89	74%
hypothetical protein [Dolichospermum circinale]	2e-88	70%
hypothetical protein [Trichormus azollae]	3e-88	73%
hypothetical protein [Anabaena sp. PCC 7108]	7e-87	74%
germination protein [Cylindrospermum stagnale]	5e-86	74%
hypothetical protein [Nodularia spumigena]	2e-84	71%
hypothetical protein [Aphanizomenon flos-aquae]	3e-84	72%
MULTISPECIES: hypothetical protein [Cylindrospermopsis]	1e-82	63%
hypothetical protein [Chlorogloeopsis fritschii]	5e-82	65%
hypothetical protein [Calothrix sp. PCC 7507]	9e-81	74%
spore germination protein [Nostoc piscinale CENA21]	5e-79	68%
hypothetical protein [Raphidiopsis brookii]	3e-77	64%
Uncharacterized protein apha_00151 [Chrysosporum ovalisporum]	5e-76	69%
germination protein [Tolypothrix sp. PCC 7601]	1e-75	75%

Table 14. BLAST analysis of Ava_2312. Comparison of the deduced amino acid sequence from *Ava_2312* of *A. variabilis* with deduced protein sequences present in genomes of different cyanobacteria. Red squares indicate protein sequences from strains forming akinetes.

3.3.1.2 Generation of the *Ava_2312* knockout mutant

To analyze the roll of the putative germination protein in cell differentiation processes, especially in akinete differentiation and germination, the gene *Ava_2312* of *A. variabilis* was inactivated by insertion of the plasmid pIM620 (see Methods) by single recombination event. After introducing the respective vector by conjugation in *A. variabilis*, streptomycin and spectinomycin-resistance colonies were obtained resulting in the mutant called *ΔAva_2312*. These underwent positive selection by growing in increasing concentrations of antibiotic. The genotypic characterization by PCR showed that the *ΔAva_2312* was fully segregated and the fragment corresponding to the amplification of the *Ava_2312* gene was only detected in the positive control (Fig. 33 b). Since pRL277 is 8,8 Kbp in size, the integrated DNA could not be amplified by Tac polymerase using the primers 1350 and 1351.

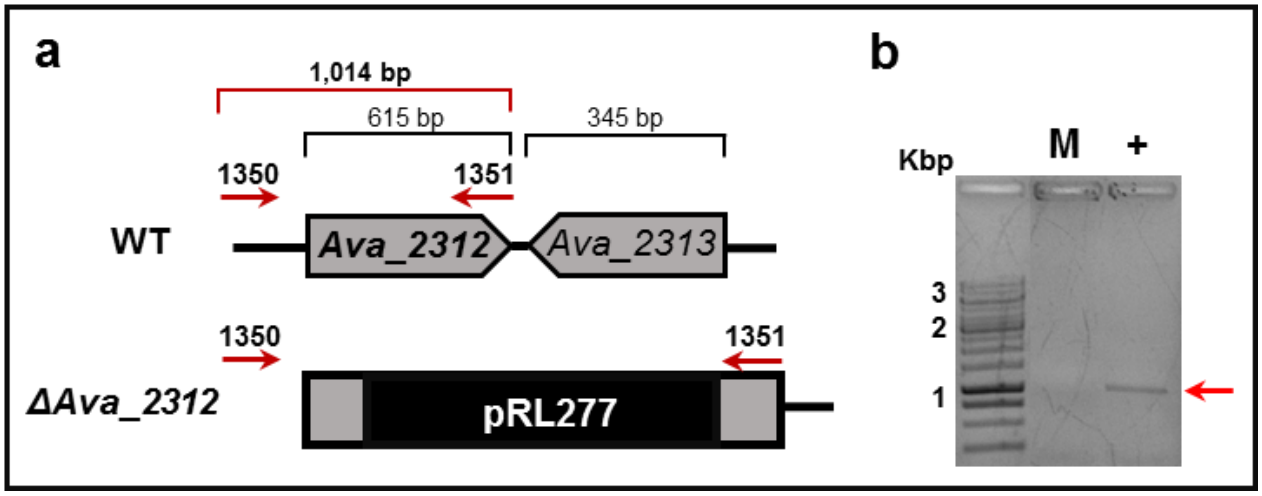

Fig. 33. Generation of the germination protein mutant in *A. variabilis*. (a) Schematic representation of the genomic organization of *Ava_2312* gene in wild-type (WT) and the mutant *ΔAva_2312*. The neighbor gene, *Ava_2313* encodes a transcriptional regulator from the ArsR family. The binding sites of the primer pairs used in PCR analysis are indicated. The gene *Ava_2312* was inactivated by insertion of the pRL277 vector by single recombination. (b) Colony PCR analysis of *ΔAva_2312* (M) and WT (+) colonies using the primers 1350 + 1351. Red arrow indicates the entire gene plus 400 bp of the upstream region (1.014bp).

3.3.1.3 Phenotype and heterocyst differentiation in the *ΔAva_2312* mutant

The *ΔAva_2312* mutant showed a very slow growth and a severe filament dystrophy in normal growth conditions independed from the antibiotic supply. The short and yellowish filaments were composed of larger and rounded cells than wild-type, and aberrant septa disposition similar to an aseriate stage (Fig. 34b). With the purpose to analyze the ability of the *ΔAva_2312* mutant to differentiate heterocysts, filaments of the wild-type and the mutant strain were washed three times with medium without combined nitrogen and incubated in this medium in presence or absence of antibiotics for 24 h. The wild-type strain showed a strong fragmentation and cell lysis in liquid medium containing the same antibiotic concentration as the resistant *ΔAva_2312* strain, showing that the filament dystrophy observed in the mutant was a consequence of the mutation and not due to an antibiotic effect (Fig. 34e). Fast bleaching, heavy filament fragmentation, inclusion bodies and absence of heterocysts were observed in the *ΔAva_2312* mutant incubated in media without NO_3^- and with antibiotics by 24 h (Fig. 34f). However, the mutant could differentiate few heterocysts and grow in media without antibiotics and NO_3^-, showing that this strain was not fully segregated even this was assumed from PCR analysis as shown in figure 26b (Fig. 34d).

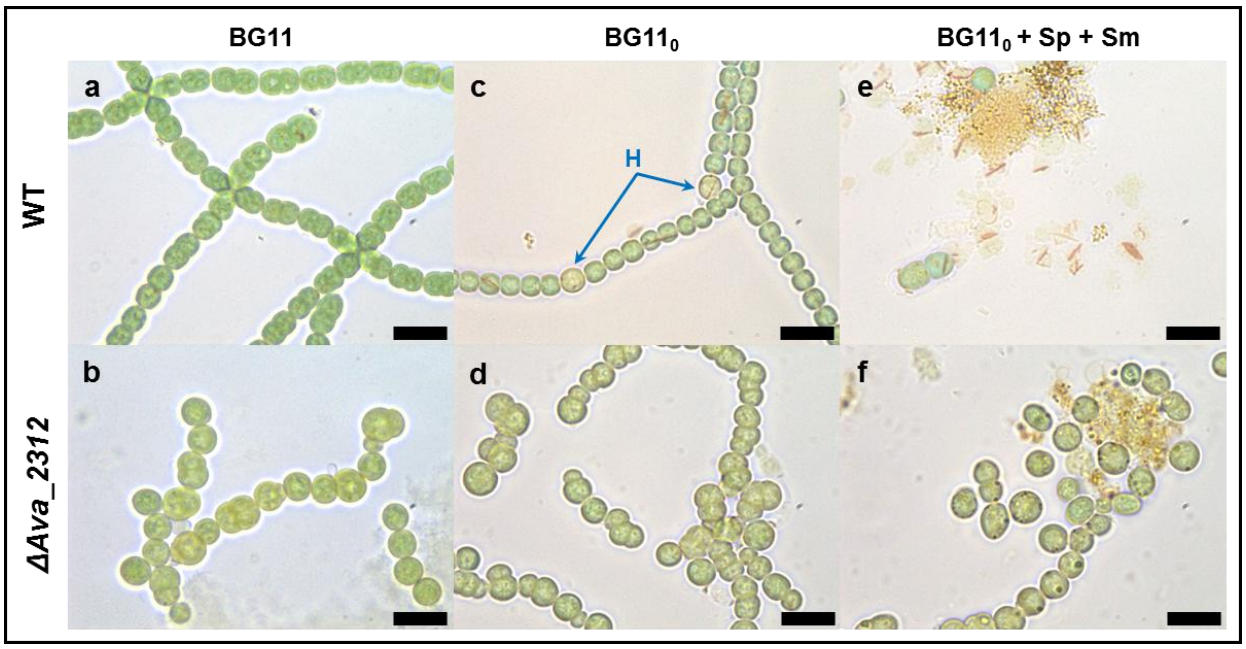

Fig. 34. Phenotype and heterocyst differentiation in the *ΔAva_2312* mutant. (a, b) Light micrographs of exponential phase cultures grown in BG11 liquid medium (+NO^-_3) or (c, d) incubated in $BG11_0$ liquid medium (-NO^-_3) by 24 hours without or (e, f) with antibiotics (Sp, Sm). (a, c, e) WT, (b, d, f) *ΔAva_2312* mutant. H, heterocyst.

3.3.1.4 Visualization of the peptidoglycan in the *ΔAva_2312* mutant

Since *ΔAva_2312* was predicted to be a cell wall protein, a Van-F staining was performed in wild-type and *ΔAva_2312* filaments incubated for 24 h in media without combined nitrogen. The Van-FL is a fluorescent vancomycin that binds *in vivo* to the free D-Ala-D-Ala dipeptides present in fresh PG and can be observed by fluorescent microcopy (Tiyanont *et al*., 2006; Lehner *et al*., 2013).

A green fluorescent stain was observed in the septa between vegetative cells, and vegetative cells and heterocyst in the wild-type strain and the mutant (Fig. 35a). However, the septa of the mutant were very extended and bind excessively Van-FL than in the wild-type strain. In addition, different sizes of cells and aberrant position of the septa were observed in the mutant (Fig. 35b-d).

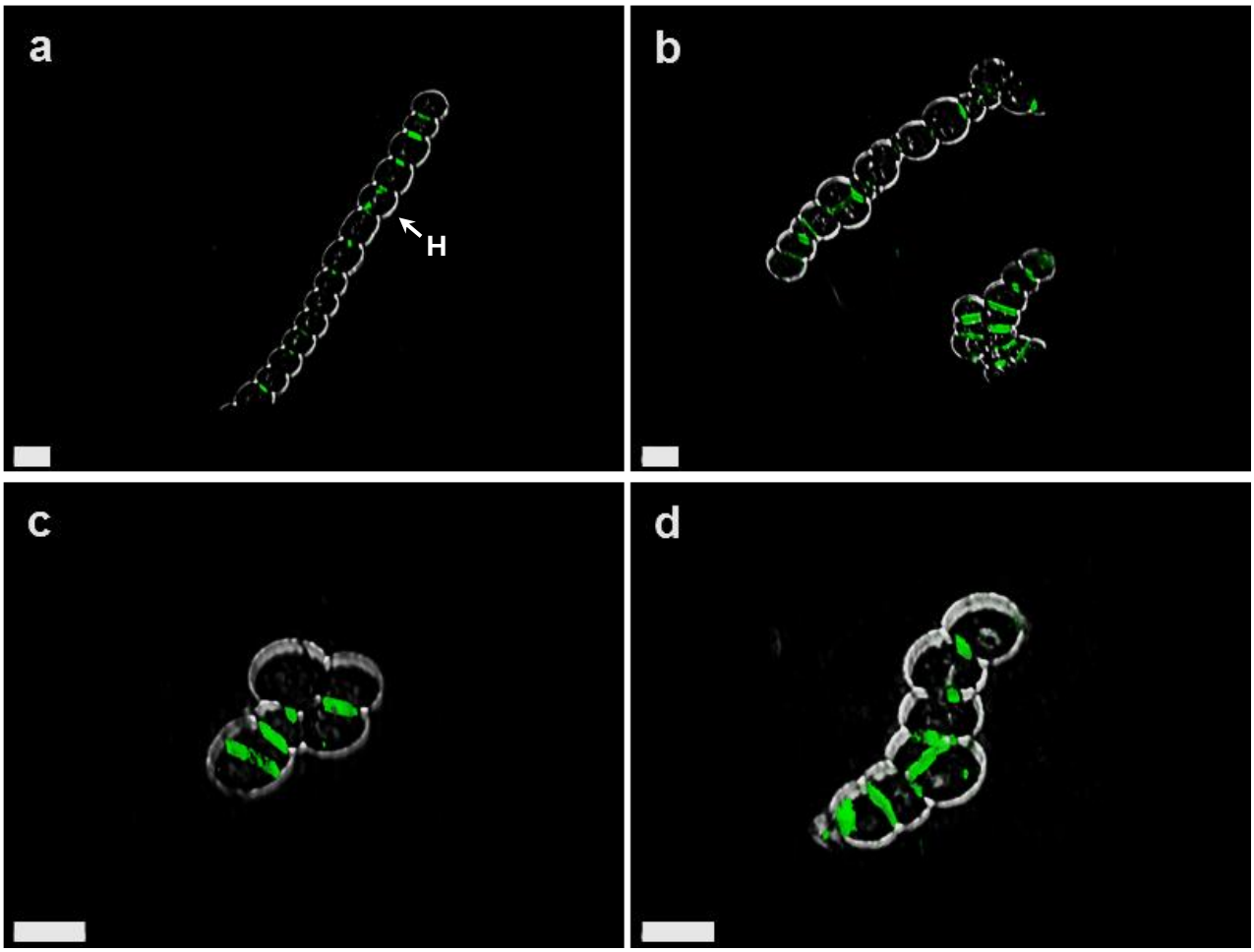

Fig. 35. Staining and visualization of the peptidoglycan in filaments of *A. variabilis* and *ΔAva_2312* strains. (a) Filaments of the wild-type and (b-d) the *ΔAva_2312* strain were incubated in $BG11_0$ for 24 hours and stained with the green fluorescent Van-FL. (a-d) Shown are overlays of Van-FL fluorescence and bright field 3D images. H, heterocyst. Bar: 5 µm.

3.3.1.5 Akinete differentiation of the *ΔAva_2312* mutant strain

In order to investigate the ability of the *ΔAva_2312* mutant to develop akinetes, stationary phase cultures of wild-type and the mutant were induced to differentiate akinetes by low light. Between 6 - 10 days of akinete induction, 90% of the wild-type cells were differentiated in akinetes that after 21 days showed the typical mature akinete morphology with oval-shape, thicker envelope and thylakoid degradation evidenced by brownish colour (Fig. 36b-d). By contrast, the *ΔAva_2312* mutant strain showed an increase in the blue-green colour and filament fragmentation after 6 days of akinete induction (Fig. 36f). Furthermore, big and rounded cells detached from the filaments started to appear after 10 days and their number increased towards

21 days (Fig. 36g, h). These akinete-like cells showed rounded-shape, absence of an envelope and intense blue-green colour (Fig. 36h).

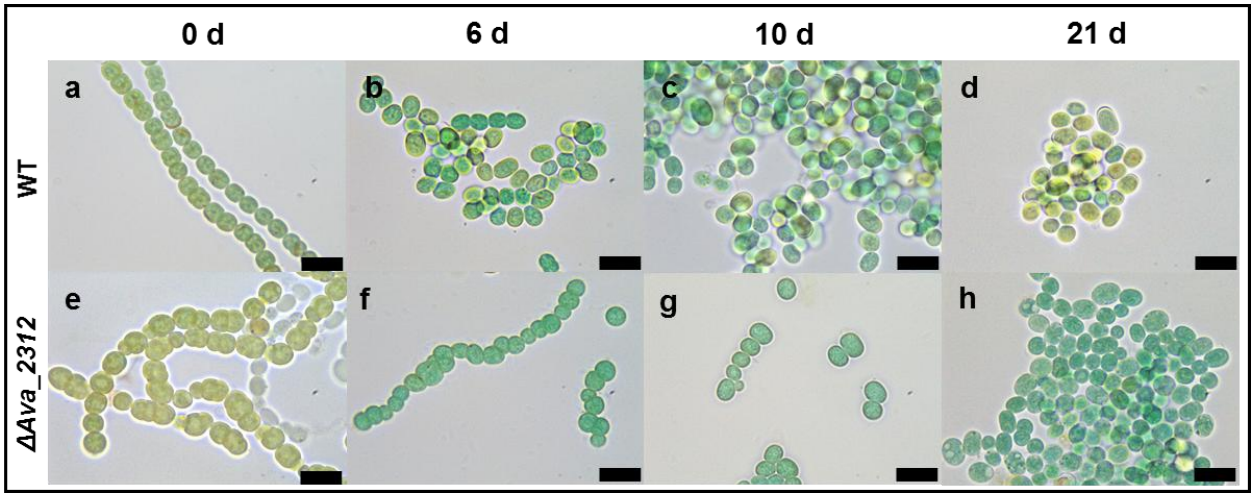

Fig. 36. Akinete differentiation in the *ΔAva_2312* mutant. (a, e) Light microscopy pictures of stationary-phase cultures exposed to normal light or (b, f,) cultures exposed to low light by 6, (c, g) 10 and (d, h) 21 days. (a-d) WT, (e-h) *ΔAva_2312* mutant. Bars: 10 µm.

3.3.1.6 Visualization of the lipid layer in akinetes-like cells of *ΔAva_2312* mutant

To investigate the presence of the lipid layer in the akinete-like cells of the *ΔAva_2312* mutant strain, a BODIPY staining was performed in wild-type and *ΔAva_2312* cultures induced to form akinetes by low light for 21days. A green-fluorescent stain was detected around of the mature akinetes in the wild-type strain as was expected (Fig. 37a, b). By contrast, the akinete-like cells from the *ΔAva_2312* mutant were not stained by BODIPY (Fig. 37 c, d). In addition, a stronger autofluorescence was detected in the these akinete-like cells in accordance of the observed blue-green colour by bright field microscopy (Fig. 37 c, d).

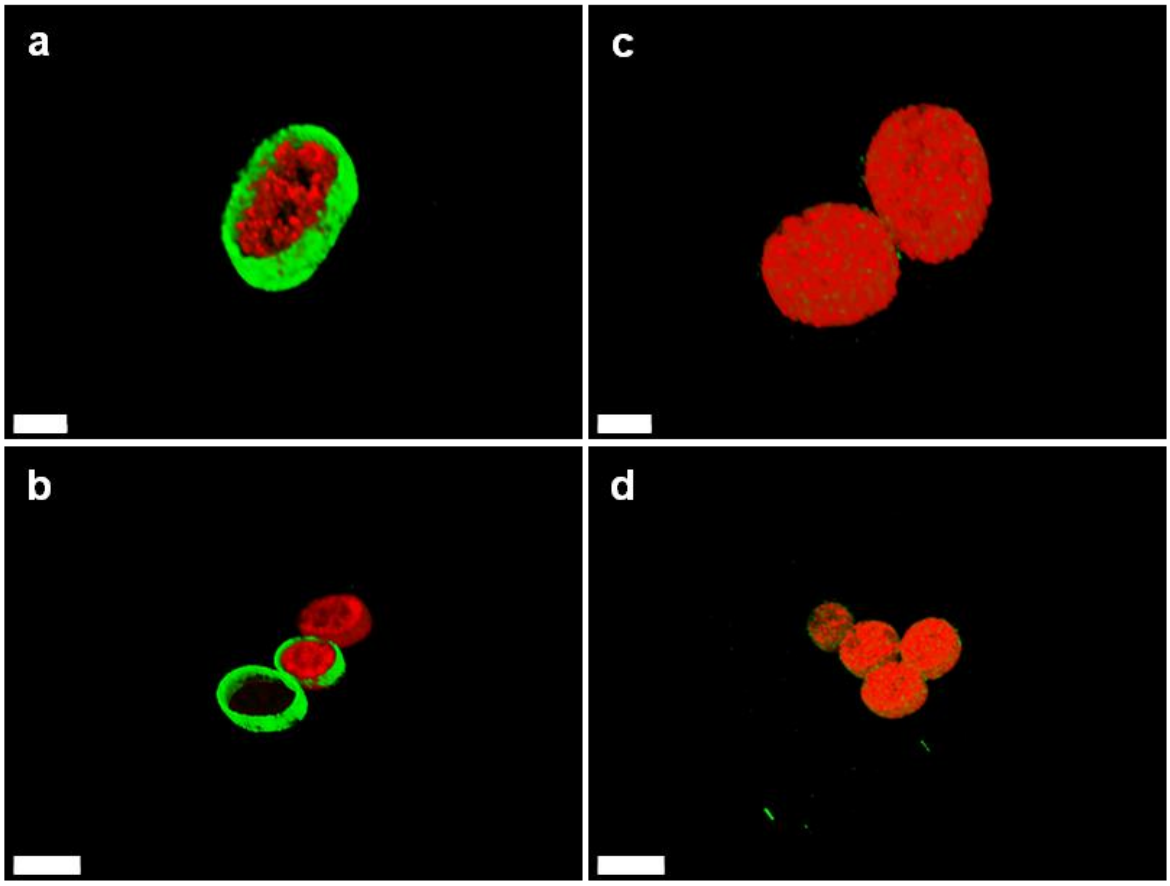

Fig. 37. Staining and visualization of akinete lipid envelope in the *ΔAva_2312* mutant strain. (a, b) cultures exposed to low light by 21 days were stained with BODIPY. Pictures show the overlay of BODIPY fluorescence and autofluorescence 3D images. (a, b) WT and (c, d) *ΔAva_2312*. (b, d) bars: 5 µm; (a, c) bars: 2 µm.

3.3.2 Generation of *ΔamiC1* and *ΔamiC2* mutant strains in *A. variabilis.*

In unicellular bacteria, the enzyme N-acetyl-muramyl-L-amidase AmiC cleaves the septal peptidoglycan in the last step of the cell division. In *N. punctiforme,* the homologue AmiC2-protein (NpF1846) drills holes into the septal peptidoglycan allowing the cell-cell communication and cell differentiation (Lehner *et al.,* 2011 & 2013).

In order to investigate the function of cell wall amidases in *A. variabilis*, the homologues *amiC*-genes *Ava_1465* (*amiC1*) and *Ava_1466* (*amiC2*) present in this strain were separately inactivated by insertion of neomycin-resistance-conferring cassette (C.K3). After introducing the respective constructs by conjugation in *A. variabilis*, neomycin-resistance colonies were obtained for *amiC1* and *amiC2* inactivation constructs. These underwent positive selection for double recombinants using the conditional lethal *sacB* gene. The genotypic characterization by

PCR showed that both mutants have the insertion of the DNA fragment bearing C.K3 by double recombination (Fig. 38b, c).

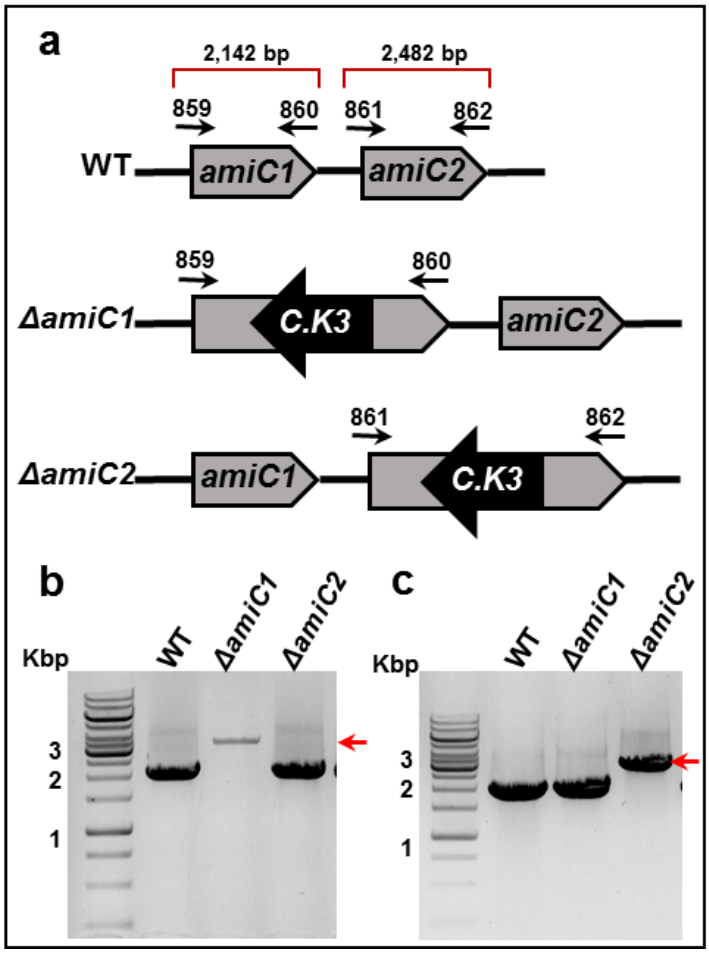

Fig. 38. Generation of *ΔamiC1* and *ΔamiC2* in *A. variabilis*. (a) Schematic representation of the genomic organization of the chromosomal amiC region of wild-type (WT) and the mutants. The genes *amiC1* and *amiC2* were separately inactivated by insertion of C.K3 cassette. The binding sites of the primer pairs used in PCR are indicated. (b) PCR analysis of *amiC1* from WT and mutants using the primers 859 + 860. (c) PCR analysis of *amiC2* from WT and mutants using the primers 861 + 862. Red arrow indicates the insertion of 1 Kbp corresponding to C.K 3 in the gen.

3.3.2.1 Phenotype of *ΔamiC1* and *ΔamiC2* mutant strains

In order to analyze the phenotype of the mutants, strains were grown in BG11 medium with or without neomycin (final concentration up to 100 µg) in standard conditions of light and agitation (see in materials and methods) and observed by light microscopy. Long filaments similar to the wild-type strain were observed in both mutants with or without neomycin in the medium (Fig.

39b, c). However, longer and very elongated cells were observed in *ΔamiC2* and *ΔamiC1* mutants respectively (wild-type: 4.110 µm; *ΔamiC1*: 6.534 µm and *ΔamiC2*: 4.744 µm).

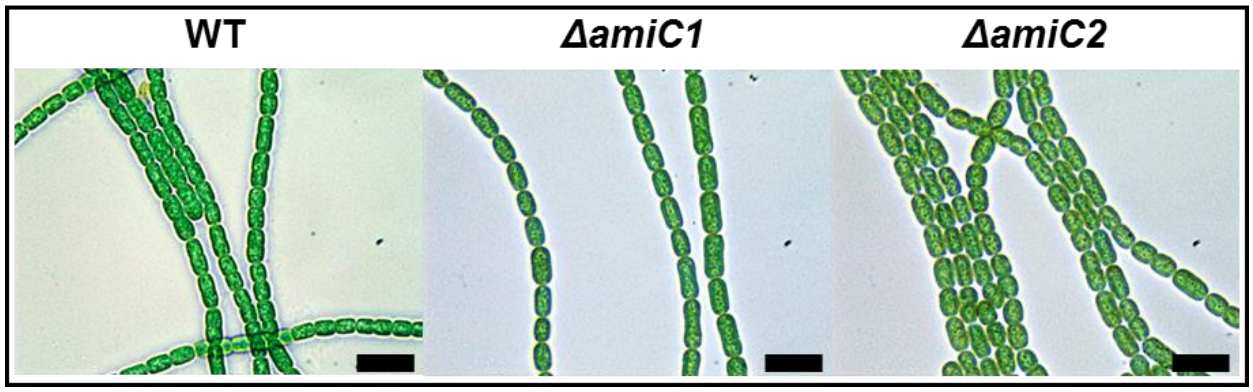

Fig. 39. Filament morphology of *ΔamiC1* and *ΔamiC2* strains. (a) Wild-type filaments grown in BG11 or (b) *ΔamiC1* and (c) *ΔamiC2* grown in BG11 with neomycin. Bars: 10 µm.

3.3.2.2 Heterocyst differentiation in *ΔamiC1* and *ΔamiC2* mutant strains

The ability to differentiate heterocyst of *ΔamiC1* and *ΔamiC2* mutant strains was investigated. Filaments in exponential growth cultures of wild-type and mutant strains that were washed three times with medium lacking combined nitrogen $BG11_0$ and maintained in the same medium for 48 h were analyzed by light microscopy. Many heterocysts with the typical shape and distribution inside of the filament were observed in the wild-type strain as expected (Fig. 40b). In contrast, aberrant heterocysts with pear shape or long heterocysts without CP polar bodies were observed in the *ΔamiC1* mutant strain. However, also few typical heterocysts were observed in this mutant strain (Fig. 40d). In addition, most of the heterocysts observed in the *ΔamiC2* mutant strain showed heterocyst with aberrant shape and yellowish filaments (Fig 40f).

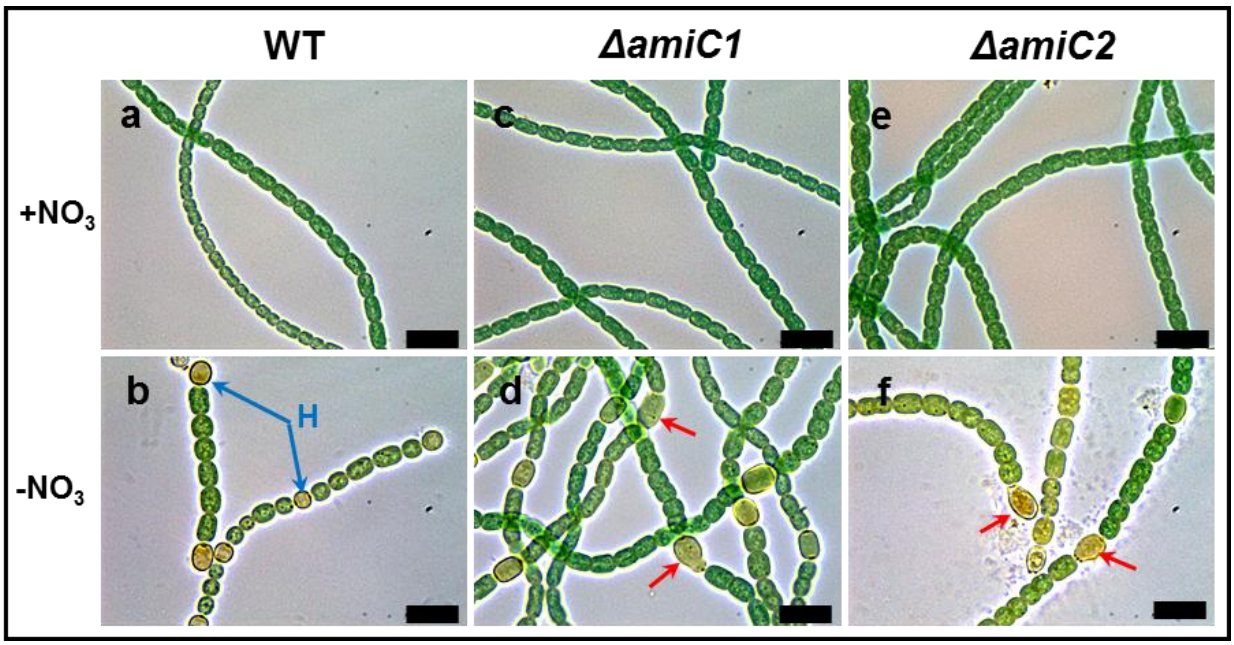

Fig. 40. Heterocyst differentiation in *ΔamiC1* and *ΔamiC2* mutant strains. (a, c, e) Light micrograph of filaments grown in BG11 liquid medium ($+NO^-_3$), (b, d, f) and after 48 hours of nitrogen step-down ($BG11_0$). (a, b) Wild-type, (c, d) *ΔamiC1* and (e, f) *ΔamiC2* mutants. Blue arrow, normal heterocysts; red arrow, aberrant heterocysts. Bars, 10 µm

In order to investigate if the mutants are able to grow under diazotrophic conditions, spot plating was done on agar lacking of a nitrogen source. After one week of incubation, green pseudo-colonies were formed for all dilutions of the wild-type strain. By contrast, both mutant strains were not able to grow without combined nitrogen after one week (Fig. 41). This phenotype is known as Fox^- mutant (Fox = fixation under oxic conditions; Elhai and Wolk, 1988).

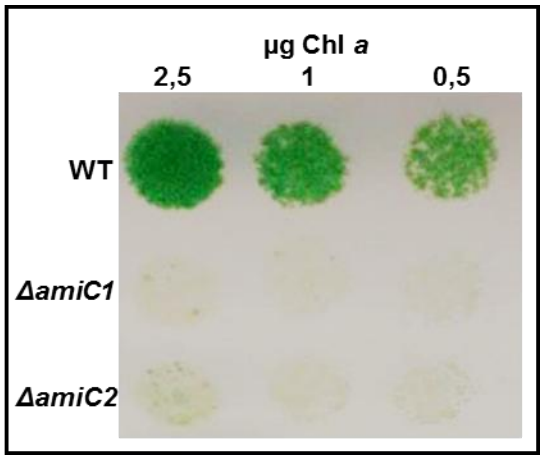

Fig. 41. Growth of wild-type, *ΔamiC1* and *ΔamiC2* pseudo-colonies without NO^-_3. Filaments of all strains were washed, resuspended in $BG11_0$ media at different chlorophyll concentrations (0,5; 1 and 2,5 µg) and incubated for 1 week in A+A agar plate medium (without NO^-_3). Chl *a*, Chlorophyll *a*.

3.3.2.3 Presence of heterocyst-specific glycolipids in the *ΔamiC1* and *ΔamiC2* mutant strains

To investigate the presence and distribution of the heterocyst specific-glycolipid, two approaches were used. First, cultures of wild-type, *ΔamiC1* and *ΔamiC2* strains that were induced to differentiate heterocysts by nitrogen step-down and after 48 h were stained with the fluorescent BODIPY stain. The glycolipid layer of the heterocyst envelope was conspicuously green fluorescent stained in wild-type cultures. Also the heterocysts didn't show autofluorenscence as expected (Fig. 42a). A green fluorescent envelope was also observed in some of the long shaped heterocysts of *ΔamiC1* mutant, but the glycolipid distribution was different from the wild-type. Two green fluorescent lines were observed in the septum between the heterocyst and the vegetative cell. In addition, the heterocyst showed autofluorescence similar to the vegetative cells (Fig. 42b). Only one green fluorescence line was observed at each pole of some of the small autofluorescent heterocyst with pear shape in the *ΔamiC2* mutant (Fig. 42c). In the majority, green BODIPY fluorescence was not observed in heterocysts from both mutant strains (not shown).

Second, the presence of heterocyst specific-glycolipids was confirmed by thin layer chromatography of lipid extracts from wild-type and mutant filaments, before and after nitrogen step-down. In the extracts from wild-type and mutant strains grown without NO_3^-, a band was detected in a region that has been attributed to heterocyst specific-glycolipid (Fig. 42d). Hence, both mutant strains can synthesize heterocyst-specific glycolipids although deposition seems to be hampered.

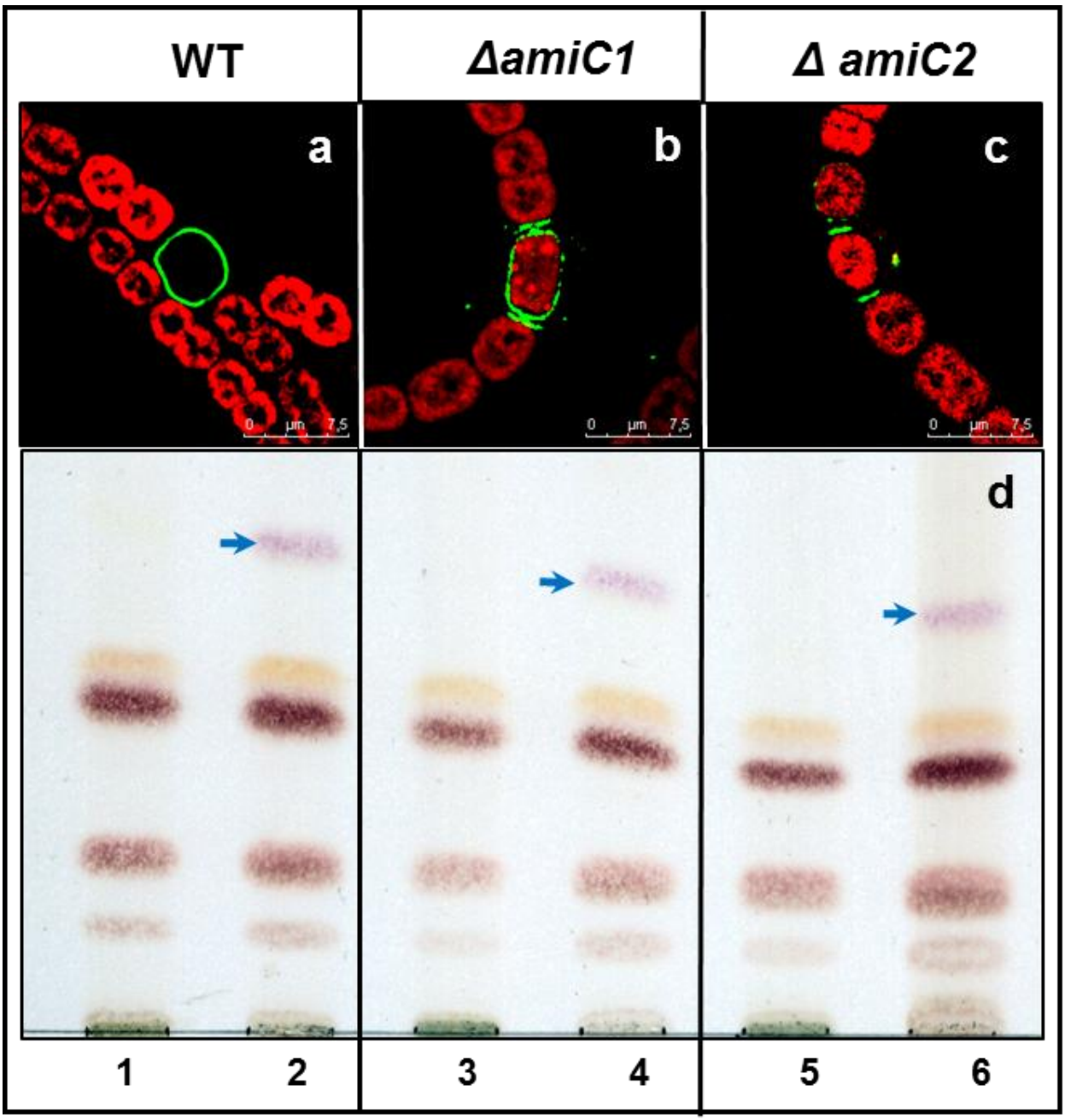

Fig. 42. The heterocyst-glycolipid layer of *ΔamiC1* and *ΔamiC2* mutants. *In vivo* BODIPY staining of (a) wild-type, (b) *ΔamiC1* and (c) *ΔamiC2* filaments washed three times and incubated in nitrogen-free medium ($BG11_0$) for 48 hours. (a-c) Shown are overlaid BODIPY fluorescence and autofluorescence images. (d) Thin-layer chromatography of lipid extracts from (1, 2) wild-type, (3, 4) *ΔamiC1* and (5, 6) *ΔamiC2* cultures containing 50 µg of chlorophyll *a*. (1, 3, 5) cultures grown in BG11 media with NO_3^- and (2, 4, 6) cultures grown in $BG11_0$ media without NO_3^- by 48 hours. Blue arrow, heterocyst-specific glycolipids.

3.3.2.4 Ultrastructure of *ΔamiC1* and *ΔamiC2* heterocysts

The ultrastructure of both mutant heterocysts together with the wild-type heterocyst were analyzed in cultures subjected to nitrogen step-down. The typical heterocyst ultrastructure with cyanophycin (CP) containing polar bodies and an envelope composed of glycolipid and exopolysaccharide layers was observed in the wild-type heterocyst after 48 hours of nitrogen deprivation (Fig. 43a). By contrast, the CP polar bodies and the glycolipid layer in the heterocyst polar region were not observed in the heterocysts of both mutants (Fig. 43b, c). A thicker peptidoglycan in the small neck between the heterocyst and the vegetative cell and around the heterocyst was observed in the *ΔamiC1* mutant. In addition, many glycogen granules were observed in heterocysts of both mutants, which is characteristic for a Fox$^-$ phenotype (Fig. 43b and S). Furthermore, an aberrant heterocyst shape was observed in the *ΔamiC2* mutant (Fig. 43c). In both mutant strains, the polar neck connecting the heterocyst and the vegetative cell differed from the wild-type (compare Figs. 43b, c with Fig. 43a). Interestingly, presumable vegetative cell showed an extra envelope, resembling the homogeneus polysaccharide layer (Fig. 43c).

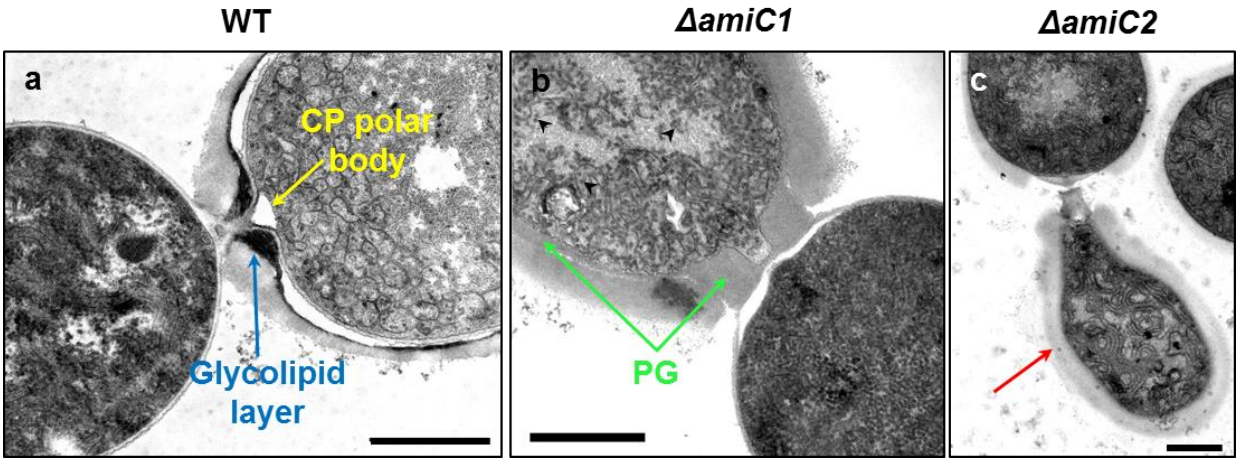

Fig. 43. Ultrastructure of heterocysts in *A. variabilis* and the amidase mutant strains. (a) Electron micrograph of heterocysts at 48 h of nitrogen step-down in wild-type and (c) *ΔamiC2* cultures or (b) at 62 h in *ΔamiC1* culture. Cp, cyanophycin; star, exopolysaccharide layer; PG, peptidoglycan; arrow head, glycogen; red arrow, aberrant heterocyst. Bars, 1 µm.

3.3.2.5 Visualization of the peptidoglycan in *ΔamiC1* and *ΔamiC2* mutant strains

In order to confirm the observation in the electron micrographs that the peptidoglycan between the heterocyst and vegetative cell is thicker in mutants than in the wild-type, a peptidoglycan stain with Van-FL was performed.

Wild-type, *ΔamiC1* and *ΔamiC2* filaments subjected to nitrogen deprivation by 48 hours, were stained *in vivo* with Van-FL stain (Fig. 44). The septa of vegetative cells from the wild-type were clearly stained. A narrow green spot in the constricted septum between the heterocyst and the vegetative cell was observed at high magnification (Fig 44a, b). In contrast, the stained area of the septa in both mutants was much broader (Fig. 44c, f). In addition, high magnification of the septa between the heterocyst and the vegetative cell in *ΔamiC1* and *ΔamiC2* mutant strains showed broader fluorescent peptidoglycan compared to the wild-type strain (Fig. 44d, f), confirming the observation by TEM (Fig. 43b).

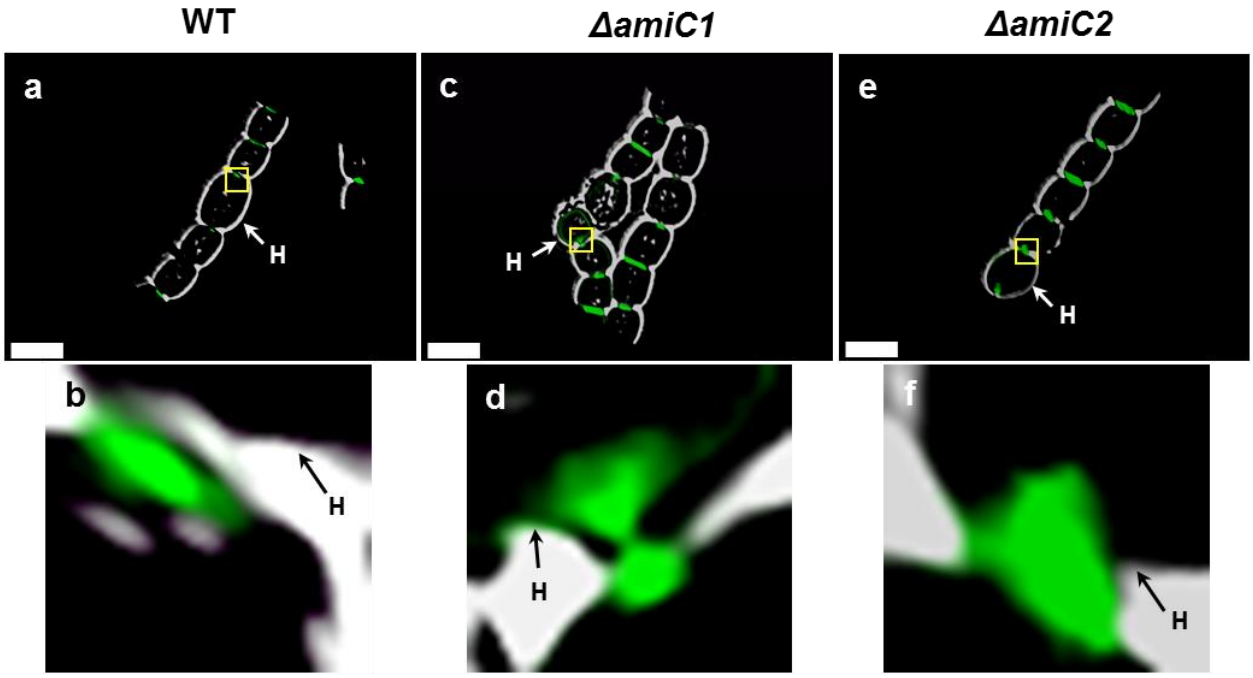

Fig. 44. Staining and visualization of the peptidoglycan in filaments of *A. variabilis* and *ΔamiC1* and *ΔamiC2* strains. (a, b) Filaments of wild-type (c, d) *ΔamiC1* and (e, f) *ΔamiC2* strains were incubated in $BG11_0$ by 24 hours and stained with the green fluorescent Van-FL. (a-f) Shown are overlaid of Van-FL fluorescence and bright field 3D images. (b, d, f) High magnification of septum between a vegetative cell and heteocyst. H, heterocyst. Yellow square, zone of amplification. Bars: 5 µm.

3.3.2.6 Akinete differentiation in *ΔamiC1* and *ΔamiC2* mutant strains

To investigate the ability of *ΔamiC1* and *ΔamiC2* mutant strains to differentiate akinetes, stationary-phase cultures of wild-type and both mutant strains were exposed to low light by 45 days. Approximately 95% of large and oval-shaped mature akinetes were observed in the wild-type culture after 45 days of induction (Fig. 45a). Most of the cells observed in the *ΔamiC1* mutant were large and detached from the filaments as mature akinetes, but with rounded-shape and in many cases without thicker envelope (Fig. 45c, d). Less and rounded-shape akinete like cells without defined envelope were developed in the *ΔamiC2* mutant in the same time period (Fig. 45e, f).

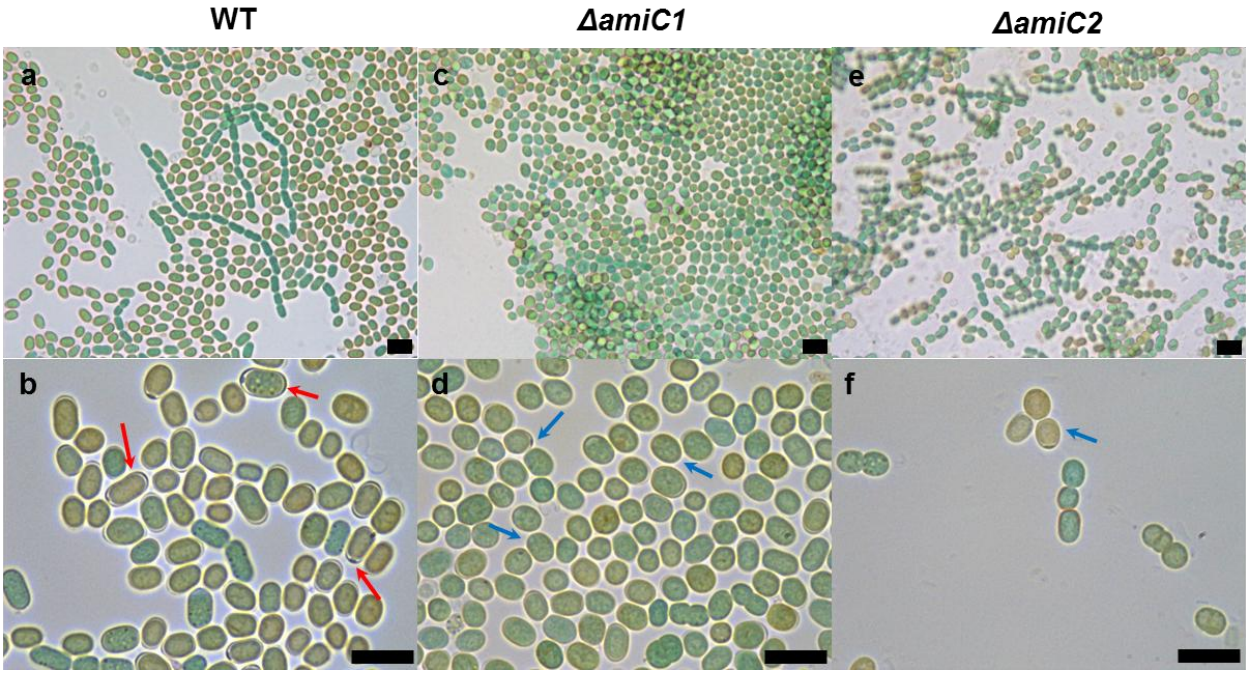

Fig. 45. Akinete differentiation in wild-type, *ΔamiC1* and *ΔamiC2* strains. (a, b) Light micrographs of WT, (c, d) *ΔamiC1* and (e, f) *ΔamiC2* strains exposed to low light by 45 days. Red arrow, akinetes. Blue arrow, rounded-shape akinetes. Bar: 10 µm.

The presence of a glycolipid layer in akinetes of *ΔamiC1* and *ΔamiC2* mutant strains were investigated by BODIPY staining. For this purpose, wild-type, *ΔamiC1* and *ΔamiC2* cultures induced to form akinetes by low light during 15 days were stained with the fluorescent BODIPY dye. The thicker glycolipid envelope in wild-type akinetes was heavily green fluorescent stained (Fig. 46a, b). In contrast, a weak and irregular staining around akinete like cells was observed in both mutant strains (Fig. 46c-f). In addition, cell division of some akinete like cells was observed

in the wild-type and in both mutant strains, showing that akinetes of both mutant strains probably will be able to germinate (Fig. 46).

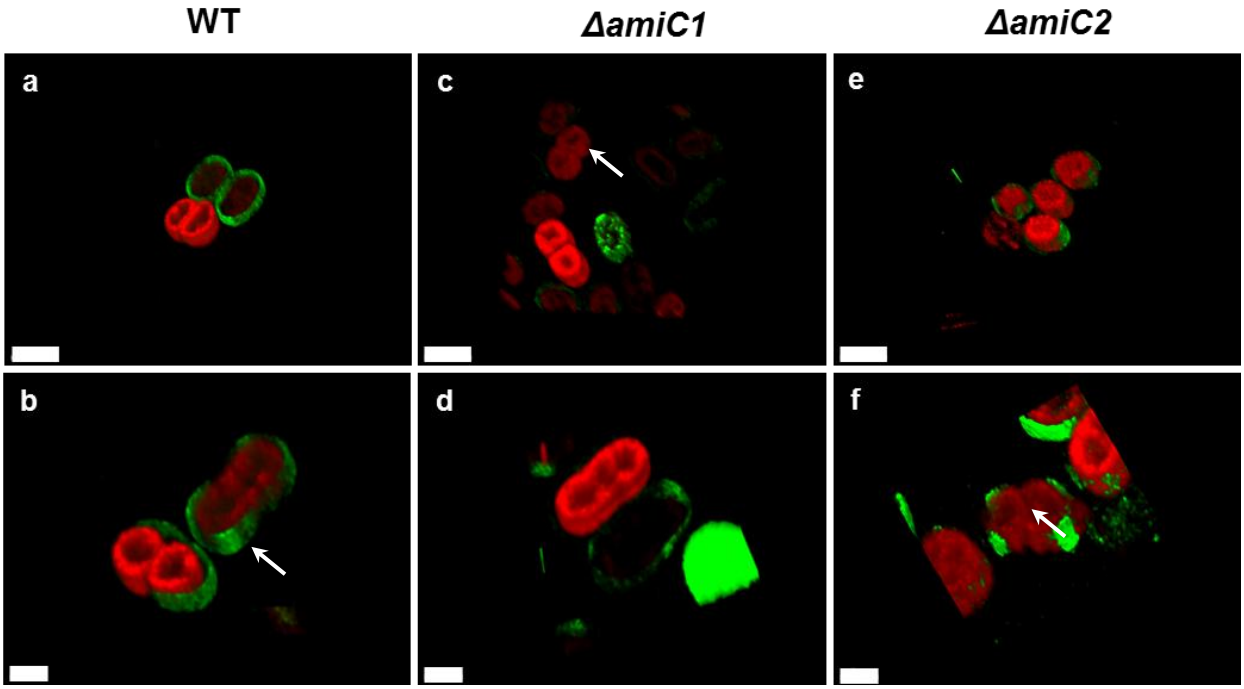

Fig. 46. Staining and visualization of akinete lipid envelope in wild-type, *ΔamiC1* and *ΔamiC2* strains. (a, b) Filaments of WT, (c, d) *ΔamiC1* and (f, g) *ΔamiC2* strains exposed to low light for 15 days were stained with BODIPY. Pictures show the overlay of BODIPY fluorescence and autofluorescence 3D images. Arrow; germinating akinete (a, c, e) bars: 5 µm. (b, d, f) bars: 2 µm.

Discussion

Akinetes are spore-like (dormant) cells that develop in asynchronous manner in stationary-phase cultures of several strains from the orders Nostocales and Stigonematales in the natural habits. The resting cell represents a survival strategy under harsh environmental conditions (Adams & Carr, 1981; Argueta & Summers, 2005). In the last decades, only rare studies on morphology and metabolism of akinetes from several species were published. The metabolic and morphologic changes during germination were also investigated in few cyanobacterial species. However, the akinete differentiation and germination processes at cellular and molecular level are still unclear (Adams & Duggan, 1999; Kaplan-Levy *et al*., 2010; Maldener *et al*., 2014).

The subject of the present study was to investigate in detail the changes in morphology and basic metabolic activities during akinete formation and germination in two model strains for cell differentiation, the planktonic freshwater strain *A. variabilis* ATCC 29143 and the terrestrial or symbiotic strain *N. punctiforme* ATCC 29133, to understand on a cellular and molecular level the adaptation mechanism of long term survival.

4.1 AKINETE DIFFERENTIATION

Akinetes were found in stationary-phase cultures of *A. variabilis* and *N. punctiforme* (Fig. 8c, d), but to obtain meaningful data on the morphological and physiological changes during akinete formation it was necessary to elucidate the best conditions to induce simultaneous akinete differentiation. Various environmental factors were reported to trigger the differentiation of akinetes in different *Nostocales* strains (Kaplan-Levy *et al.*, 2010; Maldener *et al*., 2014). Light intensity is a major, although not the only, trigger for akinete development in different *Nostocales* species (Adams & Duggan, 1999). Here, was showed that for *A. variabilis* the best inducer of akinete development was low light, and confirmed the earlier finding (Argueta & Summers, 2005; Argueta *et al*., 2006) that phosphate starvation was the best trigger for *N. punctiforme*. The triggers are apparently not genus specific, as phosphate starvation is the major trigger in *Anabaena cylindrica* (Wolk, 1965), in *Nostoc* sp. PCC 7524 the major trigger is phosphate excess (Sutherland *et al*., 1979). Others conditions were also tested to induce akinetes in *A. variabilis* and *N. punctiforme*, such as low temperature (15 °C) and phosphate starvation with nutrient enrichment (KNO_3 and fructose). These different inducing conditions had an effect on the time course of akinete formation, since all conditions tested resulted in delayed akinete formation compared to the respective optimum conditions in both strains. Low

temperature was reported as an important signal for triggering of akinete differentiation in several strains (Li *et al*., 1997). A temperature of 10 °C was the best condition to induce akinete differentiation in *Cylindrospermopsis raciborski* (Moore *et at*., 2005). The C:N ratio also appeared to be an important signal for akinete development in *Anabaena doliolum* and *Anabaena torulosa* (Rao *et al*., 1987; Sarma & Khattar, 1993; Ahuja *et al*., 2008). Deprivation of K^+ has been implicated as a trigger for akinete development in *A. ovalisporum* (Sukenik *et al*., 2007), and it was suggested that K^+ deficiency can be involved in a signal transduction cascade (Sukenik *et al*., 2013).

Low light, via photosynthesis, and phosphate starvation are leading to general low energy state. It remains to be elucidated the signalling cascade and signal sensing mechanisms responsible for the induction of akinete differentiation. Low light has an impact on the photosynthetic electron transport, which could be involved in signal transduction.

The present study provides the first ultrastructural characterization of akinetes in different stages of maturation in *A. variabilis* and *N. punctiforme*. Here, was designated as immature akinetes the stage of development represented by the presence of granules, rearrangement of thylakoid membranes, and presence of an initial or no akinete envelope. In addition, was considered mature akinetes as those with a thick envelope and presence of few or absence of granules. Sutherland *et al*., 1979 also described for *Nostoc* PCC 7524 that young akinetes first accumulate cyanophycin and then develop a multi-layered extracellular envelope. Furthermore, mature akinetes of *A. variabilis* showed a multi-layered envelope while *N. punctiforme* akinetes only two layers were detected (Fig. 13). An envelope similar to the *A. variabilis* akinetes has also been described in *Cylindrospermum* sp., *Anabaena cylindrica* and *A. variabilis* Kützing (Nichols & Adams, 1982; Cardemil & Wolk, 1981). However, it is not clear why planktonic strains as *A. variabilis* form a multi-layered envelope. One reason could be that this envelope allows enduring the high hydrostatic pressure that occurs during sedimentation in the water column during wintertime. On the other hand, it was suggested that the thicker exopolysaccharide layer present in akinetes of *N. punctiforme* play a role in the membrane stabilization during desiccation (Argueta & Summers, 2005).

The composition of the akinete envelope was investigated in detail for first time in *A. variabilis* and *N. punctiforme*. A lipid layer was detected in akinete envelopes of both strains, which were composed of the same glycolipids that form the heterocyst envelope. (Fig. 14 & 15). Three characteristic HGs were detected in the lipid extract of *A. variabilis* and *N. punctiforme* akinetes

and heterocysts (Fig. 16 & data no shown). These HGs are also present in a large number of heterocyst-forming cyanobacteria, but only in *Cyanospira rippkae* they were also identified in akinetes (Gambacorta *et al*., 1998; Wörmer *et al*., 2012; Bauersachs *et al*., 2014; Soriente *et al*., 1993). In conclusion, this result supports the idea of Wörmer *et al*., (2012), that HGs are not exclusive to heterocyst, as was shown here for *A. variabilis* and *N. punctiforme*. In addition, an unknown and new lipid was detected in the extracts of *A. variabilis* akinetes (Fig. 15 & 16). Furthermore, the akinetes and heterocysts envelopes of *A. variabilis* were positively stained with Alcian blue suggesting that the exopolysaccharide layer of both cell types were composed by similar sugars with acidic groups (Fig. 17). This result supported the earlier reports for *A. variabilis* and *A. cylindrica,* where similar polysaccharide structures were found in heterocysts and akinete envelopes (Cardemil & Wolk, 1981). In addition, the *hepA* gene encoding a putative polysaccharide exporter was required for correct deposition of the exopolysaccharide layer in both heterocyst and akinetes in *A. variabilis* (Leganés, 1994). In contrast to previous data by Argueta and Summers (2005), probably obtained with immature akinetes, most of the *N. punctiforme* akinetes were stained with Alcian blue, specially the clumpy akinetes. (Fig. 17). But profound biochemical studies are necessary to confirm that the exopolysaccharides of heterocysts and akinetes in *N. punctiforme* have the same sugar composition. In summary, these results support the hypothesis that the differentiation processes of akinete and heterocyst formation are related and that akinetes were evolutionary precursors of heterocysts (Wolk *et al*., 1994).

By Sakaguchi staining and estimation was confirmed that the granules observed in immature akinetes correspond to CP granules (Fig. 18). CP granules were not present in normal grown vegetative filaments, accumulated in immature akinetes and were reduced in mature akinetes. Immature akinetes of *N. punctiforme* accumulated the double of CP/cell than immature akinetes of *A. variabilis* (Fig. 18). Similarly, akinetes of *Anabaena torulosa* showed that CP accumulates during akinete development and decreases in mature akinetes (Sarma & Khattar, 1986). Also, *Aphanizomenon ovalisporum* accumulate CP during akinete formation induced by K^+ starvation (Sukenik *et al*., 2015). However, CP granule formation is neceessary for the normal differentiation and function of heterocysts and akinetes in *Nostoc ellipsosporum* (Leganés *et al*., 1998). The function of cyanophycin in *A. variabilis* and *N. punctiforme* needs to be investigated in future by mutational analyses.

Interestingly, a sharp increase in glycogen was detected in immature akinetes of *A. variabilis* (Fig.19). In contrast, the glycogen content did not change during akinete differentiation in *N.*

punctiforme. In other strains like *A. torulosa* and *Nostoc* PCC 7524 was also observed glycogen accumulation during akinete formation (Sarma & Khattar, 1986; Sutherland *et al*., 1979).

In addition, immature akinetes of *N. punctiforme* showed lipid droplets accumulation, which were seldom present in mature akinetes (Fig. 20). These lipid droplets were also present in vegetative cells and have recently been described as carbon storage compounds of *N. punctiforme* (Peramuna and Summers, 2014). Hence, its function during akinete development could be similar.

The measurements of storage compounds indicated that *A. variabilis* generates glycogen and cyanophycin as reserve material while *N. punctiforme* generates cyanophycin and lipid droplets (Table 15). In comparison to vegetative cells of both species, the amount of all the reserve materials was elevated in immature akinetes. This implies that in order to accomplish the differentiation process, large amounts of C and N are stored, because cell division stops but CO_2 fixation continues for a while generating these storage compound, which are probably later consumed to produce the thicker and complex akinete envelope (Fig. 47). In this context, it should be mentioned that it has been suggested that, the excess of glycogen is used to build extracellular mucilage under growth-limiting conditions in some cyanobacteria that do not develop akinetes (Stal, 2012).

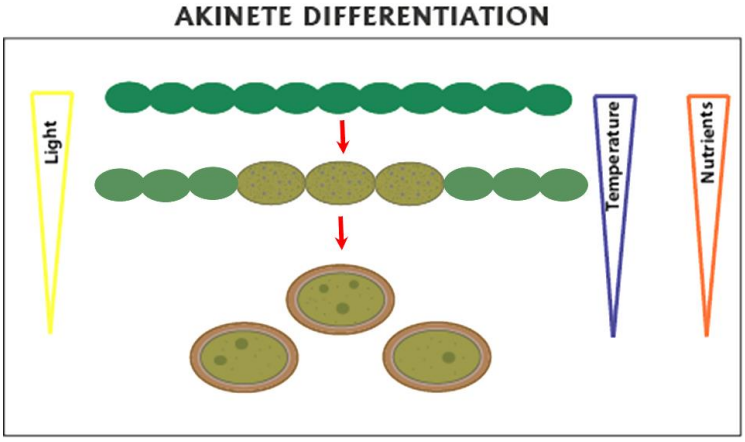

Fig. 47. Scheme of akinete differentiation process. When the environmental conditions are limiting, some of the vegetative cells that form the long filaments in *A. variabilis* and *N. punctiforme* initiate the process of akinete differentiation. In the beginning, the cells increase in size and accumulate intracellular granules of reserves as cyanophycin, glycogen and lipid droplets. Also, these cells showed a progressive loss in pigmentation because of the thylakoid degradation. Finally, the mature akinete is characterized by large size, thicker envelope composed of several layers, presence of few intracellular granules and thylakoid degradation.

In vegetative cells of both strains polyphosphate granules were present, which decreased during akinete development until they were undetectable in mature akinetes (Fig. 21). In contrast, the number of DAPI stained spots corresponding to nucleic acid highly increased in mature akinetes in comparison with vegetative cells of *A. variabilis* and *N. punctiforme* (Fig. 22). Similar results were observed in *Aphanizomenon ovalisporum*: while the nucleic acid amount increased, polyphosphate bodies disappeared in older akinetes (Sukenik *et al*., 2009). This result supports the assumption that polyphosphate bodies are used as resource to enlarge pools of nucleic acids in akinetes (Sukenik *et al*., 2012). One reason of the high DNA content in mature akinetes could be that these cells are prepared for fast cell division during germination, without requiring DNA replication.

Furthermore, this study shows the first time course of metabolic activities during akinete formation in *A. variabilis* and *N. punctiforme*. In both strains photosynthesis and respiration activities strongly decreased in cultures induced to form akinetes over 60 days (Fig. 23). It cannot be excluded that part of the residual activities came from germinating akinetes, which were frequently detected in very low percentage in the mature akinete cultures (not shown). Similarly, isolated mature akinetes of *Nostoc spongiaeforme* under conditions in which germination does not occur, showed that akinetes do photosynthesize and respire much slower than vegetative cells (Thiel & Wolk, 1983). Also, mature akinetes of *Aphanizomenon. ovalisporum* retained only residual photosynthetic activity (Sukenik *et al*., 2007 & 2015). The adaptation of metabolic activities seems to be strain specific, as the photosynthetic activity of *A. cylindrica* decreases gradually as the akinetes mature while the respiration increases (Fay, 1969). Furthermore, the oxygen produced solely by PSII was reduced to the half during akinete formation in *A. variabilis* and did not change in the case of *N. punctiforme* (Fig. 23b, e), which proves that PSII is properly working in both strains and refutes the suggestion that mature akinetes of *A. variabilis* Kützing lack functional PSII as was determined by fluorescent measurement (Bjorn *et al*., 1983). The fact that all metabolic activities in *A. variabilis* and *N. punctiforme* greatly decreased during akinete formation but PSII properly worked, showed us that reducing power and ATP were not consumed in anabolic reactions.

In summary, this study provides the first detailed characterization of akinete differentiation in two model cyanobacterial species *A. variabilis* and *N. punctiforme* and shows the marked differences in morphology, reserve materials and metabolic activity that take place during akinete differentiation (Table 15). According to Rippka *et al*., (1979), both species belong to the order Nostocales subsection IV, which form unbranched filaments and are able to fix nitrogen by

the formation of heterocysts. *A. variabilis* and *N. punctiforme* cluster in different groups in the 16S phylogenetic tree as well as in the genome-based study (Shih *et al*., 2013; Thiel *et al*., 2014). These species are also diverse with respect to the ecological niches they occupy. *A. variabilis* is a planktonic freshwater organism isolated from Mississippi river, which may require a multi-layered envelope with thicker lipid layer to survive at the bottom of sediments (Moore & Tischer, 1965). By contrast, *N. punctiforme* prevalently lives in terrestrial habitats and in symbiotic interactions with eukaryotic organisms, such as mosses, lichens and higher plants (Meeks & Elhai, 2002). In this terrestrial habitat, *Nostoc* experiences cycles of dry periods. These environments produce different stress conditions that may require specific adaptation mechanisms.

Table 15. Comparison of akinete differentiation in *A. variabilis* and *N. punctiforme*

Species	Best trigger of akinete formation	Transient reserve materials	Metabolic activities	Envelope
A. variabilis	Low light	Glycogen Cyanophycin	Gradual decrease	Multi-layered (HGs, exo-polysaccharide and $C_nH_{n-2}N_2O_8$)
N. punctiforme	Phosphate starvation	Cyanophycin Lipid droplets	Fast decrease	Two layers (HGs, exo-polysaccharide)

4.2 GERMINATION

The morphological changes and metabolic activities that take place during germination in *A. variabilis* and *N. punctiforme* were analysed in detail for the first time by this study.

Increasing the light intensity to normal level was the trigger for germination of akinetes in old medium from *A. variabilis* (Figs. 24, 25). In contrast, germination was induced by transferring akinetes to fresh medium in *N. punctiforme* (Figs. 26, 27). Germination in *A. cylindrica* and *A. variabilis* Kützing was also shown to be dependent on light intensity, and the most active spectra range for germination coincided with the maximum of the light absorption by C-

phycocyanin (Yamamoto, 1976; Braune, 1979). Furthermore, light and phosphate, but not a nitrogen source, were required for germination of *A. circinalis* and *N. spumigena* akinetes (Huber, 1985; Adams & Duggan, 1999).

During germination, the cell division took place inside the akinete envelope that was always observed in *A. variabilis* and occasionally in *N. punctiforme* (Figs. 24-27). The first cell division was observed few hours after germination was induced and long filaments were observed after just 48 h in both strains. However, mature akinetes were still detected after 24-48 h showing that germination is an asynchronous process in *A. variabilis* and *N. punctiforme* (Figs. 24, 26). Morphological changes during asynchronous germination of akintes have been also described for *Cylindrospermum*, *Aphanizomenon flos-aquae* and *A. variabilis* Kützing (Miller & Lang, 1968; Wildman *et al*., 1975; Braun, 1980). Akinetes of *Nostoc* PCC 7524 were reported to germinate synchronously after 12 h (Sutherland *et al*., 1985).

Unusual fast heterocyst differentiation compared to the heterocyst induction from vegetative filamentes was observed (6- 9 h) during germination in *A. variabilis* (Figs. 25 c, 24). It was also shown in other strains, that in absence of a nitrogen source heterocyst differentiation occurred during germination. Usually a single terminal heterocyst developed when the germling was three cells long and after 19 h in *Nostoc* PCC 7524 (Sutherland *et al*., 1985), but also proheterocysts appeared at 10-11 h in filaments of two cells in *Nostoc* PCC 6720 and *Anabaena* PCC 7937 (Skill & Smith, 1987) or after 14 h in *C. capsulata* (Sili, 1994). The fast cell division and heterocyst differentiation support the idea, that the high DNA content in mature akinetes facilitates the fast cell division during germination (Fig. 22). Moreover, an irregular plane of cell division was observed during germination in *A. variabilis* (Fig. 24). This result resembles the aseriate stage of cells observed in *Nostoc muscorum* after transfer cultures from darkness to light (Lazaroff, 1973).

Furthermore, this study shows a detailed ultrastructure characterization of germinating akinetes in *A. variabilis* and the first ultrastructure characterization of germinating akinetes in *N. punctiforme.* In the beginning of the process, the cells were characterized by undeveloped thylakoid membranes, initial carboxysomes, presence of few glycogen and cyanophycin granules (Figs. 25, 27). Similarly, few cyanophycin granules and many glycogen granules were observed in young filaments of *Nostoc* PCC 7524 (Sutherland *et al*., 1985). Cyanophycin granules were also reported in germinating cells of *A. variabilis* Kützing (Braune, 1980). In the end of the germination process, the cells that form the young filament showed the typical

structures of vegetative cells (Figs. 25f, 27f). At this point, the short filament emerged from the akinete envelope that was laterally opened in *A. variabilis* or emerged from the dissolved extracellular matrix in *N. punctiforme* (Figs. 25f, 27c & SI). In addition, a polar degradation of the akinete envelope and emergence of a young filament is a common process observed in some cyanobacterias as *Nostoc* PCC 6720, *C. rippkae* and *C. raciborskii* (Skill & Smith, 1987; Sili *et al*., 1994; Moore *et al*., 2004). By contrast, an early report described a complete degradation of the akinete wall in *N. punctiforme* (Meeks *et al*., 2002), hence, this is not always microscopically visible (Maldener *et al*., 2014). Here, an empty akinete envelope of *N. punctiforme* was observed (Figs. 27c, SI) confirming that the degradation of the akinete envelope is incomplete during germination. Similarly, empty akinete envelopes were frequently observed following germination in *Anabaena* sp. Strain CA (Adams & Duggan, 1999).

The fate of the akinete envelope during germination was observed by microscopy. The lipid layer of the akinete envelope in *A. variabilis* was detected along of the germination process and it was still attached to the young filament formed showing that this layer, and hence the akinete envelope, is not degraded during germination (Fig. 28a-d). This result strengthens the suggestion of akinete envelope rupture by high pressure due to successive cell divisions (Kaplan-Levy *et al*., 2010; Moore *et al*., 2004). In contrast, a weekly stained envelope around the germinating akinetes of *N. punctiforme* was eventaully present but was not attached to the young filaments formed (Fig. 28g, h). This result supports the idea that in *N. punctiforme* the akinete envelope could be partially degraded and this would be the reason why it is not always visible. Degradation products might be used by the growing filament before autotrophy fully works.

Although the very low conentration of cyanophycin and glycogen was not chemically determined during the process of germination (see Figs. 18, 19), the fate of these intracellular storage compounds during germination was followed by TEM. Some of the germinating akinetes of *A. variabilis* showed many glycogen granules but few or no cyanophycin granules (Fig. 25). By contrast, several cyanophycin granules but few glycogen granules were observed in germinating akinetes of *N. puntiforme* (Fig. 27). These results reinforce the observation that *A. variabilis* prefers glycogen as reserve compound while *N.punctiforme* prefers cyanophycin (Table 15). Finally, the cyanpophycin and glycogen granules were consumed or reduced during germination in both strains (Figs. 25, 27). The reduction of cyanophycin granules during germination was also observed in *C. raciborskii* (Moore *et al*., 2004). Despite, *A. variabilis* akinetes were lacking cyanophycin they were capable to germinate, and the cells of the young

filament formed in *N. punctiforme* had still small cyanophycin granules left (Figs. 25d, 27f). These results are in line with the previous assumption that cyanophycin is not a nitrogen source for protein synthesis and therefore is not essential for germination (Sutherland *et al*., 1985; Herdman, 1987).

The occurrence of lipid droplets during germination was also studied in *N. punctiforme*. Only in few germinating akinetes small weakly stained lipid droplets were detected that towards the end of the germination became larger and stronger stained (Fig. 28e-h). The fact that lipid droplets were detected in few germinating akinetes, proves that this compound could be utilized as carbon source to build the akiente envelope and that it is not used as carbone source during germination (Table 15).

Furthermore, the occurrence of polyphosphate granules during germination was investigated in *A.variabilis* and *N. punctiforme*. In both strains, polyphosphate granules were rarely detected in the begining of germination but were present towards the end of the process in all vegetative cells of the young filament (Fig. 29). Likewise, it was reported that polyphosphate granules disappear during sporulation and were resynthesized very early during germination in *N. linkia*, *A. variabilis* and *A. ferlilissima* isolated from India (Reddy, 1983). This supports the idea that the polyphosphate bodies are converted to DNA during akinete differentiation to be prepared for fast cell division during germination (Sukenink *et al*., 2012).

Finally, the present study provides to my knowckledge the first characterization on the development of photosystem and respiratory activities during akinete germination in *A. variabilis* and *N. punctiforme*. The O_2 evolution rate increased markedly 24 h after germination started, and after 72 h the O_2 evolution rate was similar to the one of vegetative cells in both strains (Figs. 30a, c; 22a, d). In addition, the colour of the cultures turned green after 24 h of germination showing a regeneration of the thylakoid membranes (Fig. S4). Chauvat *et al*., (1982) showed that in *Nostoc* PCC 7524 the photosynthetic capacities highly increased between 9-10 hours of germination but without a change in the pigments. The respiratory activity in germinating akinetes of *A. variabilis* increased during the first 12 h and then remained at a bit lower level until 48 h. Finally, after 72 h the rate had increased reaching to the respiratory activity rate of a vegetative cell culture (Fig. 30b, 23c). This result suggests that the glycogen was the substrate for respiration in the beginning of the germination, and later it was the substrate generated by the PS. The role of glycogen as respiratory substrate was previously shown for *Synechocystis* sp. PCC 6803 (Gründel *et al*., 2012). A very weak increase in the rate

of respiration was detected in germinating akinetes of *N. punctiforme* during the first 48 h because the akinetes did not contain or accumulate glycogen. The respiration rate had doubled after 72 h. Thus, for a normal rate of respiratory activity an active PS activity is necessary.

In conclusion, the germination of akinetes in *A. variabilis* and *N. punctiforme* is an asynchronous process triggered by light availability and nutrients. The cell division takes place inside the akinete envelope and does not need endogenous carbon or nitrogen resources. But, to complete the germination process the energy provided by PS and respiration activities is needed (Fig. 48).

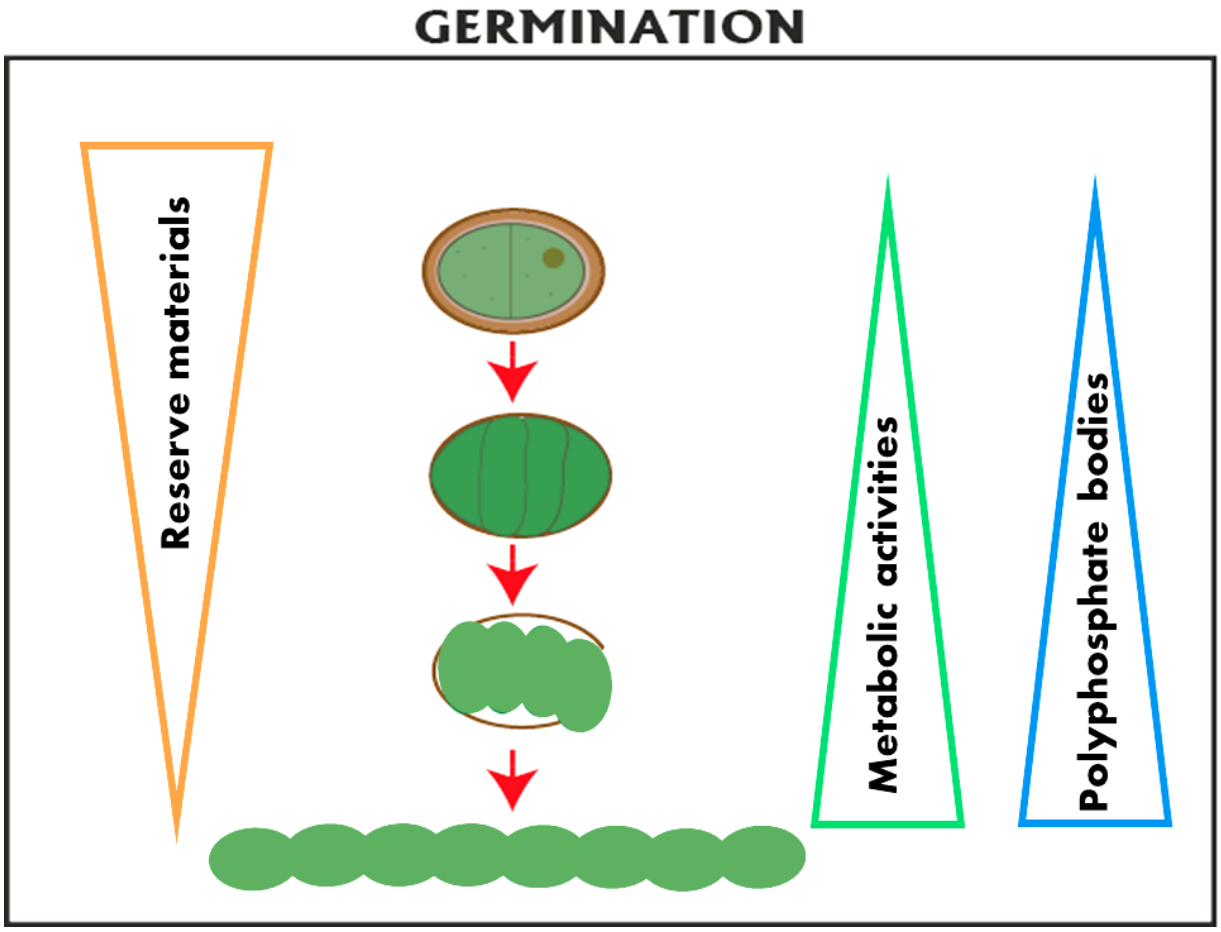

Fig. 48. Scheme of akinete germination. Light and nutrient supply are the stimulus required to start the germination of akinetes in *A. variabilis* and *N. punctiforme*. The process initiate with the first cell division inside of the akinete envelope. In that moment the cells are characterized by undeveloped thylakoid membranes, carboxysomes and presence of few storage granules as glycogen or cyanophycin. Finally, a short filament made of vegetative cells and heterocyst with the typical structures emerge from the akinete envelope. In this stage, the metabolic activities and regeneration of thylakoid membranes are observed.

4.3 CHARACTERIZATION OF CELL WALL MUTANTS IN *A. variabilis*

A global gene expression study of *N. punctiforme zwf* mutant provided valuable information about genes putatively involved in akinete formation. For example, the gene *Npun_F0437* encoding a putative spore germination protein was shown up-regulated during akinete differentiation (Campbell *et al*., 2007). In the current work, the function of the homologue gene in *A. variabilis* (*Ava_2312*) was characterized by generation of a knockout mutant called *ΔAva_2312*.

The *Ava_2312* gene is predicted to encode a putative protein containing a conserved germane domain (gerM) which is also presented in thousands of proteins encoded in *Firmicutes* and members of the other bacterial phyla (Figs. 32). In *Bacillus subtilis*, a *gerM* mutant was affected in both sporulation and germination (Sammons *et al*., 1987), and it was suggested to be involved in peptidoglycan synthesis (Slynn *et al*., 1994). The analysis of the Ava_2312 protein by CDART showed that the gerM domain is associated to other domains like Gmad2, which is an immunoglobulin-like domain of bacterial spore germination (http://pfam.xfam.org/family/PF 10648), or to the NTF2-like superfamily, which is a versatile group of protein domains sharing a common fold. It was suggested that the NTF2-like domain could regulate the activities of domains such as peptidoglycan-processing hydrolases (Eberhardt *et al*., 2013). Also, gerM domain was associated to N-acetylmuramoyl-L-alanine amidase, an autolysin that hydrolyzes the amide bond between N-acetylmuramoyl and L-amino acids in certain cell wall glycopeptides (https://www.ncbi.nlm.nih.gov/Structure/cdd/cddsrv.cgi?uid=cl02713). This protein sequence analysis suggested that Ava_2312 has a conserved domain (gerM), which function could be associated to peptidoglycan processing. Ava_2312 protein sequence showed high identity with hypothetical germination proteins of several Nostocales strains characterized by differentiation of akinetes (Table 14), suggesting that this protein is widespread in all akinete forming strains and it may be absolutely required for akinete formation and germination.

The *ΔAva_2312* mutant presented here showed a severe phenotype: filaments contained large cells with aberrant septa disposition, and it was unable to differentiate heterocysts and normal akinetes (Figs. 34, 36). A similar phenotype was reported in the *N. punctiforme amiC2*$^{-}$ mutant which forms irregular clumps of twisted cells connected by aberrant septa. This mutant was also incapable to form heterocysts and akinetes (Lehner *et al.,* 2011). Mutation of two peptidoglycan synthesis genes, *murC* and *murB* were required for heterocyst differentiation and filament integrity in *Anabaena* sp. PCC 7120 (Videau *et al.,* 2016). In conclusion, mutation in genes

associated with synthesis or remodeling of peptidoglycan lead to strains unable to differentiate heterocyst and eventually filament dystrophy as will be discussed below.

Indeed, aberrant peptidoglycan deposition was demonstrated by Van-FL staining showing broader and more stained septal peptidoglycan in the *ΔAva_2312* mutant, implying the presence of more and non-crosslinked peptide residues in the peptidoglycan (Fig. 35). Furthermore, the *ΔAva_2312* mutant formed akinete-like cells without a thick envelope suggesting that the germination protein is directly or indirectly involved in the formation of the akinete envelope (Figs. 35, 36). Similarly, the few spores formed in the *gerM* mutant of *Bacillus subtilis*, were less heat resistant and frequently, the *gerM* mutant showed multiple septa with thicker peptidoglycan suggesting a role either directly or indirectly in peptidoglycan synthesis (Sammons *et al*., 1987; Slynn *et al*., 1994). In conclusion, the function of the germination protein could be related to the AmiC amidases in *Anabaena* PCC 7120 and *N. punctiforme*, which drill holes in the peptidoglycan septa forming nanopores that constitute a frame work for the cell-joining proteins (SepJ, FraC or FraD) required for cell-cell communication and cell differentiation (Lehner *et al*., 2013; Berendt *et al*. 2011; Nürnberg *et al*., 2015).

Hence, in this study the function of the AmiC1 and AmiC2 homologues in *A. variabilis* was investigated and compared with the previously described *amiC1*/*amiC2* mutants of *N. punctiforme* and *Anabaena* sp. PCC 7120. As in the other heterocysts forming strains, these cell wall amidases were required to differentiate normal and functional heterocysts and akinetes in *A. variabilis*. Both *A. variabilis* knockout mutants showed long filaments made of elongated cells suggesting that these proteins could be involved in the regular formation of the septa, but did not affect the integrity of the filaments (Fig. 39). Similarly, the *amiC1* and *amiC2* (*hcwA*) mutants in *Anabaena* sp. PCC 7120 had no effect on filament morphology, however, in *N. punctiforme* the mutation of *amiC2* led to filament dystrophy and aberrant cell division planes (Berendt *et al.,* 2012; Lehner *et al.,* 2011). Mutation in the *conR* gene of *Anabaena* sp PCC 7120, which contains a domain associated with septum formation and cell wall maintenance leads to a similar phenotype: filaments with longer cells than normal (Mella-Herrera *et al*., 2011).

Both amidase mutants of *A. variabilis* could not grow diazotrophically and produced heterocysts with aberrant morphology (Figs. 40, 41). Similarly, *amiC1* and *hcwA* (*amiC2*) mutants in *Anabaena* sp. PCC 7120 differentiated less and non-functional heterocysts, and were unable to grow diazotrophically, however, the *amiC2* (*hcwA*) mutant generated by Berendt had the same phenotype as wild type. In the case of *N. punctiforme amiC2* mutant, the heterocysts

differentiation was totally hampered (Berendt *et al.,* 2012; Zhu *et al*., 2001; Lehner *et al.,* 2011). The heterocysts of *ΔamiC1* and *ΔamiC2* mutants in *A. variabilis* showed an abnormal or no deposition of glycolipids, which could be the reason for the Fox$^-$ phenotype (Fig. 42). In general, the mutation of genes involved in the formation of the heterocyst envelope are unable to grow diazotrophically, because a defect in the integrity of the envelope layers allowed more oxygen to enter the heterocyst inactivating the nitrogenase. For example, the *devH* mutant in *Anabaena* sp. PCC 7120, showed a Fox$^-$ phenotype associated with a defective heterocyst envelope that lacks the glycolipid layer (Ramírez *et al*., 2005). Also, mutation of the TolC-DevBCA HGL transporter leads to differentiation of non-functional immature heterocysts without glycolipid layer (Fiedler *et al*., 1998; Maldener *et al*., 1994; Staron *et al*., 2011). Finally, mutation in the HGL genes involved in glycosylation or biosynthesis of glycolipids are necessary for the formation of the laminated layer in the heterocysts envelope (Awai & Wolk, 2007; Campbell *et al*., 1997; Fan *et al*., 2005, Bauer *et al*., 1997; Black & Wolk, 1994; Maldener *et al*., 2003). The modification of the peptidoglycan by amidases and other lytic enzymes could be necessary for the correct deposition of the glycolipids, which cannot occur in the *amiC* mutants of *A. variabilis.* It remains to be shown in future studies whether the TolC-DevBCA HGL transporter cannot be assembled in the amiC mutants and where in the cell wall of *A. variabilis* the amidases are localized.

The heterocyst ultrastructure of both mutants showed the presence of glycogen granules and the absence of the CP polar bodies (Fig. 43). This observation confirmed the inactivation of the nitrogenase, because in normal conditions the excess fixed nitrogen is stored as cyanophycin in the poles (Wolk, 1994). Also, the accumulation of glycogen in the heterocyst and vegetative cells was observed in mutants where the nitrogenase activity was impaired (Valladares *et al*., 2007). Interestingly, accumulation of thicker peptidoglycan in the septum between the heterocyst and the vegetative cells of both mutants was detected (Figs. 43, 44). The results from Van-FL staining proved that the synthesis of peptidoglycan is enhanced and contains more uncrosslinked peptide residues in both amidase mutants of *A. variabilis*. Likewise, two other genes associated with synthesis or remodeling of peptidoglycan formed non-functional heterocyst, it is the case of the *pbpB* mutant in *Anabaena* sp. PCC 7120 associated to synthesis and maintenance of peptidoglycan (Lázaro *et al*., 2001). In addition, the *conR* mutant showed abnormal heterocyst and septum formation between the heterocyst and the adjacent vegetative cells resulting in Fox$^-$ phonotype (Mella-Herrera *et al*., 2011). Furthermore, mutants in the proteins SpeJ, FraC or FraD that are impaired in cell-cell communication and localized in the

septum, were also affected in maturation of functional heterocyst (Nayar *et al*., 2007; Flores *et al*., 2007; Merino-Puerto *et al*., 2010; Nürnberg *et al*., 2015 & 2016; Mariscal *et al*., 2016).

Moreover, *ΔamiC1* and *ΔamiC2* mutants formed akinete like-cells with rounded-shape, surrounded by a thin envelope or void of it (Fig. 45, 46). Conversely, the *amiC2* mutant in *N. punctiforme* was totally unable to differentiate akinetes (Lehner *et al*., 2011). The mutation in the *hepA* gene in *A. variabilis* resulted in alteration of akinete and heterocyst envelopes (Leganés, 1994). In the future, more studies are necessary to characterize deeply these akinete like-cells. However, it is feasible to suggest that due to the alteration of the envelope, these akinete- like cells are less mechanically resistant than wild type akinetes.

The results of this study support the idea that the cell wall proteins (Ava_2312, AmiC1 and AmiC2) in *A. variabilis*, are necessary for differentiation of functional heterocysts and akinetes by modification of the peptidoglycan septa.

Further morphological and physiological studies of the akinete-like cells formed in the *ΔAva_2312*, *ΔamiC1* and *ΔamiC2* mutants, are necessary to define the role of Ava_2312, AmiC1 and AmiC2 proteins in akinete differentiation and germination processes. Also, sacculi analysis by TEM and FRAP studies of these mutants together with complementation and localization of the Ava_2312, AmiC1 and AmiC2 proteins are necessaries to clarify the role of these cell wall proteins in cell-cell communication and differentiation process in *A. variabilis*.

Supplementary information

Akinete differentiation

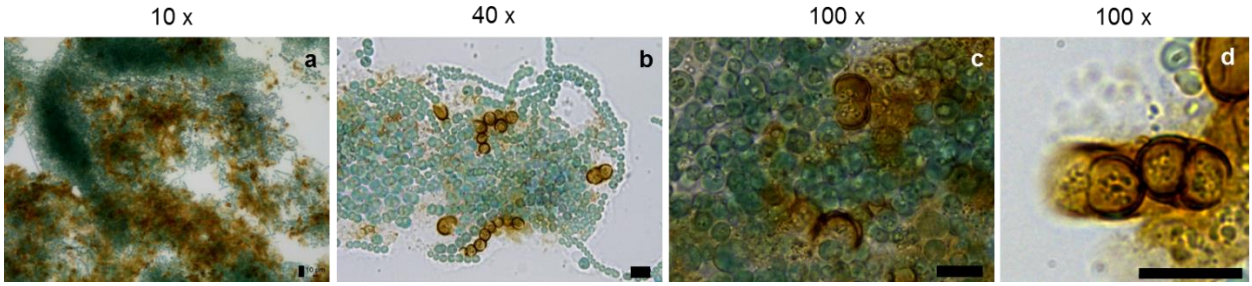

Figure S1. Light microscopy of akinetes in *N. punctiforme* (a-d). Black bars, 10 µm.

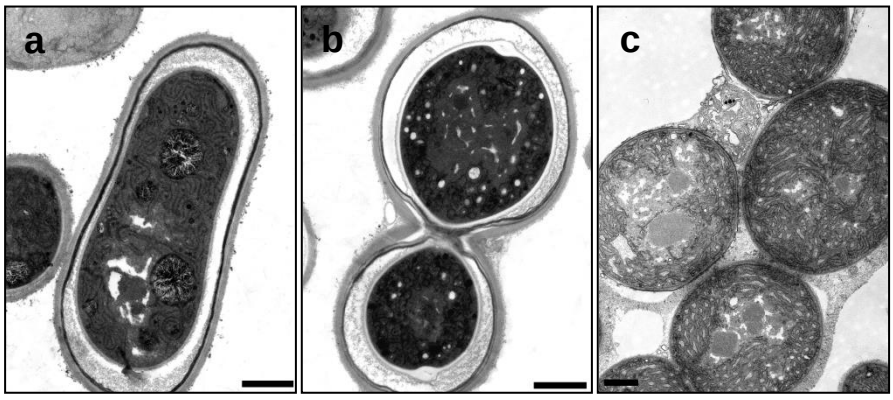

Figure S2. Ultrastructure of *A. variabilis* (a, b) and *N. punctiforme* akinetes (c). Bars, 1 µm

Akinete germination

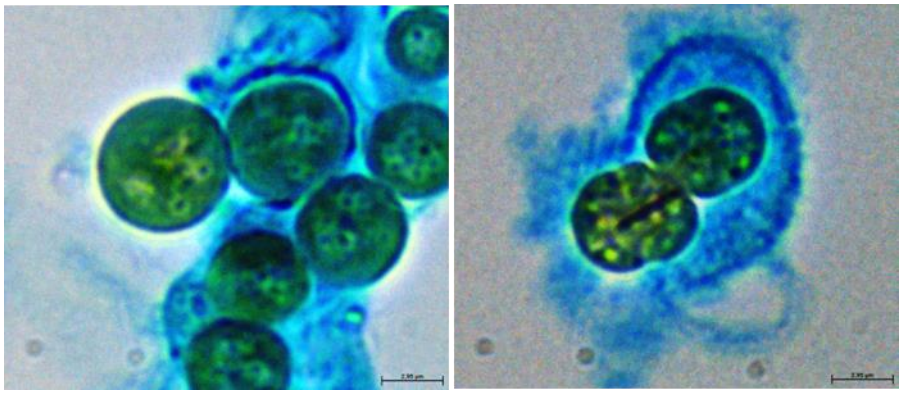

Figure S3. Alcian blue staining of germinating akinetes in *N. punctiforme*. Black bars, 2.5 µm.

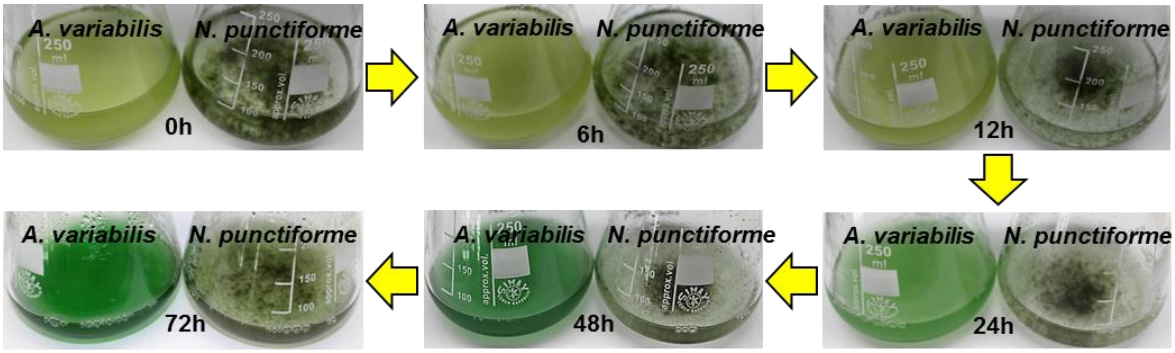

Figure S4. Regeneration of the thylakoid membranes during akinete germination in *Anabaena variabilis* and *N. punctiforme*. Cultures induced to form akinetes by phosphate starvation for 3 months were washed and transferred to conventional media and conditions. Photos were taken at 0, 6, 12, 24, 48 and 72 hours of germination.

Cell wall mutants in A. variabilis

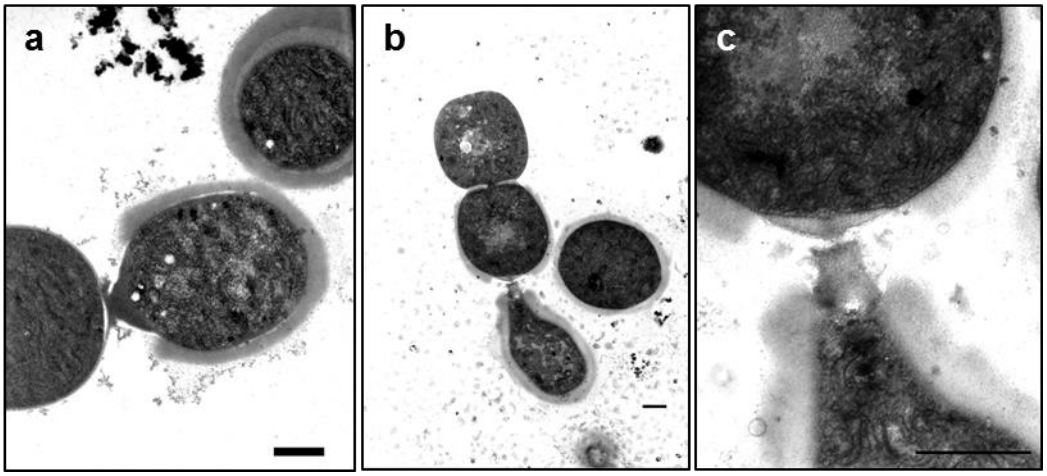

Figure S5. Ultrastructure of heterocysts in *A. variabilis* and the amidase mutant strains. (a) Electron micrograph of heterocysts at of nitrogen step-down in *ΔamiC1* and (b, c) *ΔamiC2* cultures. Bars, 1 µm.

Publications

Publications of this work:

Perez R, Forchhammer K, Salerno GL, Maldener I (2016)
Clear differences in metabolic and morphological adaptations of akinetes of two *Nostocales* living in different habitats.
Microbiology **162:** 214–223

Collaborations in other works:

Lehner J, Berendt S, Dörsam B, Pérez R, Forchhammer K, Maldener I (2013)
Prokaryotic multicellularity: a nanopore array for bacterial cell communication.
FASEB J **27:** 1–8

Bibliography

Adams DG, Duggan PS (1999) Heterocyst and akinete differentiation in cyanobacteria. New Phytol **144:** 3–33

Adams DG, Carr NG (1981) The developmental biology of heterocyst and akinete formation in cyanobacteria. CRC Critical Reviews in Microbiology **9:** 45–100

Ahuja G, Khattar JS, Sarma TA (2008) Interaction between carbon and nitrogen metabolism during akinete development in the cyanobacterium *Anabaena torulosa.* J Basic Microbiol **48:** 125–129

Argueta C, Summers ML (2005) Characterization of a model system for the study of *Nostoc punctiforme* akinetes. Arch Microbiol **183:** 338–346

Argueta C, Yuksek K, Summers M (2004) Construction and use of GFP reporter vectors for analysis of cell-type-specific gene expression in *Nostoc punctiforme*. J Microbiol Methods **59:** 181–188

Awai K, Wolk CP (2007) Identification of the glycosyl transferase required for synthesis of the principal glycolipid characteristic of heterocysts of *Anabaena* sp. strain PCC 7120. FEMS Microbiol Lett **266:** 98–102

Bauer CC, Buikema WJ, Black K, Haselkorn R (1995) A short-filament mutant of *Anabaena* sp. strain PCC 7120 that fragments in nitrogen-deficient medium. J Bacteriol **177**: 1520–1526

Bauersachs T, Compaore J, Hopmans EC, Stal LJ, Schouten S, Sinninghe Damste JS (2009) Distribution of heterocyst glycolipids in cyanobacteria. Phytochemistry **70**: 2034–2039

Berendt S, Lehner J, Zhang YV, Rasse TM, Forchhammer K, Maldener I (2012) Cell wall amidase AmiC1 is required for cellular communication and heterocyst development in the cyanobacterium *Anabaena* PCC 7120 but not for filament integrity. J Bacteriol **194**: 5218–27

Bjorn GS, Braune W, Bjorn LO (1983) Photochromic pigments in akinetes and pigment characteristics of akinetes in comparison with vegetative cells of *Anabaena variabilis*. Physiol Plant **59:** 493–500

Black TA, Cai Y, Wolk CP (1993) Spatial expression and autoregulation of *hetR*, a gene involved in the control of heterocyst development in *Anabaena*. Mol microbiol **9:** 77–84

Black TA, Wolk CP (1994) Analysis of a Het- Mutation in *Anabaena* sp. Strain PCC 7120 Implicates a Secondary Metabolite in the Regulation of Heterocyst Spacing. J Bacteriol **176:** 2282–2292

Braune W (1979) C-Phycocyanin: The main photoreceptor in the light-dependent germination process of *Anabaena* akinetes. Arch Microbiol **122:** 289–296

Braune, W. (1980) Structural aspects of akinete germination in the cyanobacterium *Anabaena variabilis*. Arch Microbiol **126:** 257–261

Büttner F, Faulhaber K, Forchhammer K, Maldener I, Stehle T (2016) Enabling cell–cell communication via nanopore formation: structure, function and localization of the unique cell wall amidase AmiC2 of *Nostoc punctiforme*. FEBS J **283**: 1336–1350

Campbell EL, Hagen KD, Cohen MF, Summers ML, Meeks JC (1996) The *devR* gene product is characteristic of receivers of two-component regulatory systems and is essential for heterocyst development in the filamentous cyanobacterium *Nostoc* sp. strain ATCC 29133. J Bacteriol **178:** 2037–2043

Campbell EL, Cohen MF, Meeks JC (1997) A polyketidesynthase-like gene is involved in the synthesis of heterocyst glycolipids in *Nostoc punctiforme* strain ATCC 29133. Arch Microbiol **167:** 251–258

Campbell EL, Summers ML, Christman H, Martin ME, Meeks JC (2007) Global gene expression patterns of *Nostoc punctiforme* in steady-state dinitrogen-grown heterocyst-containing cultures and at single time points during the differentiation of akinetes and hormogonia. J Bacteriol **189:** 5247–5256

Cardemil L, Wolk CP (1979) The polysaccharides from heterocyst and spore envelopes of a blue-green alga. Structure of the basic repeating unit. J Biol Chem **254:** 736–774

Cardemil L, Wolk CP (1981) Polysaccharides drom the envelopes of heterocysts and spores of the blue-green algae *Anabaena variabilis* and *Cylindrospermum licheniforme*. J Phycol **17:** 234–240

Castenholz RW (1969) Thermophilic blue-green algae and the thermal environment. Bacteriol Rev **33:** 476–504

Chauvat F, Corre B, Herdman M, Joset-Espardellier F (1982) Energetic and metabolic requirements for the germination of akinetes of the cyanobacterium *Nostoc* PCC 7524. Arch Microbiol **133:** 44–49

Curatti L, Giarrocco LE, Cumino AC, Salerno GL (2008) Sucrose synthase is involved in the conversion of sucrose to polysaccharides in filamentous nitrogen-fixing cyanobacteria. Planta **228:** 617–625

Dai GZ, Qiu BS Forchhammer K (2014) Ammonium tolerance in the cyanobacterium *Synechocystis* sp. strain PCC 6803 and the role of the *psbA* multigene family. Plant Cell Environ **37:** 840–851

Duggan PS, Gottardello P, Adams DG (2007) Molecular analysis of genes in *Nostoc punctiforme* involved in pilus biogenesis and plant infection. J bacteriol **189**: 4547–4551

Eberhardt RY, Chang Y, Bateman A, Murzin AG, Axelrod HL, Hwang WC, Aravind L (2013) Filling out the structural map of the NTF2-like superfamily. BMC Bioinformatics **14:** 1–11

Elhai J, Wolk CP (1988) A versatile class of positive-selection vectors based on the nonviability of palindrome-containing plasmids that allows cloning into long polylinkers. Gene **68:** 119-138

Ernst A, Black T, Cai Y, Panoff J-M, Tiwari DN, Wolk CP (1992) Synthesis of Nitrogenase in Mutants of the Cyanobacterium *Anabaena* sp. Strain PCC 7120 Affected in Heterocyst Development or Metabolism. J Bacteriol **174**: 6025– 6032

Fan Q, Huang G, Lechno-Yossef S, Wolk CP, Kaneko T, Tabata S (2005) Clustered genes required for synthesis and deposition of envelope glycolipids in *Anabaena* sp. strain PCC 7120. Mol Microbiol **58:** 227–243

Fay P. (1969) Metabolic activities of isolated spores of *Anabaena cylindrica*. J Experimental Botany **20:** 100–109

Fay P (1988) Viability of akinetes of the planktonic cyanobacterium *Anabaena circinalis*. Proc R Soc Lond B **234:** 283–301

Fiedler G, Arnold M, Hannus S, Maldener I (1998) The DevBCA exporter is essential for envelope formation in heterocysts of the cyanobacterium *Anabaena* sp. strain PCC 7120. Mol Microbiol **27:** 1193–1202

Flores E, Pernil R, Muro-Pastor AM, Mariscal V, Maldener I, Lechno-Yossef S, Fan Q, Wolk CP, Herrero A (2007) Septum-localized protein required for filament integrity and diazotrophy in the heterocyst-forming cyanobacterium *Anabaena* sp. strain PCC 7120. J Bacteriol **189:** 3884–3890

Flores E, Herrero A (2010) Compartmentalized function through cell differentiation in filamentous cyanobacteria Nature Rev Microbiol **8:** 39–50

Gambacorta A, Pagnotta E, Romano I, Sodano G, Tricone A (1998) Heterocyst glycolipids from nitrogenfixing cyanobacteria other than Nostocaceae. Phytochemistry **48:** 801–805

Garcia-Pichel F, Johnson SL, Youngkin D, Belnap J (2003) Small-scale vertical distribution of bacterial biomass and diversity in biological soil crusts from arid lands in the Colorado plateau. Microbial Ecol **46:** 312–321

Gibson D, Young L, Chuang R-Y, Venter J, Hutchison III C, Smith H (2009) Enzymatic assembly of DNA molecules up to several hundred kilobases. Nature Methods **6:** 343-345

Giddings TH, Staehelin LA (1978) Plasma membrane architecture of *Anabaena cylindrica*: occurrence of microplasmodesmata and changes associated with heterocyst development and the cell cycle. Eur J Cell Biol **16:** 235–249

Giddings HT, Staehelin LA (1981) Observation of Microplasmodesmata in both heterocyst-forming and non-heterocyst forming filamentous cyanobacteria by freeze fracture electron microscopy. Arch Microbiol **129:** 295–298

Golden JW, Yoon HS (2003) Heterocyst development in *Anabaena*. Curr Opin Microbiol **6:** 557–563

Gründel M, Scheunemann R, Lockau W, Zilliges Y (2012) Impaired glycogen synthesis causes metabolic overflow reactions and affects stress responses in the cyanobacterium *Synechocystis* sp. PCC 6803. Microbiology **158:** 3032–3043

Herdman M (1987) Akinetes: structure and function. In Fay P, van Baalen C (Ed.), The cyanobacteria (pp. 227-250). Amsterdam: Elsevier

Herdman M, Rippka R (1988) Cellular Differentiation: Hormogonia and Baeocytes. Methods Enzym **167:** 232–242

http://pfam.xfam.org/family/PF 10648

https://www.ncbi.nlm.nih.gov/Structure/cdd/cddsrv.cgi?uid=cl02713

Huber AL (1985) Factors affecting the germination of akinetes of *Nodularia spumigena* (cyanobacteriaceae) Appl Environ Microbiol **49:** 73–78

Humason GL (1967) Animal Tissue Techniques, 2nd ed. W.H. Freeman and Company, San Francisco, USA. pp 569

Kaplan-Levy RN, Hadas O, Summers ML, Rücker J, Sukenik A (2010) Akinetes: Dormant Cells of Cyanobacteria. In E Lubzens, J Cerda, M Clark eds, Dormancy and Resistance in Harsh Environments. Berlin: Springer, pp. 5–27

Kezhi B, Guoliang W, Cheng C (1985) Studies on the mechanism of light-dependent germination of akinetes of blue-green algae. Hydrobiologia **123:** 89–91

Khayatan B, Meeks JC, Risser DD (2015) Evidence that a modified type IV pilus-like system powers gliding motility and polysaccharide secretion in filamentous cyanobacteria. Mol Microbiol **98**: 1021–1036

Kumar K, Mella-Herrera RA, Golden JW (2010) Cyanobacterial heterocysts. Cold Spring Harb Perspect Biol **2:** 1–119

Lawry NH, Simon RD (1982) The normal and induced occurence of cyanophycin in inclusin bodies in several blue-green algae. J Phycol **18:** 391–399

Lazaroff N (1973) Photomorphogenesis and Nostocacea development. In NG Carr, BA Whitton eds, The Biology of Blue-Green Algae. Blackwell Scientific: Oxford, pp 279–319

Lázaro S, Fernandez-Pinas F, Fernandez-Valiente E, Blanco-Rivero A, Leganes F (2001) *pbpB*, a Gene Coding for a Putative Penicillin-Binding Protein, Is Required for Aerobic Nitrogen Fixation in the Cyanobacterium *Anabaena* sp. Strain PCC7120. J. Bacteriol. **183:** 628–636

Leganés F, Fernandez-Pinas F, Wolk CP (1994) Two mutations that block heterocyst differentiation have different effects on akinete differentiation in *Nostoc ellipsosporum*. Mol Microbiol **12:** 679–684

Leganés F, Fernandez-Pinas F, Wolk CP (1998) A transposition-induced mutant of *Nostoc ellipsosporum* implicates an arginine-biosynthetic gene in the formation of cyanophycin granules and of functional heterocysts and akinetes. Microbiology **144:**1799–1805

Lehner J, Zhang Y, Berendt S, Rasse TM, Forchhammer K, Maldener I (2011) The morphogene AmiC2 is pivotal for multicellular development in the cyanobacterium *Nostoc punctiforme*. Mol Microbiol **79:** 1655–1669

Lehner J, Berendt S, Dörsam B, Pérez R, Forchhammer K, Maldener I (2013) Prokaryotic multicellularity: a nanopore array for bacterial cell communication. FASEB J **27:** 1–8

Li R, Watanabe M, Watanabe MM (1997) Akinete formation in planktonic *Anabaena* spp (Cyanobacteria) by treatment with low temperature. J Phycol **33:** 576–584

Mackinney G (1941) Absorption of light by chlorophyll solutions. J Biol Chem **140:** 109–112

Maldener I, Ernst A, Fernández-Piñas F, Wolk CP (1994) Characterization of *devA*, a gene required for the maturation of proheterocysts in the cyanobacterium *Anabaena* sp. strain PCC 7120. J. Bacteriol. **176:** 7543–49

Maldener I, Hannus S, Kammerer M (2003) Description of five mutants of the cyanobacterium *Anabaena* sp. strain PCC 7120 affected in heterocyst differentiation and identification of the transposon-tagged genes. FEMS Microbiol Lett **224:** 205–213

Maldener I, Summers ML, Sukenik A (2014) Cellular differentiation in filamentous cyanobacteria. In E Flores, A Herrero eds, The Cell Biology of Cyanobacteria. Caister Academic Press, pp 263–291

Mariscal V, Nürnberg DJ, Herrero A, Mullineaux CW, Flores E (2016) Overexpression of SepJ alters septal morphology and heterocyst pattern regulated by diffusible signals in *Anabaena*. Mol Microbiol. doi: 10.1111/mmi.13436

Meeks J (1998) Symbiosis between nitrogen-fixing cyanobacteria and plants. BioScience **48**: 266–276

Meeks JC, Elhai J (2002) Regulation of cellular differentiation in filamentous cyanobacteria in free-living and plant-associated symbiotic growth states. Microbiol Mol Biol Rev: MMBR **66:** 94–121

Mella-Herrera RA, Neunuebel MR, Golden JW (2011) *Anabaena* sp. strain PCC 7120 *conR* contains a LytR-CpsA-Psr domain, is developmentally regulated, and is essential for diazotrophic growth and heterocyst morphogenesis. Mol Microbiol **157**: 617–626

Merino-Puerto V, Mariscal V, Mullineaux CW, Herrero A, Flores E (2010) Fra proteins influencing filament integrity, diazotrophy and localization of septal protein SepJ in the heterocyst-forming cyanobacterium *Anabaena* sp. Mol Microbiol **75:** 1159–1170

Messineo L (1966) Modification of Sakaguchi reaction – spectrophotometric determination of arginine in proteins without previous hydrolysis. Arch Biochem Biophys **117:** 534–540

Miller MM, Lang NJ (1968) The fine structure of akinete formation and germination in *Cylindrospermum*. Arch Microbiol **60:** 303–313

Miller LH (1972) Experiments in Molecular Genetics. Cold Spring Harbor Laboratory, Press Cold Spring Harbor, New York.

Moore BG, Tischer RG (1965) Biosynthesis of extracellular polysaccharides by the blue green alga *Anabaena flos-aquae*. Can J Microbiol **11:** 877–885

Moore D, McGregor G, Shaw G (2004) Morphological changes during akinete germination in *Cylindrospermopsis raciborskii* (Nostocales, cyanobacteria). J Phycol **40:** 1098–1105

Nayar AS, Yamaura H, Rajagopalan R, Risser DD, Callahan SM (2007) FraG is necessary for filament integrity and heterocyst maturation in the cyanobacterium *Anabaena* sp. strain PCC 7120. Microbiology **153:** 601–607

Nichols JM, Adams DG (1982) Akinetes. In NG Carr, BA Whitton eds, The Biology of Cyanobacteria. Oxford: Blackwell Scientific Publications, pp. 387–412

Nicolaisen K, Hahn A, Schleiff E (2009) The cell wall in heterocyst formation by *Anabaena* sp. PCC 7120. J Microbiol **49:** 5–24

Nürnberg DJ, Mariscal V, Bornikoel J, Nieves-Morión M, Krauß N, Herrero A, Maldener I, Flores E, Mullineaux CW (2015) Intercellular diffusion of a fluorescent sucrose analog via the septal junctions in a filamentous cyanobacterium. Mol Biol **6:** e02109

Omairi-Nasser A, Haselkorn R, Austin II J (2014) Visualization of channels connecting cells in filamentous nitrogen-fixing cyanobacteria. FASEB J 1–7

Pelczar M (ed) (1957). Manual for Microbiological Methods. McGraw-Hill: New York.

Peramuna A, Summers ML (2014) Composition and occurrence of lipid droplets in the cyanobacterium *Nostoc punctiforme*. Arch Microbiol **196:** 881–890

Perez R, Forchhammer K, Salerno GL, Maldener I (2016) Clear differences in metabolic and morphological adaptations of akinetes of two *Nostocales* living in different habitats. Microbiology **162:** 214–223

Ramirez ME, Hebbar PB, Zhou R, Wolk CP, Curtis SE (2005) *Anabaena* sp. strain PCC 7120 gene *devH* is required for synthesis of the heterocyst glycolipid layer. J Bacteriol **187:** 2326–2331

Rao VV, Ghosh R, Singh HN (1987) Diazotrophic regulation of akinete development in the cyanobacterium *Anabaena doliolum*. New Phytol **106:**161–168

Reddy PM (1983) Effects of temperature pre-treatment, desiccation and aging on the viability of spores of halophilic blue-green algae. Hydrobiol **106:** 235–240

Rippka R, Deruelles J, Waterbury JB, Herdman M, Stanier RY (1979) Generic assignments, strain histories and properties of pure cultures of cyanobacteria. J Gen Microbiol **111:** 1–61

Sammons RL, **Slynn GM, Smith DA** (1987) Genetical and molecular studies on *gerM*, a new developmental locus of *Bacillus subtilis*. J Gen Microbiol **133:** 3299–3312

Sambrook J, Fritsch E, Maniatis T (1989) Molecular cloning: A laboratory manual. Cold Spring Harbor Laboratory Press, Cold Spring Harbor, NY.

Sarma TA, Khattar JIS (1986) Accumulation of Cyanophycin and Glycogen during Sporulation in the Blue-Green-Alga *Anabaena torulosa*. Biochemie Und Physiologie Der Pflanzen **181:** 155–164

Sarma TA, Khattar JIS (1993) Akinete differentiation in phototrophic, photoheterotrophic and chemoheterotrophic conditions in *Anabaena torulosa*. Folia Microbiol **38:** 335–340

Shi L, Carmichael WW (1997) pp1-cyano2, a protein serine/threonine phosphatase 1 gene from the cyanobacterium *Microcystis aeruginosa* UTEX 2063. Arch Microbiol **168:** 528–531

Shih PM, Wu D, Latifi A, Axen SD, Fewer DP, Talla E, Calteau A, Cai F, Tandeau de Marsac N, other authors (2013) Improving the coverage of the cyanobacterial phylum using diversity-driven genome sequencing. Proc Natl Acad Sci USA **110:** 1053–1058

Sili C, Ena A, Materassi R, Vincenzini M (1994) Germination of desiccated aged akinetes of alkaliphilic cyanobacteria. Arch Microbiol **162:** 20–25

Simon RD (1973) Measurement of the cyanophycin granule polypeptide contained in the blue-green alga *Anabaena cylindrica*. J Bacteriol **114:**1213–1216

Simon RD (1986) Inclusion bodies in the cyanobacteria: cyanophycin, polyphosphate, and polyhedral bodies. In P Fay, C van Baalen eds, The Cyanobacteria: Current Research Amsterdam: Elsevier/North Holland Biomedical Press, pp. 199–226

Skill SC, Smith RJ (1987) Synchronous akinete germination and heterocyst differentiation in *Anabaena* PCC 7937 and *Nostoc* PCC 6720. J Gen Microbiol **133:** 299–304

Slynn GM, **Sammons RL, Smith DA, Moir A, Corfe BM** (1994) Molecular genetical and phenotypical analysis of the *gerM* spore germination gene of *Bacillus subtilis* 168. FEMS Microbiol Lett **121:** 315–320

Soriente A, Gambacorta A, Trincone A, Sili C, Vincenzini M, Sodano G (1993) Heterocyst glycolipids of the cyanobacterium *Cyanospira rippkae*. Phytochemistry **33:** 393–396

Stal LJ (2012) Cyanobacterial mats and stromatolites. In BA Whitton ed, Ecology of Cyanobacteria II: Their Diversity in Space and Time. Dordrecht: Springer, pp. 65–125

Staron P, Forchhammer K, Maldener I (2011) A novel ATP-driven pathway of glycolipid export involving TolC protein. J Biol Chem **286:** 38202–38210

Sturt H, Summons R, Smith K, Elvert M, Hinrichs K-U (2004) Intact polar membrane lipids in prokaryotes and sediments deciphered by high-performance liquid chromatography/ electrospray ionization multi stage mass spectrometry - new biomarkers for biogeochemistry and microbial ecology. Rapid Commun. Mass Spectrom. **18:** 617–628

Sukenik A, Beardall J, Hadas O (2007) Photosynthetic characterization of developing and mature akinetes of *Aphanizomenon ovalisporum* (cyanoprokaryota). J Phycol **43:** 780–788

Sukenik A, Kaplan-Levy RN, Welch JM, Post AF (2012) Massive multiplication of genome and ribosomes in dormant cells (akinetes) of *Aphanizomenon ovalisporum* (Cyanobacteria). ISME J **6:** 670–679

Sukenik A, Maldener I, Delhaye T, Viner-Mozzini Y, Sela D, Bormans M (2015) Carbon assimilation and accumulation of cyanophycin during the development of dormant cells (akinetes) in the cyanobacterium *Aphanizomenon ovalisporum*. Front Microbiol **6:** 1067

Sutherland JM, Herdman M, Stewart WDP (1979) Akinetes of the cyanobacterium *Nostoc* PCC 7524: macromolecular composition, structure and control of differentiation. J Gen Microbiol **115:** 273–287

Sutherland JM, Reaston J, Stewart WDP, HerdmanM (1985) Akinetes of cyanobacterium *Nostoc* PCC 7524 macromolecular and biochemical changes during synchronous germination. J Gen Microbiol **131:** 2855–2864

Tandeau De Marsac N (1994) The Molecular Biology of Cyanobacteria. Kluwer Academic Publishers. 825–842

Thiel T, Wolk CP (1983) Metabolic activities of isolated akinetes of the cyanobacterium *Nostoc spongiaeforme*. J Bacteriol **156:** 369–374

Thiel T, Pratte BS, Zhong J, Goodwin L, Copeland A, Lucas S, Han C, Pitluck S, Land ML, other authors (2014) Complete genome sequence of *Anabaena variabilis* ATCC 29413. Stand Genomic Sci **9:** 562–573

Tiyanont K, Doan T, Lazarus MB, Fang X, Rudner DZ, Walker S (2006) Imaging peptidoglycan biosynthesis in *Bacillus subtilis* with fluorescent antibiotics. Proc Natl Acad Sci USA **103:** 11033–11038

Valladares A, Maldener I, Muro-Pastor AM, Flores E, Herrero A (2007) Heterocyst Development and Diazotrophic Metabolism in Terminal Respiratory Oxidase Mutants of the Cyanobacterium *Anabaena* sp. Strain PCC 7120. J Bacteriol **189:** 4425–4430

Videau P, Rivers OS, Higa KC, Callahan SM (2015) ABC transporter required for intercellular transfer of developmental signals in a heterocystous cyanobacterium. J Bacteriol **197:** 2685– 2693

Vincent WF (2007) Cold Tolerance in Cyanobacteria and Life in the Cryosphere. In J Seckbach, ed, Algae and Cyanobacteria in Extreme Environments. Springer Netherlands, pp 287–301

Watzer B, Engelbrecht A, Hauf W, Stahl M, Maldener I, Forchhammer K (2015) Metabolic pathway engineering using the central signal processor PII. Microb Cell Fact **14:** 192

Whitton BA, Potts M (2012) "Introduction to the cyanobacteria". In B Whitton, ed, *Ecology of Cyanobacteria II*. Berlin: Springer, pp 1–13

Wilk L, Strauss M, Rudolf M, Nicolaisen K, Flores E, Kuhlbrandt W, Schleiff E (2011) Outer membrane continuity and septosome formation between vegetative cells in the filaments of *Anabaena* sp. PCC 7120. Cell Microbiol **13:** 1744–1754

Wildman RB, Loescher JH, Winger CL (1975) Development and germination of akinetes of *Aphanizomenon-flos-aquae*. J Phycol **11:** 96–104

Winkenbach F, Wolk CP, Jost M (1972) Lipids of membranes and of the cell envelope in heterocysts of blue-green alga. Planta **107:** 69–80

Wolk CP (1965) Control of sporulation in a blue-green alga. Dev Biol **12:** 15–35

Wolk CP, Vonshak A, Kehoe P, Elhai J (1984) Construction of shuttle vectors capable of conjugative transfer from *Escherichia coli* to nitrogen-fixing filamentous cyanobacteria. Proc Natl Acad Sci USA **81:** 1561–1565

Wolk C, Ernst A, Elhai J (1994) Heterocyst metabolism and development. *In* D Bryant, ed, Molecular Biology of Cyanobacteria. Kluwer Academic Publishers, Dordrecht, The Netherlands, pp 769–823

Wolk CP (1996) Heterocyst formation. Annu Rev Genet **30:** 59–78

Wörmer, L, Cirés S, Velázquez D, Quesada A, Hinrichs K (2012) Cyanobacterial heterocyst glycolipids in cultures and environmental samples: Diversity and biomarker potential. Limnol. Oceanogr **57:** 1775–1788

Wörmer L, Lipp J, Schröder J, Hinrichs K (2013) Application of two new LC-ESI-MS methods for improved detection of intact polar lipids (IPLs) in environmental samples. Org Geochem **59:** 10–21

Wong FC, Meeks JC (2001) The *hetF* gene product is essential to heterocyst differentiation and affects HetR function in the cyanobacterium *Nostoc punctiforme*. J Bacteriol **183:** 2654–2661

Yamamoto Y (1976) Effect of some physical and chemical factors on the germination of akinetes of *Anabaena cylindrica*. J Gen App Microbiol **22:** 311–323

Yoshinaga M, Gagen E, Wörmer L, Broda N, Meador T, Wendt J, Thomm M, Hinrichs K (2015) *Methanothermo bacter thermautotrophicus* modulates its membrane lipids in response to hydrogen and nutrient availability. Fron Microbiol **6:** 1–9

Zhu J, Jäger K, Black T, Zarka K, Koksharova O, Wolk CP (2001) HcwA, an Autolysin, Is Required for Heterocyst Maturation in *Anabaena* sp. Strain PCC 7120. J Bacteriol **183:** 6841–6851

Zhou R, Wolk CP (2002) Identification of an akinete marker gene in *Anabaena variabilis*. J Bacteriol **184:** 2529-2532